



Fisheries and Oceans
Canada

Pêches et Océans
Canada

Ecosystems and
Oceans Science

Sciences des écosystèmes
et des océans

Canadian Science Advisory Secretariat (CSAS)

Research Document 2020/071

Maritimes Region

Optical, Chemical, and Biological Oceanographic Conditions on the Scotian Shelf and in the eastern Gulf of Maine during 2019

B. Casault, C. Johnson, E. Devred, E. Head, A. Cogswell, and J. Spry

Fisheries and Oceans Canada
Bedford Institute of Oceanography
1 Challenger Drive, PO Box 1006
Dartmouth, Nova Scotia B2Y 4A2

Foreword

This series documents the scientific basis for the evaluation of aquatic resources and ecosystems in Canada. As such, it addresses the issues of the day in the time frames required and the documents it contains are not intended as definitive statements on the subjects addressed but rather as progress reports on ongoing investigations.

Published by:

Fisheries and Oceans Canada
Canadian Science Advisory Secretariat
200 Kent Street
Ottawa ON K1A 0E6

[http://www.dfo-mpo.gc.ca/csas-sccs/
csas-sccs@dfo-mpo.gc.ca](http://www.dfo-mpo.gc.ca/csas-sccs/csas-sccs@dfo-mpo.gc.ca)



© Her Majesty the Queen in Right of Canada, 2020
ISSN 1919-5044

Correct citation for this publication:

Casault, B., Johnson, C., Devred, E., Head, E., Cogswell, A., and Spry, J. 2020. Optical, Chemical, and Biological Oceanographic Conditions on the Scotian Shelf and in the eastern Gulf of Maine during 2019. DFO Can. Sci. Advis. Sec. Res. Doc. 2020/071. v + 64 p.

Aussi disponible en français :

Casault, B., Johnson, C., Devred, E., Head, E., Cogswell, A., et Spry, J. 2020. Conditions océanographiques optiques, chimiques et biologiques sur le plateau néo-écossais et dans l'est du golfe du Maine en 2019. Secr. can. de consult. sci. du MPO, Doc. de rech. 2020/071. v + 67 p.

TABLE OF CONTENTS

ABSTRACT.....	V
INTRODUCTION	1
METHODS.....	1
MISSIONS	2
High-Frequency Sampling Stations	2
Shelf Sections	2
Ecosystem Trawl Surveys	2
GEAR DEPLOYMENT	3
Conductivity, Temperature, Depth	3
Net Tows.....	3
DERIVED METRICS	3
Mixed Layer and Stratification Indices	3
Optical Properties.....	4
Vertically Integrated Variables.....	4
Phytoplankton Taxonomic Groups.....	4
SATELLITE REMOTE SENSING OF OCEAN COLOUR.....	4
ANNUAL ANOMALIES SCORECARDS	5
ACCESS TO DATA PRODUCTS	6
BEDFORD BASIN MONITORING PROGRAM.....	6
CONTINUOUS PLANKTON RECORDER.....	6
OBSERVATIONS.....	7
MIXING AND OPTICAL PROPERTIES	7
NUTRIENTS	8
High-frequency Sampling Stations	8
Broad-scale Surveys	9
PHYTOPLANKTON	10
High-frequency Sampling Stations	10
Broad-scale Surveys and Satellite Remote Sensing.....	11
ZOOPLANKTON.....	11
High-frequency Sampling Stations	11
Broad-scale Surveys	13
Indicator Species.....	13
DISCUSSION.....	14
BEDFORD BASIN MONITORING PROGRAM.....	17
PHYSICAL CONDITIONS	17
NUTRIENTS AND PLANKTON CONDITIONS.....	17
CONTINUOUS PLANKTON RECORDER.....	17
PHYTOPLANKTON	17

ZOOPLANKTON.....	18
ACID SENSITIVE ORGANISMS	18
SUMMARY	18
ACKNOWLEDGEMENTS	19
REFERENCES CITED.....	19
TABLES.....	23
FIGURES.....	24

ABSTRACT

Ocean physical conditions in the Maritimes Region in 2019 were characterized by cooler surface temperatures, continued warmer bottom temperatures and weaker stratification compared to recent years. Deep nutrient inventories were lower than normal over most of the region, with the exception of the Cabot Strait section where deep nutrients were near or higher than normal during the spring sampling and associated with record-warm water. Anomalies of surface nutrients were negative across the region, with the exception of positive anomalies observed at the deep shelf and offshore stations of the Louisbourg section. The spring phytoplankton bloom was near or slightly earlier than normal across the Scotian Shelf (SS) with near-normal duration. Peak chlorophyll *a* concentrations during the spring bloom occurred within a narrow time window across the SS. At Halifax-2 (HL2), the spring bloom was characterized by a high amplitude, and a rapid progression and decline. Plankton community changes persisted in 2019 with lower abundance of large phytoplankton (diatoms), mainly lower-than-normal biomass of zooplankton and abundance of *Calanus finmarchicus*, and higher-than-normal abundance of non-copepods. Arctic *Calanus* and warm-shelf copepods showed mixed abundance anomalies in 2019, reversing the pattern of 2018. Above-normal abundances of *Oithona atlantica*, especially at HL2, suggest a greater influence of offshore waters in recent years. Surface temperature in the Bedford Basin was near normal in 2019 with mainly cooler-than-normal temperatures from January to June and near- or slightly-above-normal temperatures from July to December. Bottom temperature and salinity were below normal in 2019 with near- or slightly-above-normal conditions at the start of the year and progressing toward cooler and fresher water from February to December. Surface and deep nitrate, phosphate and silicate were near or below normal, with surface phosphate reaching a record low in 2019. The 2018 Continuous Plankton Recorder data indicated an annual abundance of diatoms close to normal for the Eastern (ESS) and Western Scotian Shelf (WSS), while the abundance of dinoflagellates and the Phytoplankton Colour Index values were near (WSS) or above (ESS) normal. The annual abundance of *Calanus* CI-IV was near normal (ESS) or slightly below normal (WSS), while *C. finmarchicus* CV-VI levels were slightly below (ESS) or below (WSS) normal. The abundance of *Calanus glacialis* (ESS, WSS) and *Paral/Pseudocalanus* and *Limacina* spp. (WSS) were lower than normal, while that of coccolithophore (ESS, WSS), and copepod nauplii and foraminifera (ESS) was higher than normal.

INTRODUCTION

The Atlantic Zone Monitoring Program (AZMP) was implemented in 1998 to enhance Fisheries and Oceans Canada's (DFO's) capacity to understand, describe, and forecast the state of the marine ecosystem (Therriault et al. 1998). The AZMP derives its information on the marine environment and ecosystem from data collected at a network of sampling locations (fixed-point, high-frequency sampling stations, cross-shelf sections, ecosystem trawl surveys) in four DFO regions (Québec, Gulf, Maritimes, and Newfoundland), sampled at a frequency of twice-monthly to once-annually. The sampling design provides basic information on the variability in physical, chemical, and biological properties of the Northwest Atlantic continental shelf on annual and inter-annual scales. Ecosystem trawl surveys and cross-shelf sections provide information about broad-scale environmental variability (Harrison et al. 2005) but are limited in their seasonal coverage. High-frequency sampling stations complement the broad-scale sampling by providing detailed information on annual changes in ocean properties. In addition, the North Atlantic Continuous Plankton Recorder (CPR) survey provides monthly sampling along commercial shipping routes between Reykjavik and the New England coast, via the Scotian Shelf (SS). The CPR sampling extends a dataset started in 1960, allowing present-day observations to be set within a longer time frame. *In situ* sampling is also complemented by remote sensing ocean colour measurements providing additional information of the distribution of phytoplankton on a broad scale. This report provides an assessment of the distribution and variability of nutrients, oxygen, and plankton on the SS and in the eastern Gulf of Maine (GoM), focusing on conditions observed during 2019. It complements assessments for the physical environment of the Maritimes Region (e.g., Hebert et al. in preparation)¹ and for the state of the Canadian Northwest Atlantic shelf system as a whole (DFO 2020).

The SS is located in a transition zone influenced by both sub-polar waters, mainly flowing into the region from the Gulf of St. Lawrence and the Newfoundland Shelf, and warmer offshore waters. The deep-water properties of the western SS exhibit significant shifts in temperature, reflecting changes in the source of deep slope water to the shelf between cold, low-nutrient Labrador Slope Water, and warm, nutrient-rich slope water that can be driven by changes in large-scale atmospheric pressure patterns (Petrie 2007). Temperature and salinity on the SS are also influenced by heat transfer between the atmosphere and ocean, local mixing, precipitation, and runoff from land. Changes in the physical pelagic environment influence both plankton community composition and annual biological production cycles, with implications for energy transfer to higher trophic-level production. The status of nutrients, oxygen, and plankton in the region in 2019 are reported here in the context of warmer conditions in the marine environment observed in recent years.

METHODS

To the extent possible, sample collection and processing conform to established standard protocols (Mitchell et al. 2002). Non-standard measurements or derived variables are described below.

¹ Hebert, D., Pettipas, R., and Brickman, D. Meteorological, Sea Ice and Physical Oceanographic Conditions on the Scotian Shelf and in the Gulf of Maine during 2019. DFO Can. Sci. Advis. Sec. Res. Doc. In preparation.

MISSIONS

AZMP-DFO Maritimes Region sea-going staff participated in three missions (two ecosystem trawl surveys and one seasonal cross-shelf oceanographic survey) during the 2019 calendar year, in addition to day trips to the two high-frequency sampling stations. The fall seasonal cross-shelf survey was cancelled due to vessel unavailability. A total of 299 hydrographic station occupations were completed with net samples collected at 161 of these stations (Table 1).

High-Frequency Sampling Stations

The Halifax-2 (HL2) and Prince-5 (P5) high-frequency sampling stations (Figure 1) were sampled 18 and 12 times, respectively, in 2019, similar to the sampling frequencies achieved in recent years. There was no sampling between mid-August and mid-October at HL2 due to lack of ship availability.

The standard sampling suite for the high-frequency stations includes the following:

- a Conductivity, Temperature, Depth (CTD; measured using a Sea-Bird instrument) profile with dissolved oxygen, fluorescence, and Photosynthetically Active Radiation (PAR),
- Niskin water bottle samples at standard depths for nutrient analyses, salinity and oxygen calibration, and chlorophyll *a* and accessory pigments analyses,
- Niskin water bottle samples for phytoplankton enumeration,
- vertical ring net tows (202 µm mesh net) for zooplankton biomass (wet and dry weights) and abundance, and
- Secchi depth measurement for light attenuation when possible.

Shelf Sections

The four primary sections (Cabot Strait [CSL]; Louisbourg [LL]; Halifax [HL]; Browns Bank [BBL]; Figure 1), and a number of ancillary sections/stations (gray markers in Figure 2) were sampled in spring only (Table 1). Results from the ancillary sections/stations are not reported here.

The standard sampling suite for the section stations is the same as for the high-frequency sampling stations as listed above, except for phytoplankton enumeration. In addition to the standard suite of analyses from water samples, particulate organic carbon is measured at standard depths.

Ecosystem Trawl Surveys

AZMP-DFO Maritimes Region participated in two primary ecosystem trawl surveys in 2019. The February-March winter survey on the western SS and Georges Bank (GB) took place in two legs that were assigned different mission identifiers. The summer survey on the SS and the eastern GoM took place from early July to mid-August. Both ecosystem trawl surveys were led by the DFO Science Population Ecology Division with AZMP participation.

The sampling suite for the ecosystem trawl survey stations includes the measurements listed above for the high-frequency sampling stations, but the standard set of water bottle sampling depths is reduced, and vertical ring net tows (202 µm mesh net) are only collected at a subset of stations (Table 1 and Figure 3).

The sum of nitrate and nitrite is reported here as “nitrate.” For the summer ecosystem trawl survey, bottom nitrate concentrations were interpolated on a three-minute latitude-longitude grid

using optimal estimation (Petrie et al. 1996) to generate fields of bottom properties within the ecosystem trawl survey strata. The interpolation method uses the three nearest neighbours, with data near the interpolation grid point weighted proportionately more than those farther away. The weighting scheme is described in Petrie and Dean-Moore (1996), with horizontal length scales of 30 km, a vertical length scale of 15 m (for depth <50 m) or 25 m (for depths between 50 and 500 m). Bottom oxygen concentrations were optimally interpolated using the same technique as for nitrate. Oxygen concentrations were measured using a CTD-mounted oxygen sensor which was calibrated against oxygen concentrations measured by Winkler titration. Anomalies of bottom oxygen are not presented here, due to insufficient quality of oxygen data collected prior to 2015.

GEAR DEPLOYMENT

Conductivity, Temperature, Depth

The CTD is lowered to a target depth within 2 m of the bottom.

Standard depths for water samples include:

- High-frequency sampling stations:
 1. HL2: 1, 5, 10, 20, 30, 40, 50, 75, 100, 140 m
 2. P5: 1, 10, 25, 50, 95 m
- Seasonal sections: near-surface, 10, 20, 30, 40, 50, 60, 80, 100, 250, 500, 1000, 1500, 2000 m, near-bottom (depths sampled are limited by bottom depth)
- Ecosystem trawl surveys: 5, 25, 50 m, and near bottom when possible

Net Tows

Ring nets of a standard 202 μm mesh are towed vertically from near bottom to surface at approximately $1 \text{ m}\cdot\text{s}^{-1}$. In deep offshore waters, the maximum tow depth is 1000 m. Samples are preserved in buffered formalin and analyzed according to the protocol outlined in Mitchell et al. (2002).

DERIVED METRICS

Mixed Layer and Stratification Indices

Two simple indices of the vertical physical structure of the water column are computed:

1. The Mixed Layer (ML) depth is determined from CTD observations as the minimum depth where the density gradient is equal to or exceeds $0.01 \text{ kg}\cdot\text{m}^{-4}$.
2. The Stratification Index (SI) is calculated as:

$$\text{SI} (\text{kg}\cdot\text{m}^{-4}) = (\sigma_{t-50} - \sigma_{t-z_{\min}})/(50 - z_{\min})$$

where σ_{t-50} and $\sigma_{t-z_{\min}}$ are interpolated values of density (σ_t) at 50 m and z_{\min} , the minimum depth of reliable CTD data, which is typically around 1 or 2 m and always less than approximately 5 m.

Optical Properties

The optical properties of seawater (attenuation coefficient [K_d], euphotic depth [Z_{eu}]) are derived from *in situ* light extinction measurements using a rosette-mounted PAR meter and from Secchi disk, according to the following procedures:

1. The downward vertical attenuation coefficient for PAR ($K_{d- PAR}$) is estimated as the slope of the linear regression of $\ln(E_d(z))$ versus depth z (where $E_d(z)$ is the value of downward irradiance at depth z) in the depth interval from minimum depth to around 50 m. The minimum depth is typically around 2 m although the calculation is sometimes forced below that target when near-surface PAR measurements appear unreliable.
2. The value of the light attenuation coefficient $K_{d- Secchi}$ from Secchi disc observations is found using:

$$K_{d_secchi} \text{ (m}^{-1}\text{)} = 1.44 / Z_{sd}$$

where Z_{sd} is the depth (in m) at which the Secchi disc disappears from view (Holmes 1970).

Estimates of the euphotic depth (Z_{eu}), defined as the depth where PAR is 1% of the surface value, are obtained using the following expression:

$$Z_{eu} \text{ (m)} = 4.6 / K_d$$

Vertically Integrated Variables

Integrated chlorophyll *a* and nutrient inventories are calculated over various depth intervals (e.g., 0–100 m for chlorophyll *a*, and 0–50 m and 50–150 m for nutrients) using trapezoidal numerical integration. When the maximum depth at a given station is shallower than the lower depth limits noted above, the inventories are calculated by setting the lower integration limit to the maximum depth at that station (e.g., 95 m for P5). Data at the surface (0 m) is taken as the closest-near-surface sampled value. Data at the lower depth is taken as:

1. the interpolated value when sampling is below the lower integration limit; or
2. the closest-deep-water sampled value when sampling is shallower than the lower integration limit.

Phytoplankton Taxonomic Groups

Phytoplankton abundance and taxonomic composition at the high-frequency sampling stations are estimated from pooled aliquots of water collected in the upper 100 m using the Utermöhl technique (Utermöhl 1931).

SATELLITE REMOTE SENSING OF OCEAN COLOUR

In previous reports (e.g., Johnson et al. 2020 and Casault et al. 2020), near-surface chlorophyll *a* estimates from ocean colour data collected by different sensors (i.e., Sea-viewing Wide Field-of-view Sensor [SeaWiFS], the Moderate Resolution Imaging Spectroradiometer [MODIS] “Aqua” sensor, and the Visible Infrared Imaging Radiometer Suite [VIIRS]) were merged for the purpose of constructing semi-monthly, composite time series for different statistical sub-regions. However, our previous analyses revealed possible sensor bias, particularly with the introduction of the VIIRS dataset. In order to eliminate any potential bias,

the present report uses exclusively chlorophyll *a* estimates collected from the MODIS sensor² for which the time series extend from July 2002 to present for the selected sub-regions of the Maritimes Region (Cabot Strait [CS], Eastern Scotian Shelf [ESS], Central Scotian Shelf [CSS], Western Scotian Shelf [WSS], Lurcher Shoal [LS], Georges Bank [GB]; Figure 4). The OC3M band-ratio algorithm is used to derive chlorophyll *a* concentration from remote sensing reflectance as described in O'Reilly et al. (1998) with coefficients of the algorithm accessible on [NASA's OceanColor Web chlorophyll-a](#) website (accessed on July 30, 2020). Note that the OC3M algorithm was modified to account for bias at low chlorophyll *a* concentration according to Hu et al. (2012). Basic statistics (mean and standard deviation) are extracted from weekly composites for the purpose of visualizing the annual cycle and the inter-annual variability of surface chlorophyll *a* for the sub-regions. Characteristics of the spring bloom are estimated from the weekly MODIS data using the shifted Gaussian function of time model (Zhai et al. 2011). Four metrics are computed to describe the spring bloom characteristics: start date (day of year), cycle duration (days), magnitude (the integral of chlorophyll *a* concentration under the Gaussian curve), and amplitude (maximum minus the background chlorophyll *a* concentration).

ANNUAL ANOMALIES SCORECARDS

Scorecards of key indices, based on normalized, seasonally-adjusted annual anomalies, represent physical, chemical, and biological observations in a compact format. Annual estimates of water column inventories of nutrients, chlorophyll *a*, and the mean abundance of key zooplankton species or groups, at both the high-frequency sampling stations and as an overall average along each of the four standard sections, are based on general linear models (R Core Team 2020) of the form:

$$Density = \alpha + \beta_{YEAR} + \delta_{MONTH} + \varepsilon \text{ for the high-frequency sampling stations, and}$$
$$Density = \alpha + \beta_{YEAR} + \delta_{STATION} + \gamma_{SEASON} + \varepsilon \text{ for the sections.}$$

Density is in units of m⁻² (or L⁻¹ for microplankton abundance), α is the intercept and ε is the error. For the high-frequency sampling stations, β and δ are categorical effects for year and month, respectively. For the sections, β , δ and γ take into account the effect of year, station and season, respectively.

This approach is also used to calculate annual seasonal estimates of zooplankton indices (i.e., zooplankton biomass and *Calanus finmarchicus* abundance) for the individual sections (spring and fall) and the ecosystem trawl surveys (winter and summer) (e.g., Figures 26-29). In this case, a reduced model including the year and station effects is fitted to the seasonal data subsets. Note that for 2019, seasonal estimates were only calculated for the spring due to the absence of a fall mission. For the ecosystem trawl surveys data, the station term corresponds to the subset of strata that have been sampled in at least ten years since 1999.

The general linear-model approach is also applied to the remote sensing data to calculate annual estimates of near-surface chlorophyll *a*. In this case, the model is fitted for each selected sub-region (i.e., CS, ESS, CSS, WSS, LS and GB) using year and decimal month (e.g., 2.375 representing week 2 of February) as categorical variables.

Density in terms of zooplankton or phytoplankton abundance is log-transformed [$\log_{10}(n+1)$] to normalize the skewed distribution of the observations, and one is added to the *Density* term to include observations for which the value equals zero. Integrated inventories of nutrients,

² Information about the MODIS sensor can be found on the [NASA's OceanColor Web MODIS](#) webpage (accessed on July 30, 2020).

chlorophyll *a*, and zooplankton biomass are not log-transformed. An estimate of the least-squares means based on Type III Sums of Squares (Lenth et al. 2020) is used as the measure of the overall year effect.

Annual anomalies are calculated as the deviation of an individual year from the mean of the annual estimates over the period 1999–2015, except for the remote sensing surface chlorophyll *a* and bloom metrics for which a reference period of 2003–2015 is used to account for missing data prior to 2003. The annual anomalies are expressed either in absolute units or as normalized quantities (i.e., by dividing by the standard deviation of the annual estimates over the same period).

A standard set of indices representing anomalies of nutrient availability, phytoplankton biomass, and the abundance of dominant copepod species and groups (*C. finmarchicus*, *Pseudocalanus* spp., total copepods, and total non-copepods) are produced in each of the AZMP regions, including the Maritimes. To visualize Northwest Atlantic shelf scale patterns of environmental variation, a zonal scorecard including observations from all of the AZMP regions is presented in DFO's Science Advisory Report (DFO 2020).

ACCESS TO DATA PRODUCTS

Data products presented in Figures 6, 8, 10, 11, 15–18, and 21–31 are published on the Government of Canada's Open government website; a link to the data is available upon request to the [corresponding author](#). Chlorophyll *a* weekly estimates presented in Figure 19 are available at the DFO Maritimes [MODIS FTP website](#) (accessed on July 30, 2020) and bloom metrics used to generate Figure 20 are available upon request to the [corresponding author](#).

BEDFORD BASIN MONITORING PROGRAM

The Compass Station (44° 41' 37" N, 63° 38' 25" W) has been occupied weekly as part of the Bedford Basin Monitoring Program since 1992 (Li 2014). Regular occupations consist of a CTD equipped with a [standard suite of sensors](#) (accessed on July 30, 2020) and a vertical net tow for zooplankton identification and enumeration using AZMP protocols. Water samples are collected in Niskin bottles for a [variety of analyses](#) (accessed on July 30, 2020) at 2, 5, 10, and 60 m depths. Only zooplankton samples from 1999–2002 and 2012–2017 have been analyzed and archived in a local database; thus, only the CTD sensor and bottle observations are reported in this summary of 2019 conditions.

For ease of interpretation, surface conditions are expressed as the mean conditions at 2, 5, and 10 m. There is a strong seasonal agreement between these depths for the physical and chemical conditions being measured and generally a minor difference in magnitude.

CONTINUOUS PLANKTON RECORDER

The Continuous Plankton Recorder (CPR) is an instrument towed by commercial ships that collects plankton at a depth of approximately 7 m on a long continuous ribbon of silk (approximately 260 µm mesh). The position on the silk corresponds to the location of the different sampling stations. CPR data are analyzed to detect differences in the surface indices of phytoplankton (colour and relative numerical abundance of large taxa) and zooplankton relative abundance for different months, years, or decades in the Northwest Atlantic. The indices are used to indicate relative changes in concentration over time (Richardson et al. 2006). The sampling methods from the first surveys in the Northwest Atlantic (1960 for the continental shelf) to the present ones have been exactly the same so that valid comparisons can be made between years and decades.

The tow routes between Reykjavik and the GoM are divided into eight regions: WSS, ESS, the south Newfoundland Shelf, the Newfoundland Shelf, and four regions in the Northwest Atlantic sub-polar gyre, divided into 5 degrees of longitude bins (Figure 5). Only CPR data collected on the SS since 1992 are reported here, since these are comparable to AZMP survey results, which date back to 1999. CPR data collected in all regions and all decades (i.e., including the four regions in the sub-polar gyre east of 45° W) are presented in annual Atlantic Zone Offshore Monitoring Program reports (e.g., Yashayaev et al. 2016). In 2018, there was CPR sampling during 11 months on the WSS and 10 months on the ESS.

Monthly abundances of 14 taxa [$\log_{10}(n+1)$ transformed] and the Phytoplankton Colour Index (PCI), a semi-quantitative measure of total phytoplankton abundance, are calculated by averaging values for all individual samples collected within either the WSS or ESS region for each month and year sampled. The examined taxa include: the PCI, diatoms and dinoflagellates (phytoplankton), four groups of *Calanus* species/stages, three representative small copepod taxa, two macrozooplankton taxa, and three acid-sensitive taxa.

Climatological seasonal cycles are obtained by averaging monthly averages for 1992–2017, and these are compared with values in the months sampled in 2018. Details are presented for three indices of phytoplankton abundance and for the *Calanus* I-IV and *C. finmarchicus* V-VI taxa. Annual abundances and their anomalies are calculated only for years during which there were 8 or more months of sampling, with no gaps of 3 or more consecutive months, conditions that were met in both regions in 2018.

OBSERVATIONS

MIXING AND OPTICAL PROPERTIES

At HL2, the ML is deepest and SI lowest during the winter months when surface heating is weak and wind-driven mixing is strong (Figure 6). The ML shoals in the spring to minimum depth values from June to August and deepens in the last four months of the year. Similarly, SI increases in the spring to maximum values in August and September and then declines during the fall months. Since SI is calculated using a reference depth of 50 m, low values of the SI typically concur with ML depths deeper than 50 m. Conversely, shallow ML depths (<50 m) correspond to higher SI values that are determined by the strength of the pycnocline below the ML.

In 2019, ML at HL2 was significantly shallower than normal in winter (about 20 m shallower except in mid-February), then near normal in spring, and again shallower than normal in summer (Figure 6). The deepest winter ML, and the corresponding lowest winter SI, occurred in mid-February in response to daily wind gusts of around 80 km·h⁻¹ having occurred in the days prior to the sampling date (Figure 7). The passage of hurricane Dorian on September 7, 2019, was accompanied by daily maximum wind gusts in excess of 100 km·h⁻¹ as recorded at Halifax airport (Figure 7). However, its effect on the mixing at HL2 could not be measured due to the absence of sampling in late summer. Deeper-than-normal ML and associated lower-than-normal SI were observed in late fall, which coincided with strong wind events observed in November/December (Figure 7).

At P5, the ML is typically deeper and more variable, and stratification weaker, than at HL2 due to strong tidal mixing. The SI normally remains low (below 0.01 kg·m⁻⁴) for most of the year and ML depths vary from nearly full depth (90 m) in winter to approximately 40 m in summer (Figure 6).

In 2019, ML and SI at P5 were near normal in winter and spring, and ML was shallower and SI higher than normal in summer (Figure 6). The higher-than-normal value of SI in May is likely

associated with the spring flooding of the St. John river into the coastal environment resulting in a freshwater layer at the surface. Deeper-than-normal ML were observed in late fall while the SI remained near normal values. The trajectory of hurricane Dorian was south of P5 and the resulting winds recorded at Grand Manan were not considerably higher than normal (Figure 7). Therefore, the effect of the hurricane on the mixing at P5 appeared to have dissipated at the time of sampling, which occurred eight days after the passage of the hurricane.

Euphotic depths are generally deepest during the winter months and after the decline of the spring phytoplankton bloom and shallowest during the period of the bloom when light attenuation in the water column is maximal (Figure 8). In 2019, Z_{eu} depths based on PAR measurements at HL2 remained near normal values throughout most of the year except for shallower euphotic depths observed during the summer (Figure 8). The unusual Secchi-based euphotic depth recorded on April 15, 2019 was due to a shallow Secchi depth measurement taken around 9:00 AM local time under rainy conditions.

At P5, Z_{eu} depths are relatively constant year-round since the primary attenuator is non-living suspended matter due to tidal action and continental freshwater input (Figure 8). In 2019, the PAR-based and the Secchi-based euphotic depths were near normal throughout the year at P5, with the exception of shallower-than-normal values in September and October where departure from the climatology was highest (Figure 8).

NUTRIENTS

The primary dissolved inorganic nutrients (nitrate, silicate, and phosphate) measured by the AZMP strongly co-vary in space and time (Petrie et al. 1999). For this reason and because the availability of nitrogen is most often associated with phytoplankton growth limitation in coastal waters of the Maritimes Region (DFO 2000), this report focuses mainly on variability patterns for nitrate, with information on silicate and phosphate concentrations presented mainly to help interpreting phytoplankton taxonomic group succession at HL2 and P5.

High-frequency Sampling Stations

At HL2, the highest surface nitrate concentrations are observed in the winter when the water column is well mixed and primary production is low (Figure 9). Surface nitrate declines with the onset of the spring phytoplankton bloom, and the lowest surface nitrate concentrations are observed in the late spring through early fall. Deep-water nitrate concentrations are lowest in the late fall and early winter, and they increase from February to August, perhaps reflecting sinking and decomposition of the spring phytoplankton bloom (Petrie and Yeats 2000).

Nitrate concentrations in the upper 50 m were higher than normal at HL2 in 2019 (Figure 10). The surface nitrate was quickly depleted with the onset of the phytoplankton spring bloom that occurred around mid-March. Surface nitrate depletion lasted until the end of November, about two weeks later than normal (Figures 9 and 10), although, no measurements were taken in August and September to confirm the trend. In general, surface nutrients remained below the climatology values in summer and fall. Surface nitrate depletion during the summer and fall months also penetrated deeper than normal into the water column as evidenced in the deep-nutrient inventory (Figure 9). Deep nitrate concentrations were near- or below-normal levels with the exception of transient pulses of higher nitrate concentrations in early February and late March (Figure 9 and 10). Deep nitrate concentrations were lower than normal in the summer months perhaps indicative of lower-than-normal contribution of external sources (e.g., water intrusion onto the shelf). A mixing event that took place in November appeared to have contributed to an upward flux of nitrate at the surface, but diluted the water column resulting in below-normal bottom concentrations (Figures 9 and 10). Overall, the surface and deep nitrate

annual inventories at HL2 were slightly below average in 2019 for a fourth consecutive year (Figure 11). In parallel with the nitrate conditions, the surface and deep inventories of silicate and phosphate annual were also below or slightly below normal at HL2 in 2019 (Figure 11).

The nitrate dynamics at P5 differ considerably from those at HL2 because of nutrient input from the effluent of the nearby St. John River, combined with the strong tidal mixing which contributes to a lower nitrate replenishment of the deep water while maintaining a higher overall surface inventory. The highest nitrate concentrations are observed in the winter and late fall, when the water column is well mixed from surface to bottom and phytoplankton growth is minimal due to light limitation (Figure 9). Nitrate concentrations start to decline in the upper water column when the spring phytoplankton bloom starts in April or May, and the lowest surface nitrate concentrations are typically observed from June to August.

At P5, nitrate concentrations in 2019 were lower than normal throughout the entire water column during winter, early spring, summer, and fall, except for small pulses in May and July (Figure 9). Consequently, the surface and deep nitrate inventories were both lower than normal during these periods (Figure 10). Strong phytoplankton activity that peaked in September contributed in prolonging the depletion of surface nitrate beyond its normal duration. Overall, the surface and deep nitrate annual inventories at P5 were below average in 2019 for a seventh consecutive year (Figure 11). In parallel with the nitrate conditions, the surface and deep annual inventories of silicate and phosphate were also below normal at P5 in 2019 (Figure 11).

Broad-scale Surveys

There was no seasonal survey in the fall of 2019 and, therefore, the analysis of the broad-scale nutrients on the core sections is limited to the spring observations. The highest nitrate concentrations on the sections are typically observed in the deep waters of the Scotian slope, CSL, and Emerald Basin (i.e., the deep HL3 station on the shelf portion of the Halifax section) as was the case in spring 2019 (Figure 12). Surface nitrate concentrations observed on the sections in spring are dependent upon the timing of the sampling relative to the timing of the spring phytoplankton bloom. Low, near-surface nitrate concentrations were observed at all stations of all sections in spring 2019 (Figure 12), consistent with sampling timing during, or shortly after, the peak of the phytoplankton bloom at CSL and across the SS. Anomalies of near-surface nitrate concentrations were negative at nearly all core stations, with the exception of LL3, LL5, and LL8-9, perhaps indicative of spatial patchiness in the bloom conditions. Positive anomalies of nitrate concentrations were particularly observed in the mid- and bottom depths on CSL, below the surface at the offshore stations of LL, and in the deep water at the offshore stations of BBL (Figure 12). Consequently, the 0–50 m annual nitrate inventory was below average on all sections with the exception of LL where it was slightly above normal, and the 50–150 m nitrate inventory was also below average on all sections, with the exception of CSL, where it was slightly above average (Figure 11). The higher-than-normal nitrate concentrations observed at mid-depth on CSL were associated with a record-high, warm-water layer in the 100–300 m range that extended across the whole section as reported by Hebert et al. (in preparation). Similar to nitrate, the surface and deep annual inventories of silicate and phosphate were below or slightly below normal on all sections in 2019, with the exception of CSL's deep inventory (Figure 11).

Anomalies of bottom nitrate concentration for the 2019 summer ecosystem trawl survey showed high variability between positive and negative values. Positive anomalies were observed on several relatively shallow banks on the SS (e.g., Misaine Bank, Middle Bank, Emerald Bank, and LaHave Bank), in the upper Bay of Fundy (BoF), in the deeper waters of Emerald Basin, the Laurentian Channel, the Northeast Channel, and in the slope water off central and western SS

(Figure 13). Negative anomalies were observed in inshore and offshore bottom waters of the Eastern SS, shallow portions of the SS, and on Browns Bank and in the eastern GoM.

The lowest oxygen saturation levels are typically observed in deep basins and deep slope waters where nutrient concentrations are highest. In July 2019, bottom oxygen-saturation values near or below 60% were observed mainly in Emerald Basin, LaHave Basin, the Laurentian Channel, the slope water off central and western SS, and the Northeast Channel (Figure 14).

PHYTOPLANKTON

Although phytoplankton temporal and spatial variability is high in coastal and shelf waters, a recurrent annual pattern, including a pronounced diatom-dominated spring phytoplankton bloom and smaller secondary summer-fall blooms, is observed across the SS. A bloom develops as phytoplankton growth outpaces losses such as grazing and sinking (Behrenfeld and Boss 2014). Spring bloom initiation is thought to be regulated by the light environment of phytoplankton as well as temperature, starting when the water column stabilizes in late winter/early spring (Sverdrup 1953). Bloom magnitude is thought to be regulated largely by nutrient supply, and bloom duration is regulated by nutrient supply and, secondarily, by loss processes such as aggregation-sinking, grazing by zooplankton (Johnson et al. 2012), and lysis (Mojica et al. 2016).

High-frequency Sampling Stations

In 2019, the spring phytoplankton bloom at HL2 was characterized by a rapid biomass build-up, a higher-than-normal intensity, and an equally rapid biomass decline (Figure 15). The initiation of the bloom was slightly delayed and its duration was also shorter than normal. Higher-than-normal chlorophyll *a* concentrations were measured in the 0–50 m layer during the bloom, resulting in a peak value of the 0–100 m integrated chlorophyll *a* more than 1.5 times the climatological value (Figure 15). The spring bloom was largely dominated by diatoms, accounting for over 95% of the total phytoplankton abundance (Figure 16). Chlorophyll *a* levels remained near normal throughout the summer months with a well-defined sub-surface chlorophyll maximum (Figure 15) dominated by flagellates (Figure 16). The summer sub-surface chlorophyll *a* concentrations were higher than normal (Figure 15) and likely responsible for the shallower euphotic depths observed during the summer (Figure 8). Fall bloom conditions were observed in October and November in response to an upward flux of nitrate, as mentioned earlier. However, Figure 15 depicts a fall bloom that appears exaggerated due to interpolation artifacts resulting from the absence of sampling between mid-August and mid-October. The phytoplankton community in the fall was also dominated by flagellates (Figure 16). Overall at HL2, the annual anomaly of the 0–100 m chlorophyll *a* inventory was near normal in 2019 with no clear sign of temporal trend over the recent years (Figure 17). The abundance of diatoms and dinoflagellates remained lower than average while the abundance of flagellates and ciliates was higher than average in 2019, continuing the trend of the last 5 to 7 years (Figure 17).

At P5, the spring phytoplankton bloom was later and shorter than normal, with an amplitude near the climatological value despite higher than normal chlorophyll *a* concentrations measured in the 0–15 m layer (Figure 15). A second bloom occurred in September which appears to be later than normal and perhaps emphasized by the low temporal resolution of monthly sampling. The second bloom was also shorter in duration with an intensity slightly above normal (Figure 15). The higher-than-normal chlorophyll *a* concentrations in the surface layer measured in September were associated with the shallower-than-normal euphotic depth measured at that time (Figure 8). For both the June and September blooms, the phytoplankton community was completely dominated by diatoms (Figure 16). Overall at P5, the chlorophyll *a* inventory was below normal in 2019, with no clear sign of a temporal trend over the last few years (Figure 17).

The abundance of diatoms remained lower than average while the abundance of dinoflagellates and ciliates was higher than average in 2019, continuing the trend of the last 9 to 11 years (Figure 17). Flagellates do not exhibit any trends but rather strong inter-annual variability (Figure 17).

Broad-scale Surveys and Satellite Remote Sensing

The 2019 annual integrated chlorophyll *a* inventory indicated slightly higher-than- or near-normal chlorophyll *a* levels on CSL, HL and BBL, and slightly lower-than-normal levels on LL (Figure 18). On the other hand, near-surface chlorophyll *a* concentrations measured from remote sensing indicated higher-than-normal values on CS and the SS (ESS, CSS, and WSS) sub-regions in 2019 (Figure 18). Since 2016, there is a clear contradictory pattern between the *in situ* integrated chlorophyll *a* inventory, which has shown predominantly negative anomalies across the region, and the remote sensing surface chlorophyll *a*, which has shown predominantly positive anomalies across the region (Figure 18). Such contradictory pattern is also noticeable in previous years (e.g., 2006, 2010 and 2013). These apparent inconsistencies could be attributed in part to the inherent differences between the two indices such as the vertical extent of the signal they capture (i.e., surface vs. water column integrated), the temporal resolution of the observations (weekly vs. semi-annual), and the spatial extent they represent (averaging boxes vs. sections).

The weekly surface chlorophyll *a* estimates indicated that the timing of the peak amplitude of the spring bloom occurred within a narrow window of time of about one week across the SS as shown on the ESS, CSS, and WSS plots (Figure 19a and 19b). Overall, the spring bloom initiation was slightly earlier than normal on the eastern sub-regions (CS and ESS), and near-normal on the other sub-regions (Figure 20), following a trend of mostly earlier blooms over the last 4 years. Bloom duration was longer than normal on CS and near normal on the SS sub-regions, while bloom amplitude was slightly below normal on CS and near normal on the SS sub-regions (Figure 20). Longer duration combined with near- or slightly-higher-than-normal amplitude resulted in mostly higher-than-normal bloom magnitude for CS and the SS sub-regions (Figure 20). Fall bloom conditions were particularly noticeable for CS and ESS in 2019 (Figure 19a), in agreement with the observations at HL2, which showed a relatively large fall bloom and unusual strong depletion of the surface nitrate.

For the westernmost areas of the Maritimes region, the annual surface chlorophyll *a* concentration was slightly lower than normal on GB in 2019 (Figure 18) despite a spring bloom amplitude nearly twice the climatological value, the highest in the last 3 years (Figure 19b). The low annual variability in the surface chlorophyll *a* in the tidally mixed LS sub-region is such that bloom conditions are hardly discernible (Figure 19b) and therefore, the resulting bloom metrics should be interpreted with caution for that sub-region.

ZOOPLANKTON

High-frequency Sampling Stations

Zooplankton biomass is presented here in terms of the total wet biomass for zooplankton larger than 0.202 mm and the dry biomass for zooplankton in the size range of 0.202 mm to 10 mm. Consequently, the dry biomass estimates are a close representation of the mesozooplankton size class while the wet biomass estimates can represent both mesozooplankton and macrozooplankton, including gelatinous plankton. However, as Figure 21 suggests, there is strong similarity in the annual variability pattern of dry and wet biomass at both the HL2 and P5 stations.

At HL2, zooplankton biomass and total abundance are typically lowest in January and February, and increase to maximum values in April, similar to the spring phytoplankton bloom peak timing, before declining to low levels again in the fall (Figure 21 and 22). In 2019, there was considerable variability in the wet and dry zooplankton biomass, and in total zooplankton abundance. Biomass was near or below normal in winter and spring, back to normal in summer, and mostly above normal in fall (Figure 21). On the other hand, total zooplankton abundance was near normal in winter and early spring, below normal in late spring, higher than normal in summer, and back to normal in fall (Figure 22). Overall, the zooplankton biomass was near normal at HL2 in 2019 (Figure 23).

At P5, zooplankton biomass and total abundance are typically lowest in January–May and increase to maximum values in July–October, lagging the increase in phytoplankton by about a month, before declining to low levels again in the late fall (Figure 21 and 22). In 2019, zooplankton biomass was near normal throughout most of the year, except lower than normal in early summer and higher than normal in August and December (Figure 21). This resulted in an annual mean mesozooplankton biomass that was near normal in 2019 (Figure 23). Similarly, total zooplankton abundance in 2019 was near normal throughout most of the year with near- or below-normal levels in spring and higher-than-normal levels in early fall (Figure 22).

The zooplankton community at HL2 in 2019 was dominated by copepods, representing roughly 95% of the total zooplankton abundance throughout most of the year (Figure 22). Overall at HL2 in 2019, copepod abundance was slightly above normal while that of non-copepods was near normal (Figure 23). Similarly, copepods at P5 represented on average about 85% of the annual total zooplankton abundance in 2019 (Figure 22). Overall at P5 in 2019, the annual mean abundance of copepods was higher than normal and that of non-copepods was near normal (Figure 23).

At HL2, the timing of *C. finmarchicus* production was normal in 2019 although the abundance was near or below normal from winter to around mid-June (Figure 24). The lower-than-normal abundance in mid-June was associated with low levels of early stages CI and CII. A second generation developed in August although it is not possible to infer how long it was sustained due to the absence of sampling between mid-August and mid-October. The abundance of *C. finmarchicus* was normal at the end of 2019, with a higher-than-normal relative abundance of stage CV (Figure 24). Overall at HL2, the abundance of *C. finmarchicus* was near normal in 2019 (Figure 23). At P5, the timing of development of the early *C. finmarchicus* stages closely followed the climatological pattern (Figure 24). Periods when the overall *C. finmarchicus* abundance was higher than normal coincided with periods dominated by late copepodite stage CV in August and December, and when the abundance of adult CVI was higher than normal in May (Figure 24). The abundance of *C. finmarchicus* was above normal at the end of 2019, with stage CV representing about 95% of the *C. finmarchicus* population (Figure 24). Overall at P5, the abundance of *C. finmarchicus* was above normal in 2019 (Figure 23).

At HL2, higher-than-normal abundance of copepods was recorded in mid-summer (Figure 25a) which coincided with a mesozooplankton biomass level more than twice the normal level recorded for the mid-July sample (Figure 21). This peak in biomass was due in part to higher abundances of *C. finmarchicus* and *C. hyperboreus* (respectively about two to four times the July mean abundance) and, to a certain degree, higher abundances of *Pseudocalanus* spp., *Oithona atlantica*, and *Centropages* spp. (approximately four to five times the July mean abundance). Two of the dominant small copepods at HL2, *Oithona similis* and *Pseudocalanus* spp., were slightly more abundant than normal in 2019 (Figure 25a). Among the sub-dominant copepods, the abundances of *Metridia lucens*, *Centropages* spp., *Oithona atlantica*, and *Temora longicornis* were higher or slightly higher than normal in 2019 and continued trends of the last 6 years (or longer for *O. atlantica*, especially). At P5, the abundance of the dominant

Pseudocalanus spp. was slightly below normal in 2019 (Figure 23). The abundances of the small dominant copepod *O. similis* and the sub-dominant *Centropages* spp., *Paracalanus* spp., and *Eurytemora* were either near or higher than normal in 2019 and continuing patterns of the last 8 to 10 years (Figure 25b).

Broad-scale Surveys

Mesozooplankton biomass during the spring 2019 survey was lower than normal on CSL, LL, and HL, and slightly above normal on BBL (Figure 26). This pattern was also observed in the annual biomass anomalies estimated with the statistical model (Figure 23), which could be indicative of the model estimates being biased due to the absence of fall data. The slightly positive biomass anomaly observed in spring on BBL appeared to be driven by the high biomass value recorded at station BBL5 (Figure 26). Mesozooplankton dry biomass during the 2019 winter ecosystem survey indicated a strong positive anomaly for GB (Figure 27). Out of the 7 samples collected within the GB strata, four of them reported biomass in excess of $8 \text{ g} \cdot \text{m}^{-2}$, which is more than six times the annual mean, thus contributing to the higher-than-normal biomass anomaly value for 2019. High biomass values were also recorded in the eastern GoM near the entrance of the BoF. On the other hand, mesozooplankton dry biomass during the SS summer ecosystem survey was near normal (Figure 27). Although relatively high biomass values were recorded during that survey, some of those samples were located outside the SS strata used to calculate the annual biomass estimates.

The abundance of *C. finmarchicus* during the spring 2019 survey was lower than normal on CSL, LL, and HL, and near normal on BBL (Figure 28). This pattern was also observed in the anomalies of the annual *C. finmarchicus* abundance (Figure 23), which again, could be indicative of the model estimates being biased due to the absence of fall data. The highest abundances of *C. finmarchicus* were recorded in spring on BBL and at the slope water stations of HL, although, on average, they did not translate into higher-than-normal anomalies (Figure 28). The abundance of *C. finmarchicus* was below average during the 2019 winter ecosystem survey on GB, and near normal during the SS summer survey (Figure 29). The near-normal abundance of *C. finmarchicus* for the summer survey was influenced by an exceptionally high abundance (about 20 times the overall average value) recorded on the ESS, which could be indicative of spatial patchiness (Figure 29).

The annual abundance in 2019 for *Pseudocalanus* spp., a dominant small copepod species on the SS, was near or above normal on LL, HL, and BBL, and lower than normal on CSL, continuing the trend of the last 4 years for CSL (Figure 23). Total copepod abundance was below normal on CSL, near normal on LL and HL, and slightly above normal on BBL, in 2019 (Figure 23). For CSL, the trend in copepod abundance somewhat follows that of *C. finmarchicus* over the last 9 years (Figure 23). Non-copepod abundance was near or higher than normal on all sections in 2019, as has been the case over the last 6 to 8 years (Figure 23). The Ostracoda group continued to be much less abundant in 2019 (Figure 30). Other groups, including Gastropoda, Chaetognatha, Polychaeta, Bivalvia, and Echinodermata, shifted from near- or above-normal abundance in 2018 to below-normal levels in 2019 (Figure 30). Cirripedia and Larvacea showed the strongest positive abundance anomalies in 2019 (Figure 30).

Indicator Species

Indicator species provide insights into the response of the copepod community to changes in water mass properties. Arctic *Calanus* species (*Calanus hyperboreus* and *Calanus glacialis*) have been mainly less abundant than normal on the SS since 2012. However, mixed signals were observed in 2019, with higher-than-normal abundance recorded on LL, BBL, and at HL2, while CSL, HL, and P5 showed negative abundance anomalies (Figure 31). On the other hand,

warm offshore species (*Clausocalanus* spp., *Mecynocera clausi*, and *Pleuromamma borealis*) have been generally more abundant than normal on the SS since 2012. This pattern continued in 2019, with only CSL and BBL indicating near- or lower-than-normal abundances (Figure 31). Warm-shelf copepod species (the summer-fall copepods *Paracalanus* spp. and *Centropages typicus*) were mainly near or less abundant than normal in 2019, with the exception of HL where the abundance was well above normal (Figure 31). In most cases, this represents a shift from consistently higher-than-normal abundance in 2018 to near- or below-normal levels in 2019 (Figure 31).

DISCUSSION

In the Maritimes Region, the SS is characterized by a strong annual cycle of temperature and stratification, and spatial variability in the form of longitudinal and cross-shelf gradients. While the temperature annual cycle and its perturbations are mostly the response to meteorological forcing, spatial variability is mostly the result of interacting water inputs with the advection of cold fresh waters onto the inshore ESS from the Gulf of St. Lawrence in the northeast and the intrusion of warm and salty slope waters onto the WSS and CSS in the southwest (Hebert et al. in preparation). These temporal and spatial patterns result in different water masses having direct and indirect influence on the distribution and the dynamics of plankton and nutrients in the region.

Ocean temperatures on the SS and in the GoM have exhibited strong inter-decadal variability since the 1950s, with recent years (2010 and onward) being generally warmer than the long-term average over that period. In 2019, ocean temperatures in the upper water column were near normal in most sub-regions of the SS, following the cooling trend of the last 4–5 years. Annual sea surface temperatures were below normal in ESS and CSS, and near normal in WSS and eastern GoM. In all sub-regions, the annual sea surface temperature was the coolest since the record high values of 2012. Sea surface temperatures across the region were particularly warmer than normal during the months of August and November, and cooler than normal during the winter and spring months, and also in September, likely in response to the passage of hurricane Dorian. On the other hand, water temperatures measured in deep basins or near the bottom were mostly warmer than normal and continued the warming trend of the last 8–10 years. Stratification was higher in 2019 than 2018 but remained below the 70-year increasing trend. Similarly, the cold intermediate layer volume was higher than the previous 5 years, although still below the 30-year mean value (Hebert et al. in preparation).

In parallel with, or perhaps in response to changes in the SS physical environment of the recent years, changes have also taken place in nutrients, phytoplankton, and zooplankton community levels. Deep nutrient concentrations have been mainly lower than normal since 2013 for silicate and phosphate, and since 2016 for nitrate. Phytoplankton community changes have been characterized by mainly negative anomalies in the abundance of diatoms and other large phytoplankton since 2009. Zooplankton community changes have been characterized by mainly negative anomalies in biomass since 2010, *C. finmarchicus* abundance since 2011, and Arctic *Calanus* abundance since 2012, while abundance anomalies of warm offshore copepods and non-copepods have been mainly positive in the central and western parts of the region since 2012.

The nutrient environment on the SS is influenced directly or indirectly by water inputs from upstream, for example the Labrador Current and the outflow from the Gulf of St. Lawrence, as well as by intrusions of slope water and Gulf Stream meanders (Pepin et al. 2013). Surface nutrients display a strong seasonality associated with phytoplankton production, with higher production typically associated with surface nutrient depletion. Deep nutrients, on the other hand, provide a better representation of the nutrient pool available for new primary production.

Pepin et al. (2013) reported below-average concentrations of all deep nutrients on the SS in the years leading to 2010, with a low level of variability which was deemed uncharacteristic for the area. With the exception of CSL, deep nutrients were below normal across the region in 2019, continuing a pattern of lower-than-normal concentrations observed over the last four to six years. For CSL, the positive anomaly was associated with record-warm and nutrient-rich water (Hebert et al. in preparation). The recent shift in deep-nutrients inventory is likely linked to changes in shelf circulation as well as changes in the Gulf Stream transport. A decrease in the deep nutrient concentrations coupled with the observed increase in stratification on the SS (Hebert et al. in preparation) could imply a lower productivity and potential impacts on the structure and functioning of the food web.

In ocean regions where annual-scale environmental variability is a dominant frequency, plankton life history, behavior, and physiology provide adaptations that focus reproductive effort on favorable times of year and minimize exposure to risk at unfavorable times of year. However, unpredictable perturbations in the range of environmental seasonality and in seasonal timing can disrupt these adaptations (Greenan et al. 2008; Mackas et al. 2012). Large-scale shifts in water mass boundaries also influence local plankton community composition (e.g., Keister et al. 2011). The main recurring feature of phytoplankton dynamics on the SS and in the GoM is the spring bloom which develops under favourable conditions of increased insolation, warming temperature, and water column stratification. However, Ross et al. (2017) observed spring blooms on the SS when stratification is at its lowest, water temperature at its coldest, and surface mixed layer still much deeper than the euphotic depth, which is in apparent contradiction of the critical-depth hypothesis. Phytoplankton biomass declines after the bloom peak as grazing increases or growth becomes nutrient limited. In summer, sporadic occurrence of sub-surface chlorophyll maxima reflect regenerated production within the stratified upper water column.

The spring phytoplankton bloom initiation on the SS in 2019, as inferred from remote sensing ocean color observations, occurred in early to mid-March, which was on average near or slightly earlier compared to normal conditions. Peak bloom amplitudes were observed almost simultaneously in each sub-region of the SS, which is somewhat contrary to the general pattern of westward progression (Song et al. 2010). The spring phytoplankton bloom also occurred when sea surface temperatures were nearly 1°C below normal levels (Hebert et al. in preparation). Spring bloom initiation when the surface-water temperature is near its minimum is not unusual, at least for the CSS (Shadwick et al. 2011). The duration of the spring bloom on the SS was on average near or slightly longer than normal, which concurs with observations by Friedland et al. (2016) suggesting that early blooms typically last longer in regions where spring blooms are a recurring feature.

At the finer scale, the initiation of the spring bloom at HL2 in 2019 was slightly delayed, shorter in duration, but with an amplitude higher than normal. Zhai et al. (2011) suggest that the bloom amplitude correlates with the surface nitrate inventory at the end of the winter, which was higher than normal in 2019. A relatively intense sub-surface chlorophyll maximum was observed in July which was dominated by flagellates. Sub-surface chlorophyll maxima follow the nitracline and occur at a depth where both light and nutrient can sustain production. Sub-surface summertime chlorophyll maxima are typically dominated by small cell assemblages for which chlorophyll is a poor proxy of the phytoplankton biomass (Craig et al. 2015). The sub-surface chlorophyll maxima is often overlooked in favour of the spring or the fall bloom. However, it is an important feature of the phytoplankton dynamics through its significant contribution to the annual primary production on the SS (Ross et al. 2017). Observations at HL2 in 2019 also confirmed the continued trend toward lower abundance of diatoms and dinoflagellates, and higher abundance of ciliates and flagellates. A shift toward smaller phytoplankton assemblages could be

associated with warmer ocean conditions on the SS, as has been observed in other areas of the ocean (Doney et al. 2012).

Zooplankton biomass on the SS and in the eastern GoM is normally dominated by large, energy-rich copepods, mainly *C. finmarchicus*, which are important prey for planktivorous fish such as Herring and mackerel, North Atlantic Right Whales, and other pelagic species. The population response of *C. finmarchicus* to environmental changes is complex due to interactions among transport by ocean circulation, annual primary production cycles, and the *Calanus* life history, that focuses reproductive effort on spring bloom production of diatoms and can include a period of late-juvenile-stage dormancy in deep water during less-productive seasons. The winter abundance level of *C. finmarchicus* is an indicator of initial conditions for production, while the late-fall abundance level is an indicator of the overwintering stock for production in the following year. The smaller copepods *Pseudocalanus* spp. are less energy-rich but are also important prey for small fish due to their large abundance and wide spatial distribution.

A persistent change in the zooplankton assemblage on the SS has been evident since around 2010, marked most notably by the decline in the abundance of *C. finmarchicus*. Since *C. finmarchicus* is a biomass-dominant member of zooplankton assemblage, the decline in its abundance tracks a similar decline in the mesozooplankton biomass over that same period. On the other hand, copepod abundance has been mostly higher than normal since around 2014, as has been the abundance of non-copepods since around 2012. Higher abundances of smaller species have been observed consistently at HL2 during the last six to ten years for *Centropages* spp., *T. longicornis*, and *Oithona* spp. *Pseudocalanus* spp. abundances have been more variable with lower-than-normal abundance during 2010–2012 and 2017–2018, and higher-than-normal abundance during 2013–2015 and 2019. In the GoM, warming has been linked to a decline in the summer and fall abundance of *C. finmarchicus*, and an increase in their winter abundance since 2010 (Pershing and Stamieszkin 2020; Record et al. 2019). In contrast, *C. finmarchicus* abundance at HL2 in 2019 was lower than normal in winter and spring, and near or above normal in summer and fall, perhaps in response to cooler conditions in 2019 compared to previous years. The combined freshening and warming trends observed on the SS certainly have impacts on the zooplankton community; however, any in-depth analyses of these factors is beyond the scope of the present document.

2019 was marked by the passage of hurricane Dorian along part of the SS in early September. Neither its immediate or its broad-scale residual effect on the nutrient and plankton environment could be assessed due to sampling deficiencies at HL2 between mid-August and mid-October and the absence of sampling on the sections in the fall. Annual estimates of key nutrient and plankton abundance/biomass indices presented in this report are derived from model fits, which compensate for missing sampling events. Assessing the extent of bias in the annual estimates resulting from the absence of sampling over prolonged periods or for entire surveys is recommended, especially for metrics that display strong seasonality combined with the occurrence of significant perturbations in the environmental conditions.

Although ocean conditions in the Maritimes Region were not systematically as warm in 2019 as in previous years, recent trends in nutrient inventories and phytoplankton and zooplankton community indices have persisted. Observations in recent years provide increasing evidence of decreased deep-nutrient availability coupled with a shift in both phytoplankton and zooplankton communities away from the dominance of large phytoplankton cells and large, energy-rich copepods like *C. finmarchicus* and toward smaller phytoplankton and copepod species and particle-feeding, opportunistic non-copepod species such as Larvacea. Since “classical” type food webs dominated by diatoms and *C. finmarchicus* are associated with higher transfer efficiency of energy to higher trophic level pelagic animals than are food webs dominated by small phytoplankton cells and small zooplankton taxa, this shift may indicate a change to less

productive conditions for planktivorous fish, North Atlantic Right Whales, and pelagic-feeding seabirds in the Maritimes Region.

BEDFORD BASIN MONITORING PROGRAM

PHYSICAL CONDITIONS

Surface-water temperature conditions in 2019 were near normal (-0.25 sd) compared to the reference period 2000–2015 (Figure 32). Surface salinity, density, and stratification annual conditions were also near normal. Monthly anomalies for surface temperature in 2019 were warmer than normal for 6 of the 12 months (Figure 33). Conditions for the first half of the year (January to June) were either at or below normal with the second coolest June since 2002 (-1.71 sd). From July until December, surface temperatures were at or slightly above normal (Figure 33).

Bottom conditions are generally stable within the basin unless otherwise perturbed by periodic intrusions of shelf water (Kerrigan et al. 2017). In 2019, temperature conditions at 60 m were the 5th coolest on record (-0.91 sd) (Figure 34), a sharp departure from the positive anomaly in 2018 (+1.00 sd). Bottom salinity (-0.62 sd) and density (-0.07 sd) also returned to below-normal in 2019 after warmer, saltier and denser water occupied the basin in 2018. This is a return to negative, or near-normal, annual bottom salinity and density anomalies that extended from 2010 to 2017 (Figure 34). These cooler- and fresher-than-normal bottom conditions began in February and persisted throughout the remainder of the year, with the 3rd coolest and 2nd freshest December for the time series (-1.39 and -1.68 sd) (Figure 35 and 36).

NUTRIENTS AND PLANKTON CONDITIONS

Surface annual anomalies for all nutrients and chlorophyll were below normal (Figure 32). Nitrate was the lowest annual anomaly since 1997 (-0.58 sd), while nitrite, ammonia, and phosphate were the lowest annual anomalies of the time series (-0.97, -0.73, and -1.58 sd). Surface phosphate continues a 9-year trend (2011–2019) of negative annual anomalies (Figure 32). Particulate Organic Carbon (POC) and Particulate Organic Nitrogen (PON) (+0.63 and +0.97 sd) anomalies were positive, with the 2nd highest values of the time series (Figure 32). Surface chlorophyll *a* was slightly below-normal concentrations, as were the other indices of the phytoplankton community (Figure 32). The conditions at 60 m were somewhat dissimilar from surface values, with slightly negative nitrate and silicate anomalies (-0.26 and -0.24 sd), likely indicative of the absence of intrusion of new water into the basin throughout the year, and the highest nitrite annual anomaly on record (+3.13 sd) (Figure 34). Surface and bottom phosphate continues the trend of below-average concentrations since 2010 (Figure 32 and 34), following the broader scale trend described earlier.

CONTINUOUS PLANKTON RECORDER

PHYTOPLANKTON

Average monthly PCI values and diatom abundances (1992–2015) on the ESS and WSS show the spring bloom occurring in March–April, with low values in summer (Figure 37). In fall and winter, the PCI is low, but diatom abundance increases over the fall, remaining relatively high in winter, and dinoflagellate abundance shows no clear seasonal cycle. In 2018, PCI values during March and/or April were higher (lower) than normal on the ESS (WSS). This pattern was also seen in satellite observations of sea-surface chlorophyll *a*, reported previously (Casault et al. 2020). Monthly diatom abundances were near normal on the WSS, but unusually low (July, October) and high (January, August–September) on the ESS. Monthly dinoflagellate

abundances in 2018 were mainly close to (WSS) or higher than (ESS) normal, although low in November in both regions. Annual abundance anomalies for dinoflagellates and the PCI were near (higher than) normal on the WSS (ESS), while diatom abundances were near normal in both regions (Figure 38).

ZOOPLANKTON

CPR-derived, climatological (1992–2015) seasonal cycles for *Calanus* I-IV (mostly *C. finmarchicus*) and *C. finmarchicus* CV-VI have broad spring–summer (April–July) peaks in abundance on the WSS (Figure 39). On the ESS, *Calanus* CI-IV has a similar, lower-magnitude peak, but *C. finmarchicus* CV-VI does not. In 2018, on the WSS, monthly abundances for both taxa were generally slightly lower than normal, although both were much less (more) abundant than normal in March (December) and *Calanus* CI-IV abundance was also very low in April. On the ESS, abundances were close to or slightly below normal, although *Calanus* CI-IV abundance was relatively high in December. The annual average abundance anomalies were near normal (slightly below) for *Calanus* CI-IV for the ESS (WSS), and slightly below (below) normal for *C. finmarchicus* CV-VI for the ESS (WSS) (Figure 38). Year-round *in situ* vertical net tow sampling at HL2 has indicated low *C. finmarchicus* abundances compared with the 1999–2015 average values since 2011, but this decrease is not observed in CPR samples, since it is due to decreasing abundances of CVs at-depth in summer and/or over winter (Casault et al. 2020).

Among the zooplankton of other taxa in 2018, most were at near-normal abundance levels in both regions, although *Calanus glacialis* (both regions) and *Paral/Pseudocalanus* (WSS) abundances were lower than normal and copepod nauplii were more abundant than normal on the ESS (Figure 38).

ACID SENSITIVE ORGANISMS

In 2018, coccolithophores were more (WSS) or much more (ESS) abundant than normal, as were foraminifera on the ESS. The abundance of *Limacina* spp. was near normal on the WSS and below normal on the ESS (Figure 38).

SUMMARY

- Observations in 2019 provided evidence that changes in the plankton community observed in recent years have persisted despite the evidence of cooling surface-water temperatures, compared to the warm conditions of previous years. These changes are likely to alter the fate of production in the ecosystem, with negative impacts already observed in the feeding habitat for specialized planktivores such as North Atlantic Right Whales.
- In 2019, surface and deep inventories of silicate and phosphate were mainly lower than average on the SS following a trend started around 2014. Deep nitrate, silicate, and phosphate inventories were near or above average on CSL and associated with record warm water.
- Phytoplankton spring bloom on the SS, as observed from satellite remote sensing, was either near or slightly earlier than normal, mainly longer in duration with higher-than-normal magnitude. At HL2, the spring bloom was intense with a rapid progression and a rapid decline.
- *C. finmarchicus* abundance was mainly near or slightly lower than average on the SS while mesozooplankton biomass was below or slightly below average in the eastern part and near or slightly above average in the western part of the region. Non-copepod abundance was

mainly near or higher than average across the region, continuing a pattern that started around 2012.

- Anomalies of copepod indicator species abundance were mixed in 2019, especially for Arctic *Calanus* and warm-shelf species, which both showed shifts in anomalies (i.e., positive to negative, and vice-versa) between 2018 and 2019. Warm-water offshore species were mostly more abundant than average in 2019 and continued a trend that started in 2012.
- Surface temperature in Bedford Basin was near normal in 2019 with mainly cooler temperatures from January to June and mainly slightly warmer temperatures from July to December. Surface nitrite, ammonia, and phosphate reached their lowest levels of the time series in 2019.
- Bottom temperature and salinity in Bedford Basin were below normal in 2019 and progressively went from near- or slightly-above-normal levels in January to below-normal levels in December. Bottom nitrate reached its lowest level of the time series in 2019.
- In 2018, CPR observations indicated that annual average PCI values and dinoflagellate abundances were near normal on the WSS and above normal on the ESS, while annual average diatom abundances were near normal in both regions.
- In 2018, CPR observations indicated that annual abundances for the *Calanus* copepodite I-IV taxon (mostly *C. finmarchicus* CI-IV) were near normal (ESS) and slightly below normal (WSS), while the *C. finmarchicus* CV-VI annual average abundance was slightly below (below) normal for the ESS (WSS). On the ESS, average annual abundances for copepod nauplii, coccolithophores, and forams were higher than normal, while *Limacina* spp. abundance was lower than normal. The average annual abundance of *C. glacialis* CV-VI was lower than normal in both regions.

ACKNOWLEDGEMENTS

The authors thank the personnel at the Bedford Institute of Oceanography and St. Andrews Biological Station who contributed to sample collection, sample analysis, data analysis, data management, and data sharing. We also thank the officers and crews of the Canadian Coast Guard Ships *Alfred Needler*, *Coriolis II*, *Sigma-T*, *Teleost*, and *Viola M. Davidson* for their assistance in the collection of oceanographic data during 2019. Reviews by Gary Maillet and Stéphane Plourde improved the manuscript.

REFERENCES CITED

- Behrenfeld, M.J., and Boss, E.S. 2014. [Resurrecting the Ecological Underpinnings of Ocean Plankton Blooms](#). *Annu. Rev. Mar. Sci.* 6: 167–194.
- Casault, B., Johnson, C., Devred, E., Head, E., and Spry, J. 2020. [Optical, Chemical, and Biological Oceanographic Conditions on the Scotian Shelf and in the Eastern Gulf of Maine in 2018](#). DFO Can. Sci. Advis. Sec. Res. Doc. 2020/037. v + 66 p.
- Craig, S.E., Thomas, H., Jones, C.T., Li, W.K., Greenan, B.J., Shadwick, E.H., and Burt, W.J. 2015. [The effect of seasonality in phytoplankton community composition on CO₂ uptake on the Scotian Shelf](#). *J. Mar. Syst.* 147:52–60.
- DFO. 2000. [Chemical and Biological Oceanographic Conditions in 1998 and 1999 – Maritimes Region](#). DFO Sci. Stock Status Rep. G3-03 (2000).

-
- DFO. 2020. [Oceanographic Conditions in the Atlantic Zone in 2019](#). DFO Can. Sci. Advis. Sec. Sci. Advis. Rep. 2020/028.
- Doney, S.C., Ruckelshaus, M., Duffy, J.E., Barry, J.P., Chan, F., English, C.A., Galindo, H.M., Grebmeier, J.M., Hollowed, A.B., Knowlton, N., Polovina, J., Rabalais, N.N., Sydeman, W.J., and Talley, L.D. 2012. [Climate change impacts on marine ecosystems](#). *Annu. Rev. Mar. Sci.* 4:11–37.
- Friedland, K.D., Mouw, C.B., Asch, R.G., Ferreira, A.S.A, Henson, S., Hyde, K.J.W., Morse, R.E., Thomas, A.C., and Brady, D.C. 2018. [Phenology and time series trends of the dominant seasonal phytoplankton bloom across global scales](#). *Glob. Ecology Biogeography*. 27(5):551–569.
- Greenan B.J.W., Petrie B.D., Harrison W.G., Strain P.M. 2008. [The onset and evolution of a spring bloom on the Scotian Shelf](#). *Limnol. Oceanogr.* 53.
- Harrison, G., Colbourne, E., Gilbert, D., and Petrie, B. 2005. [Oceanographic Observations and Data Products Derived from Large-scale Fisheries Resource Assessment and Environmental Surveys in the Atlantic Zone](#). *AZMP/PMZA Bull.* 4: 17–23.
- Holmes, R.W. 1970. [The Secchi Disk in Turbid Coastal Waters](#). *Limnol. Oceanogr.* 15(5): 688–694.
- Hu, C., Lee, Z., and Franz, B. 2012. [Chlorophyll a algorithms for oligotrophic oceans: A novel approach based on three-band reflectance difference](#). *Journal of Geophysical Research*, 117(C1).
- Johnson, C., Harrison, G., Head, E., Casault, B., Spry, J., Porter, C., and Yashayaeva, I. 2012. [Optical, Chemical, and Biological Oceanographic Conditions in the Maritimes Region in 2011](#). DFO Can. Sci. Advis. Sec. Res. Doc. 2012/071.
- Johnson, C., Devred, E., Casault, B., Head, E., Cogswell, A., and Spry, J. 2020. [Optical, Chemical, and Biological Oceanographic Conditions on the Scotian Shelf and in the Eastern Gulf of Maine During 2017](#). DFO Can. Sci. Advis. Sec. Res. Doc. 2020/002. v + 66 p.
- Keister, J.E., Di Lorenzo, E., Morgan, C.A., Combes, V., and Peterson, W.T. 2011. [Zooplankton species composition is linked to ocean transport in the Northern California Current](#). *Global Change Biol.* 17: 2498–2511.
- Kerrigan, E.A., Kienast, M., Thomas, H., and Wallace, D.W.R. 2017. [Using oxygen isotopes to establish freshwater sources in Bedford Basin, Nova Scotia, a Northwestern Atlantic fjord](#). *Estuar. Coast. Shelf. Sci.* 199, pp. 96–104.
- Lenth, R., Singmann, H., Love, J., Buerkner, P., and Herve, M. 2020. [emmeans: Estimated Marginal Means, aka Least-Squares Means](#). R package version 1.3.4.
- Li, W.K.W. 2014. [The state of phytoplankton and bacterioplankton at the Compass Buoy Station: Bedford Basin Monitoring Program 1992–2013](#). *Can. Tech. Rep. Hydrogr. Ocean Sci.* 304.
- Mackas, D.L., Greve, W., Edwards, M., Chiba, S., Tadokoro, K., Eloire, D., Mazzocchi, M.G., Batten, S., Richardson, A.J., Johnson, C., Head, E., Conversi, A., and Pelosi, T. 2012. [Changing zooplankton seasonality in a changing ocean: Comparing time series of zooplankton phenology](#). *Progr. Oceanogr.* 97-100: 31–62.
- Mitchell, M., Harrison, G., Pauley, K., Gagné, A., Maillet, G., and Strain, P. 2002. [Atlantic zonal monitoring program sampling protocol](#). *Can. Tech. Rep. Hydrogr. Ocean Sci.* 223.
-

-
- Mojica, K.D.A., Huisman, J., Wilhelm, S.W., and C.P.D. Brussaard. 2016. [Latitudinal variation in virus-induced mortality of phytoplankton across the North Atlantic Ocean](#). ISME J 10, 500–513.
- O'Reilly, J.E., Maritorena, S., Mitchell, B. G., Siegel, D. A., Carder, K. L., Garver, S. A., Kahru, M., and McClain, C. R. 1998. [Ocean color chlorophyll algorithms for SeaWiFS](#). J. Geophys. Res. 103, 24937–24953.
- Pepin, P., Maillet, G.L., Lavoie, D., and Johnson, C. 2013. Temporal trends in nutrient concentrations in the Northwest Atlantic basin. Ch. 10 (p. 127–150) In: [Aspects of climate change in the Northwest Atlantic off Canada](#) [Loder, J.W., G. Han, P.S. Galbraith, J. Chassé and A. van der Baaren (Eds.)]. Can. Tech. Rep. Fish. Aquat. Sci. 3045: x + 190 p.
- Pershing, A.J. and Stamieszkin, K. 2020. [The North Atlantic Ecosystem, from Plankton to Whales](#). Annu. Rev. Mar. Sci. 12(1):339–359.
- Petrie, B. 2007. [Does the north Atlantic oscillation affect hydrographic properties on the Canadian Atlantic continental shelf?](#) Atmos. Ocean 45(3): 141–151.
- Petrie, B., and Dean-Moore, J. 1996. Temporal and Spatial Scales of Temperature and Salinity on the Scotian Shelf. Can. Tech. Rep. Hydrogr. Ocean Sci. 177.
- Petrie, B., and Yeats, P. 2000. [Annual and interannual variability of nutrients and their estimated fluxes in the Scotian Shelf - Gulf of Maine region](#). Can. J. Fish. Aquat. Sci. 57: 2536–2546.
- Petrie, B., Drinkwater, K., Gregory, D., Pettipas, R., and Sandström, A. 1996. [Temperature and Salinity Atlas for the Scotian Shelf and the Gulf of Maine](#). Can. Data. Rep. Hydrog. Ocean Sci. 171.
- Petrie, B., Yeats, P., and Strain, P. 1999. [Nitrate, Silicate and Phosphate Atlas for the Scotian Shelf and the Gulf of Maine](#). Can. Tech. Rep. Hydrogr. Ocean Sci. 203.
- R Core Team. 2020. [R: A language and environment for statistical computing](#). R Foundation for Statistical Computing, Vienna, Austria.
- Record, N.R., et al. 2019. [Rapid Climate-Driven Circulation Changes Threaten Conservation of Endangered North Atlantic Right Whales](#). Oceanography. 32(2) : 162 :169.
- Richardson, A.J., Walne, A.W., John, A.W.G., Jonas, T.D., Lindley, J.A., Sims, D.W., Stevens, D., and Witt, M. 2006. [Using continuous plankton recorder data](#). Progr. Oceanogr. 68: 27–74.
- Ross, T., Craig, S.E., Comeau, A., Davis, R., Dever, M., and Beck, M. 2017. [Blooms and subsurface phytoplankton layers on the Scotian Shelf: Insights from profiling gliders](#). J Marine Syst. 172, 118–127.
- Shadwick, E.H., Thomas, H., Azetsu-Scott, K., Greenan, B.J.W., Head, E., and Horne, E. 2011. [Seasonal variability of dissolved inorganic carbon and surface water pCO₂ in the Scotian Shelf region of the Northwestern Atlantic](#). Mar. Chem. 124, 23–37.
- Song, H., Ji, R., Stock, C., and Wang, Z. 2010. [Phenology of phytoplankton blooms in the Nova Scotian Shelf–Gulf of Maine region: remote sensing and modeling analysis](#). J. Plankton Res., 32(11), 1485–1499.
- Sverdrup, H.U. 1953. [On Conditions for the Vernal Blooming of Phytoplankton](#). J. Cons. Perm. Int. Explor. Mer. 18: 287–295.

-
- Therriault, J.-C., Petrie, B., Pepin, P., Gagnon, J., Gregory, D., Helbig, J., Herman, A., Lefaiivre, D., Mitchell, M., Pelchat, B., Runge, J., and Sameoto, D. 1998. [Proposal for a Northwest Atlantic Zonal Monitoring Program](#). Can. Tech. Rep. Hydrogr. Ocean Sci. 194.
- Utermöhl, von H. 1931. [Neue Wege in der quantitativen Erfassung des Plankton.\(Mit besonderer Berücksichtigung des Ultraplanktons.\)](#). Verh. Int. Verein. Theor. Angew. Limnol., 5, 567–595.
- Yashayaev, I., Head, E.J.H., Azetsu-Scott, K., Devred, E., Ringuette, M, Wang, Z., and Punshon, S. 2016. [Environmental Conditions in the Labrador Sea during 2015](#). NAFO SCR Doc. 16/018. Serial N6559. 34 p.
- Zhai, L., Platt, T., Tang, C., Sathyendranath, S., and Hernández Walls, R. 2011. [Phytoplankton Phenology on the Scotian Shelf](#). ICES J. Mar. Sci. 68:781–791.

TABLES

Table 1. Atlantic Zone Monitoring Program sampling missions in the Maritimes region in 2019.

Group	Location	Mission ID	Dates	# Hydro Stations	# Net Stations
Ecosystem Trawl Survey	Western Scotian Shelf	TEL2019-102	Feb 12, 18 Mar 07–22	73	17
Ecosystem Trawl Survey	Georges Bank	TEL2019-002	Feb 19–24, 28 Mar 01–07	47	9
Ecosystem Trawl Survey	Scotian Shelf	NED2019-030	Jul 03–Aug 10	84	40
Seasonal Sections	Scotian Shelf	COR2019-001	Apr 07–25	73	73
High-frequency Stations	Halifax-2	BCD2019-666	Jan 01–Dec 31	18(10) ¹	18(10) ¹
	Prince-5	BCD2019-669	Jan 01–Dec 31	12	12
<i>Total:</i>				299	161

¹Total station occupations, including occupations during trawl surveys and seasonal sections (dedicated occupations with mission ID as listed at left are in parentheses).

FIGURES

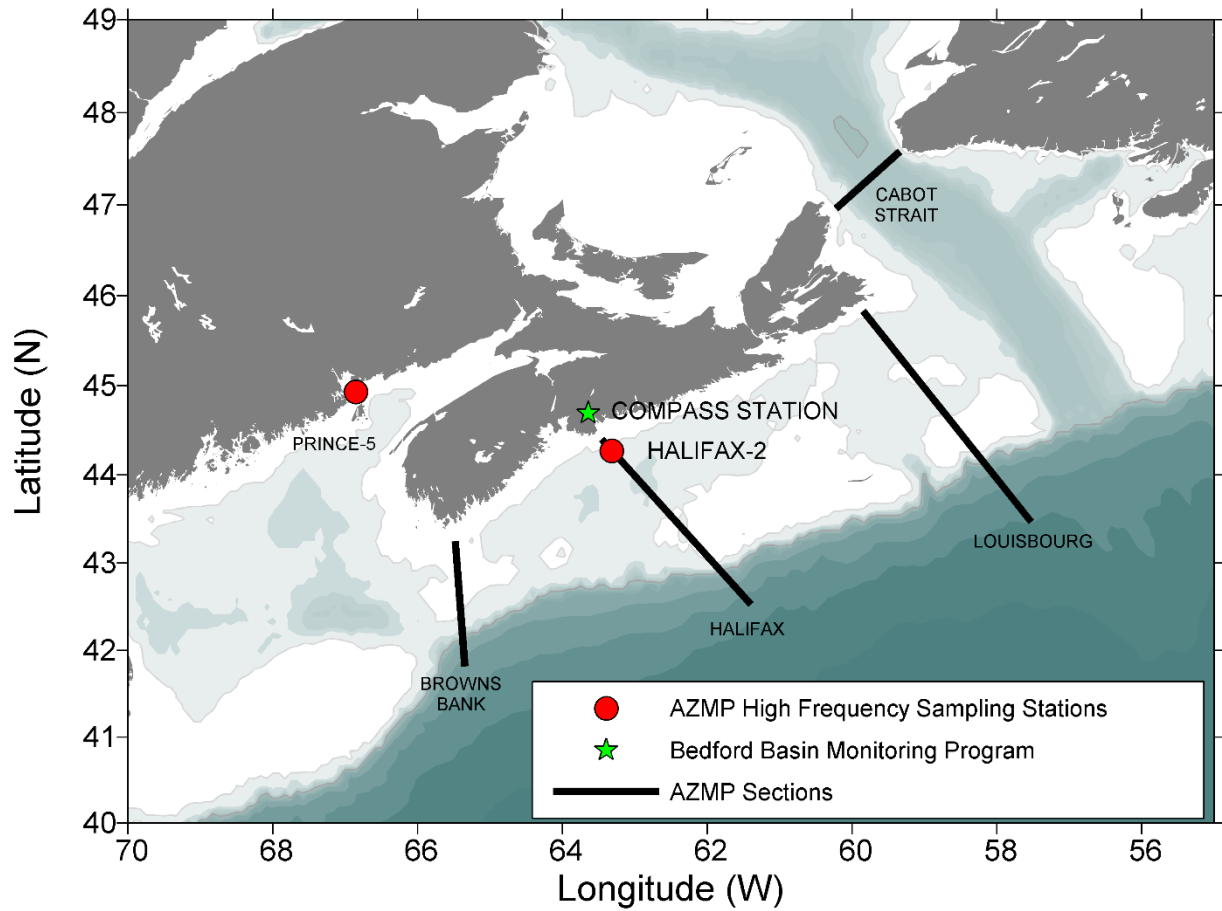


Figure 1. Map of primary sections (Cabot Strait [CSL]; Louisbourg [LL]; Halifax [HL]; Browns Bank [BBL]) and high-frequency sampling stations (Halifax-2 [HL2]; Prince-5 [P5]) sampled in the DFO Maritimes Region. The Compass Station is sampled as part of the Bedford Basin Monitoring Program.

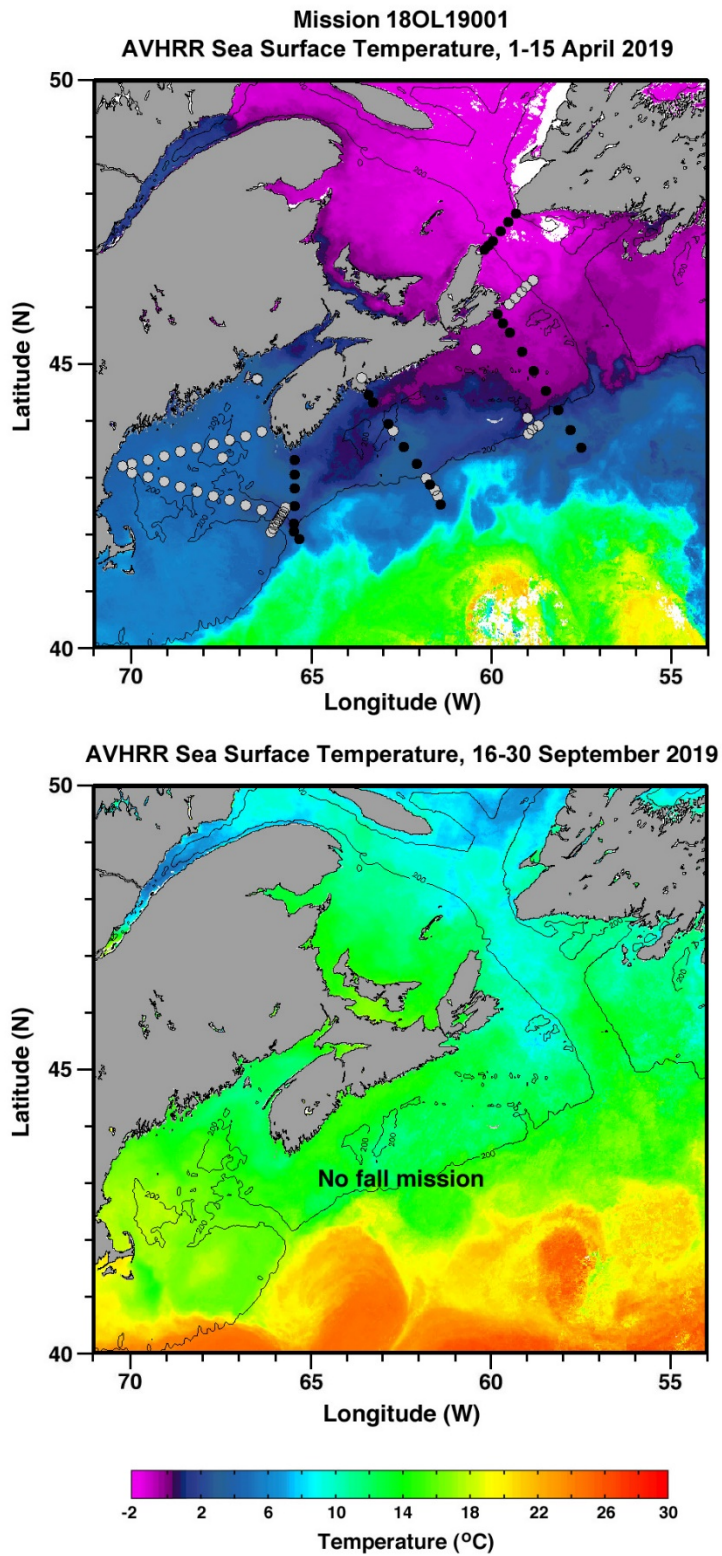


Figure 2. Stations sampled during the 2019 spring survey. Station locations are superimposed on sea-surface-temperature composite images for dates close to the mission dates. Black markers indicate core stations, and gray markers indicate stations sampled for ancillary programs.

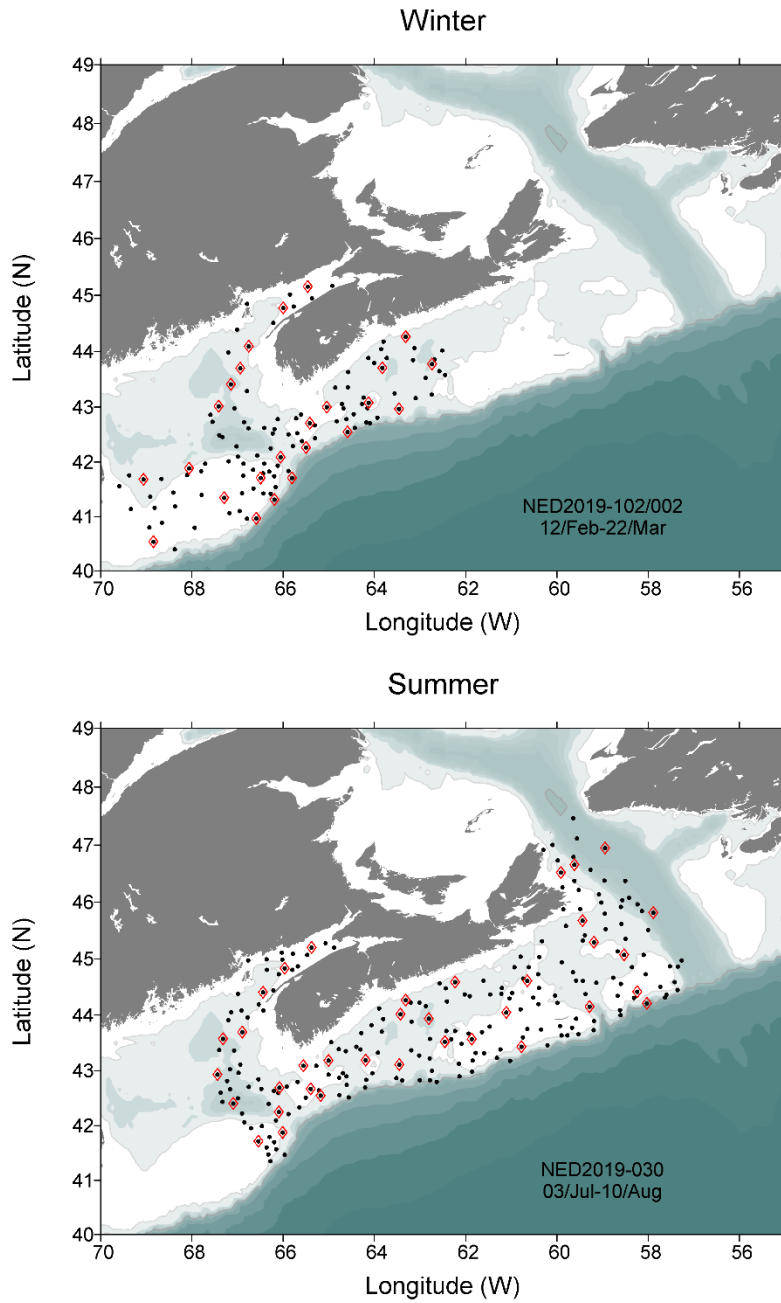


Figure 3. Stations sampled during primary Maritimes Region ecosystem trawl surveys in 2019. Black solid markers are hydrographic stations; red open diamonds are stations where vertical nets tows were taken in addition to hydrographic measurements.

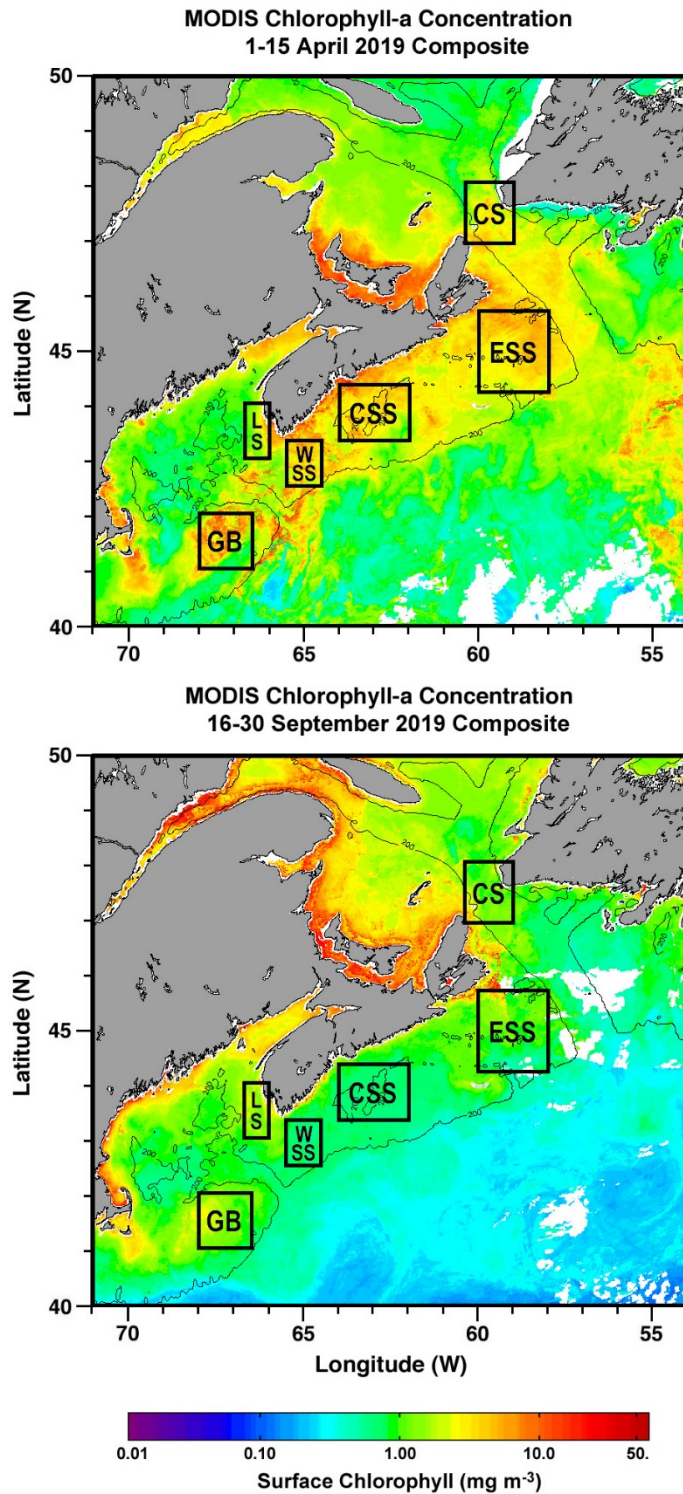


Figure 4. Statistical sub-regions in the Maritimes region identified for spatial/temporal analysis of satellite ocean colour data. Sub-regions are superimposed on surface chlorophyll a composite images for dates close to the mission dates (spring mission only). Cabot Strait [CS]; Eastern Scotian Shelf [ESS]; Central Scotian Shelf [CSS]; Western Scotian Shelf [WSS]; Lurcher Shoal [LS]; Georges Bank [GB].

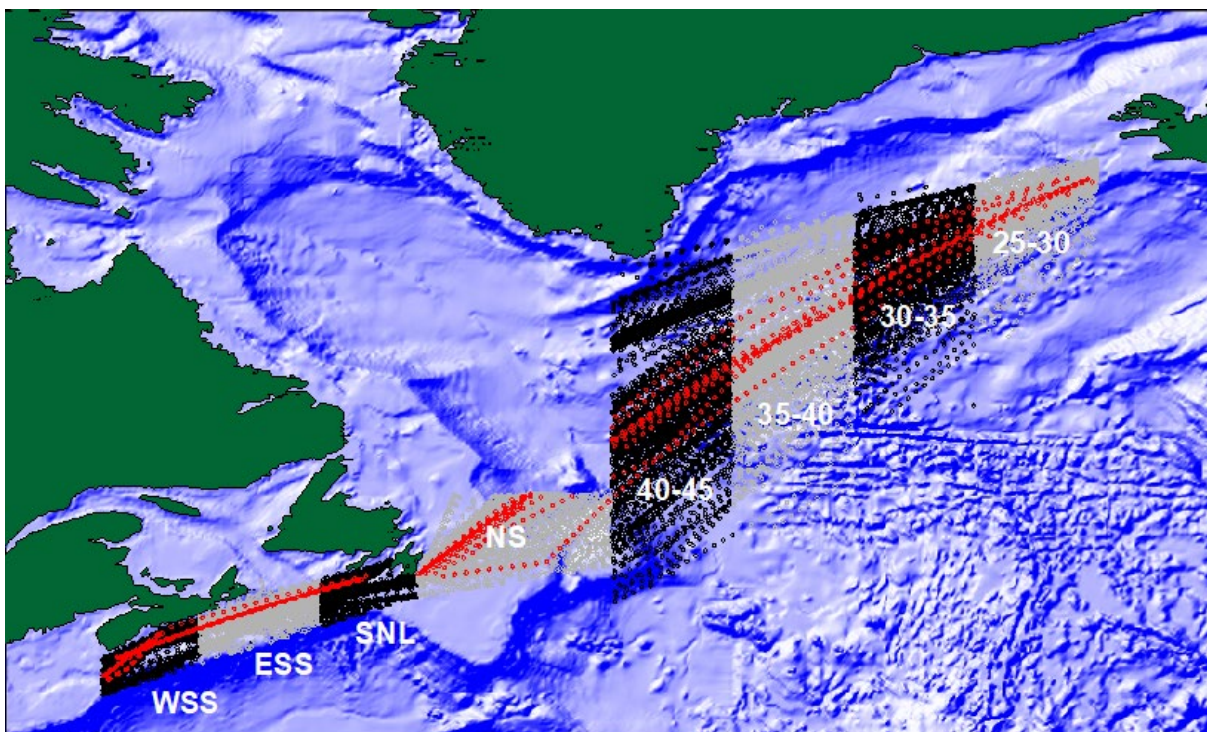


Figure 5. Continuous Plankton Recorder (CPR) lines and stations 1957 to 2018. Stations sampled in 2018 are shown in red. Data are analysed by region. Regions are: Western Scotian Shelf (WSS), Eastern Scotian Shelf (ESS), South Newfoundland Shelf (SNL), Newfoundland Shelf (NS), and between longitudes 40–45°W, 35–40°W, 30–35°W, 25–30°W.

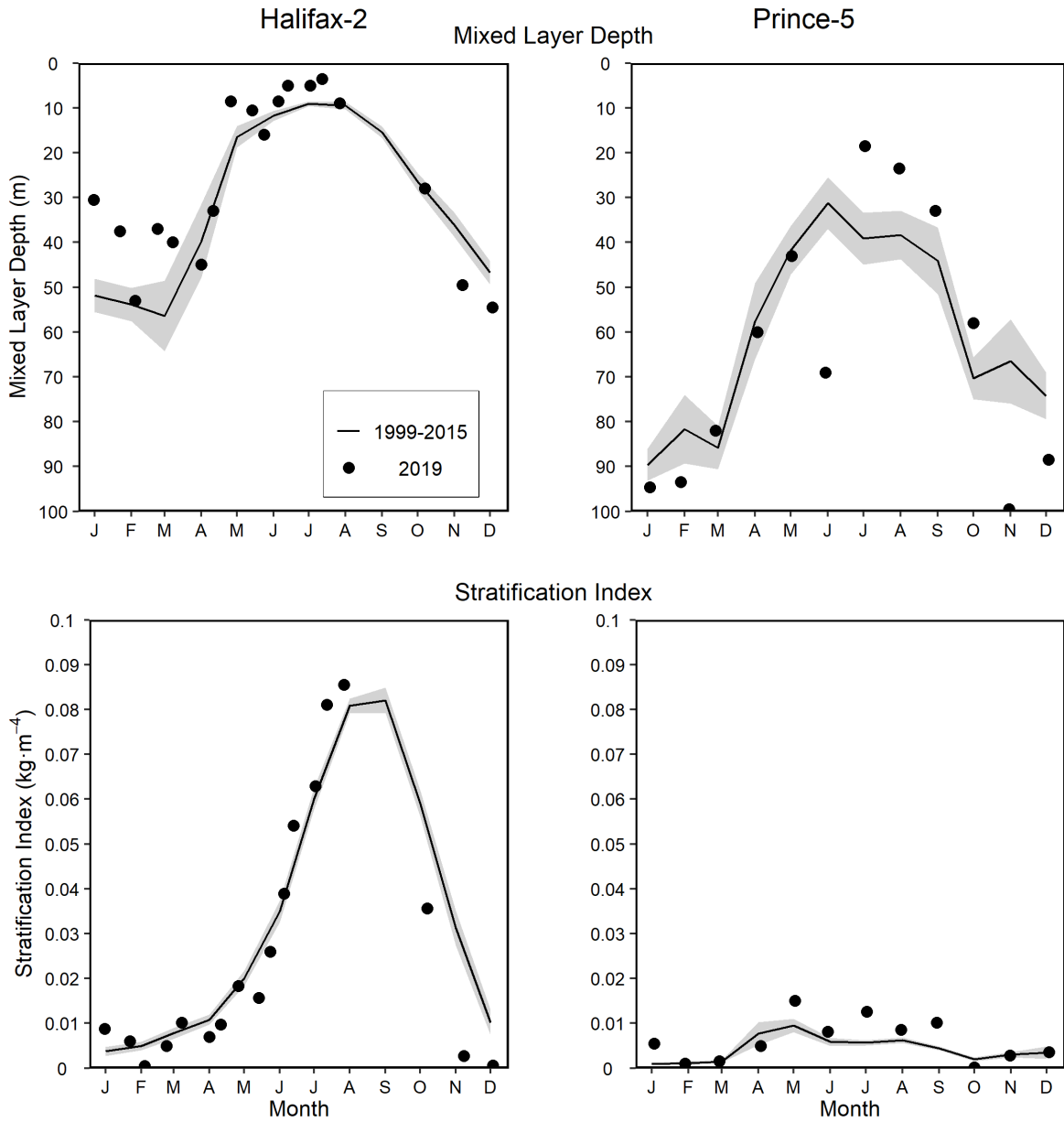


Figure 6. Mixing properties (mixed-layer depth, stratification index) at the Maritimes high-frequency sampling stations comparing 2019 data (solid circle) with mean conditions from 1999–2015 (solid line). The gray shaded area represents the standard error of the monthly means. Tick marks on the horizontal axes indicate the 15th day of the month.

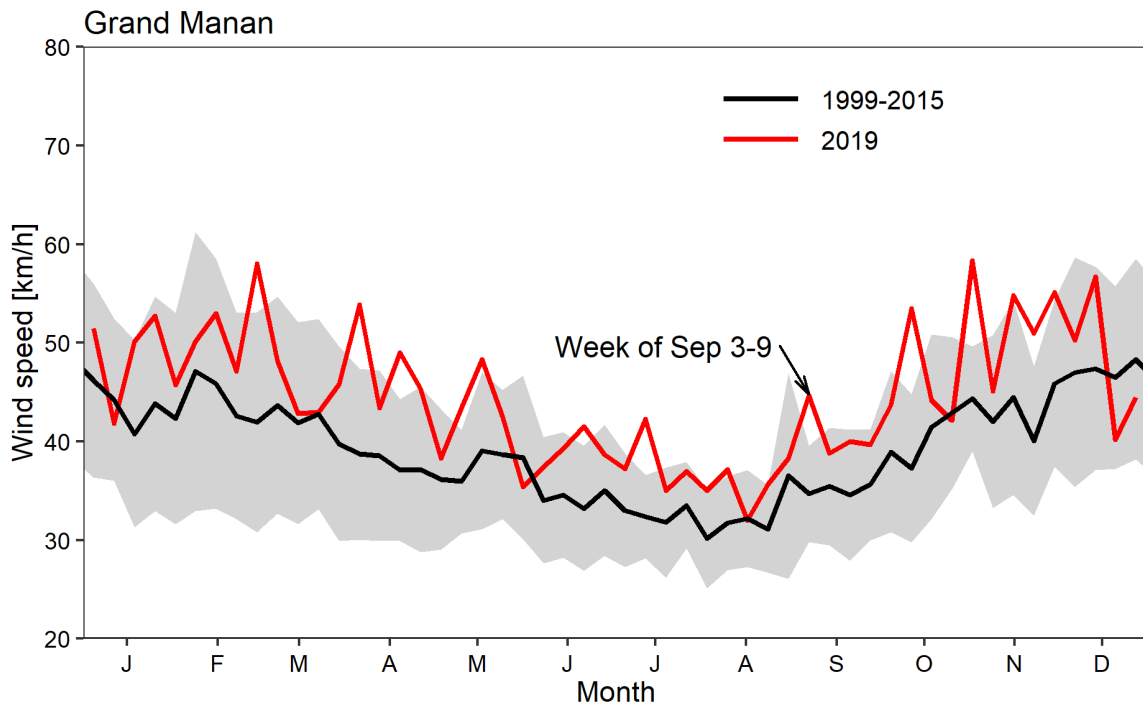
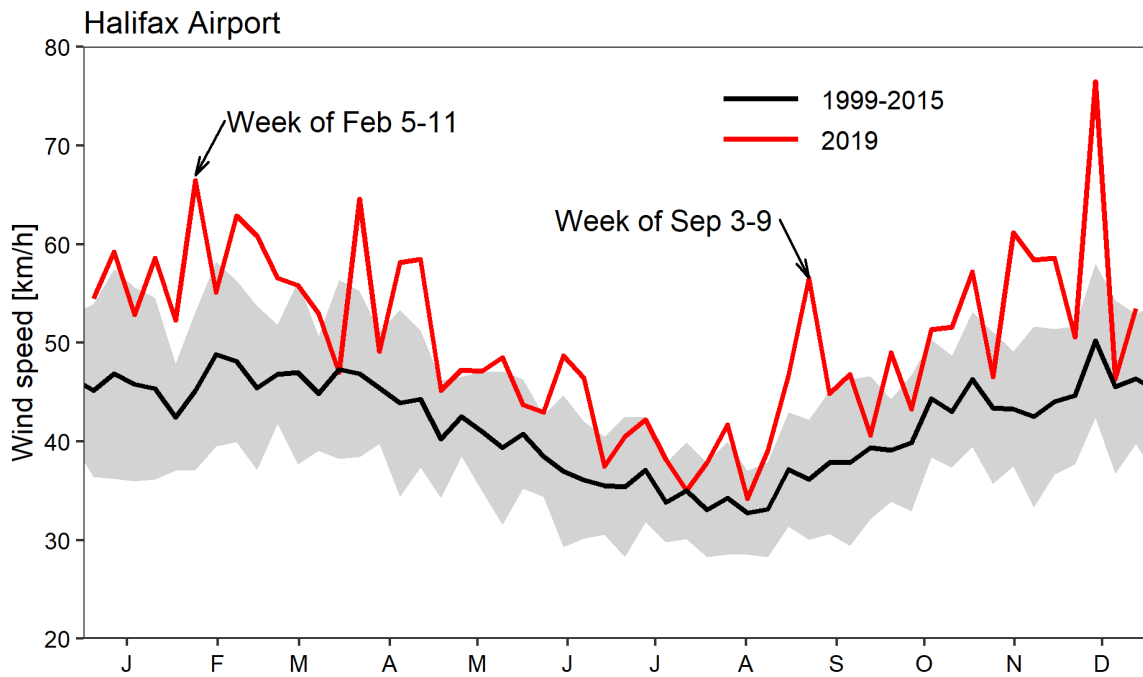


Figure 7. Weekly mean of maximum daily wind gust at Halifax International airport (representative of wind conditions at Halifax-2) and Grand Manan Island (representative of wind conditions at Prince-5) for the year 2019 (red line) and the 1999–2015 climatology (black line). The gray shaded area represents the standard deviation to the climatology computed over 17 years. Tick marks on the horizontal axes indicate the 15th day of the month.

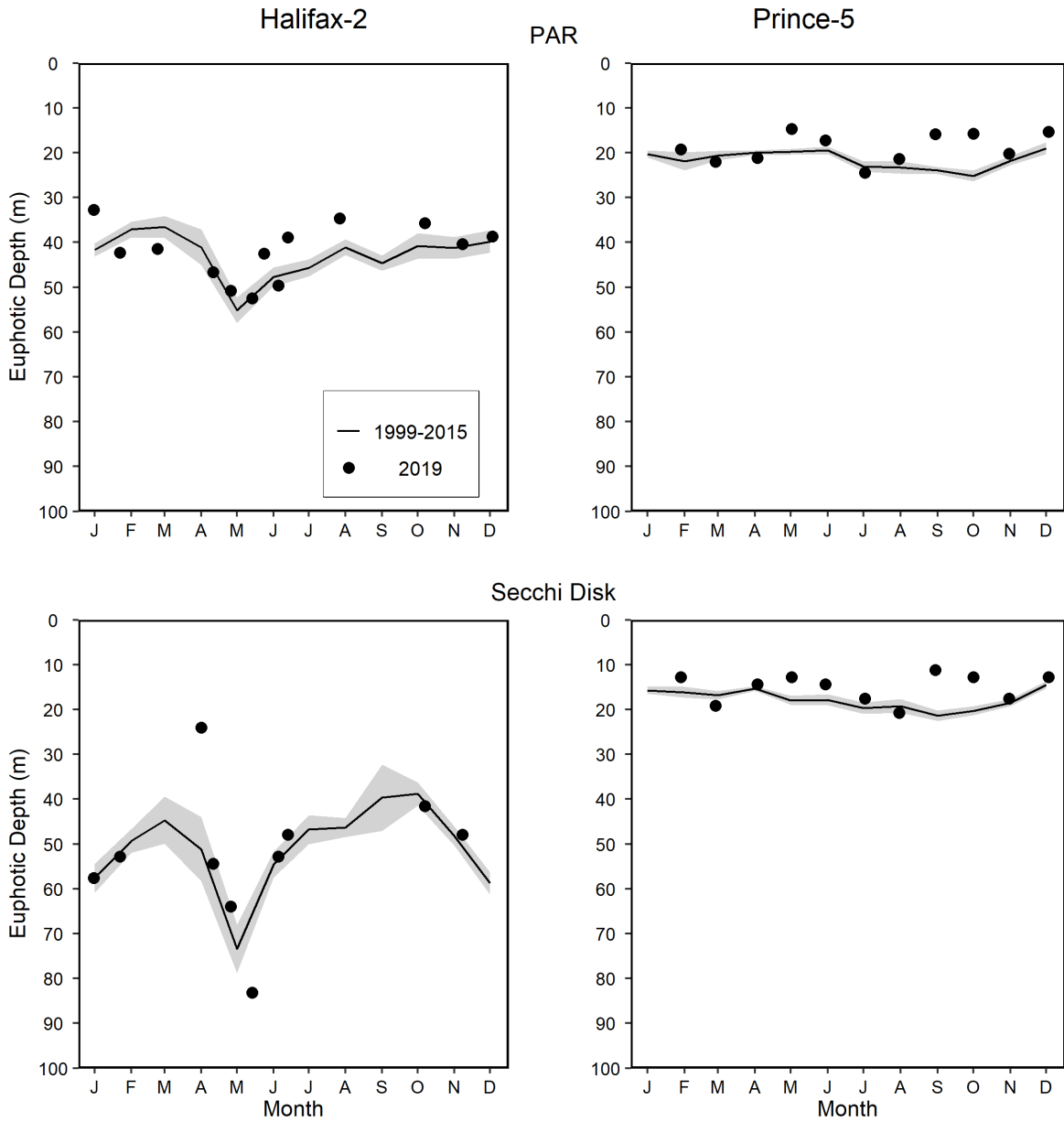


Figure 8. Optical properties (euphotic depth from PAR irradiance meter and Secchi disc) at the Maritimes high-frequency sampling stations. Year 2019 data (solid circle) compared with mean conditions from 1999–2015 (solid line), except 2001–2015 for euphotic depth from PAR at Prince-5. The gray shaded area represents the standard error of the monthly means. Tick marks on the horizontal axes indicate the 15th day of the month.

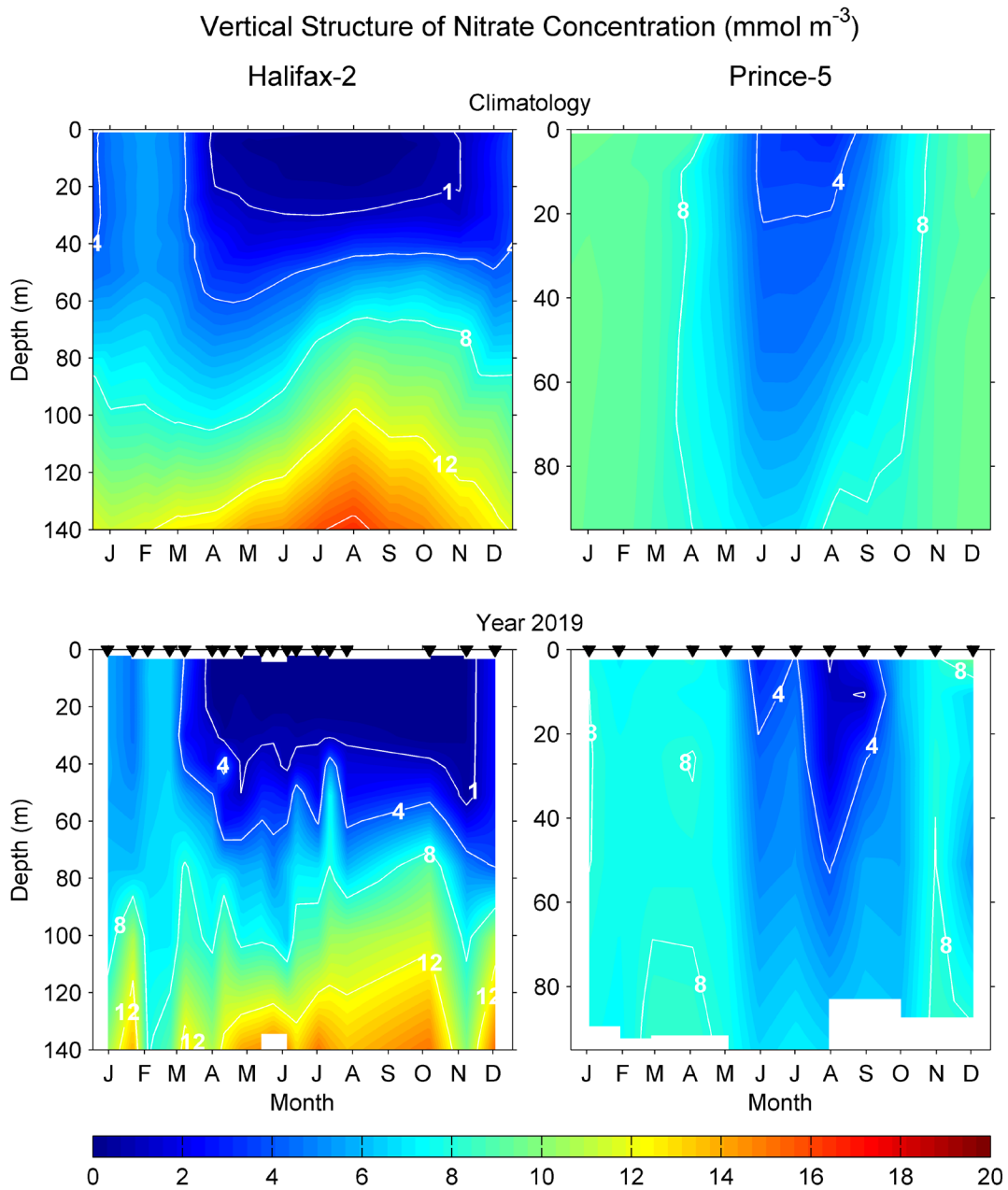


Figure 9. Comparison of annual changes in the vertical structure of nitrate concentrations ($\text{mmol}\cdot\text{m}^{-3}$) in 2019 (bottom panels) with climatological mean conditions from 1999–2015 (upper panels) at the Maritimes high-frequency sampling stations. Black triangles in the bottom panels indicate sampling dates. Tick marks on the horizontal axes indicate the 15th day of the month. White areas indicate no data.

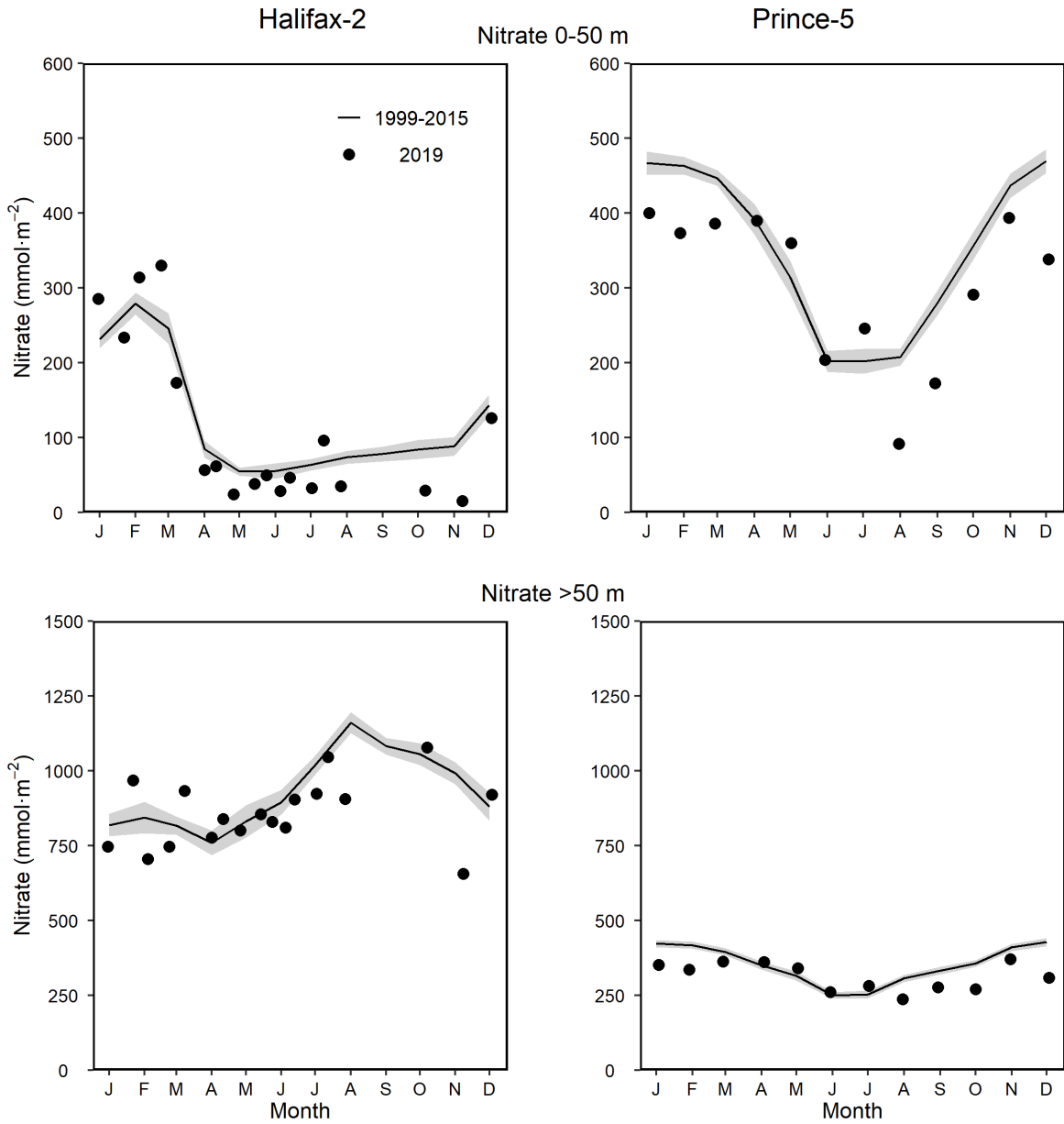


Figure 10. Comparison of 2019 (solid circle) data with mean conditions from 1999–2015 (solid line) at the Maritimes high-frequency sampling stations. Upper panels: surface (0–50 m) nitrate inventory. Lower panels: deep (50–150 m for Halifax-2 and 50–95 m for Prince-5) nitrate inventory. The gray shaded area represents the standard error of the monthly means. Tick marks on the horizontal axes indicate the 15th day of the month.

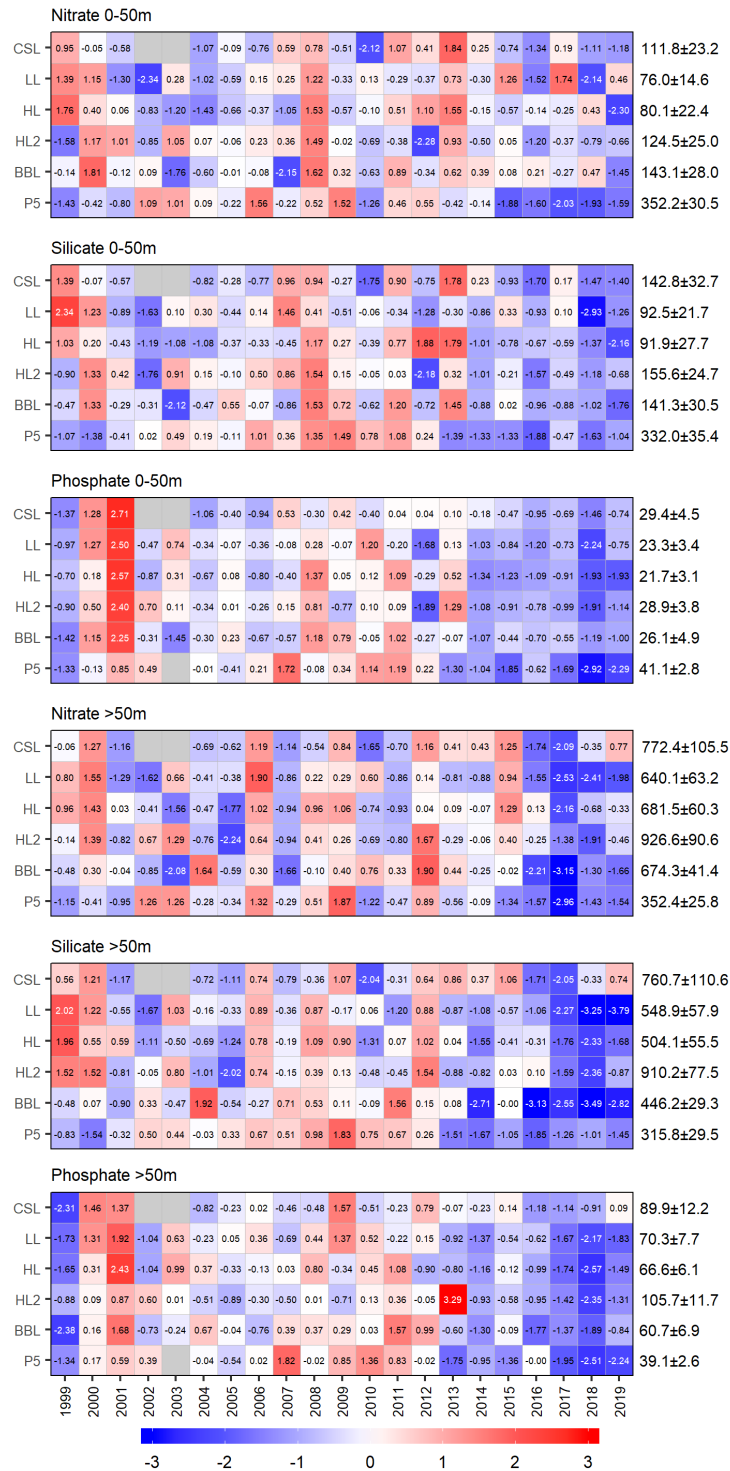


Figure 11. Annual anomaly scorecard for surface (0–50 m) and deep (>50 m) nitrate, silicate and phosphate inventories. Values in each cell are anomalies from the mean for the reference period, 1999–2015, in standard deviation (sd) units (mean and sd listed at right). A grey cell indicates missing data. Red (blue) cells indicate higher- (lower-) than-normal nutrients. CSL: Cabot Strait section; LL: Louisbourg section; HL: Halifax section; HL2: Halifax-2; BBL: Browns Bank section; P5: Prince-5.

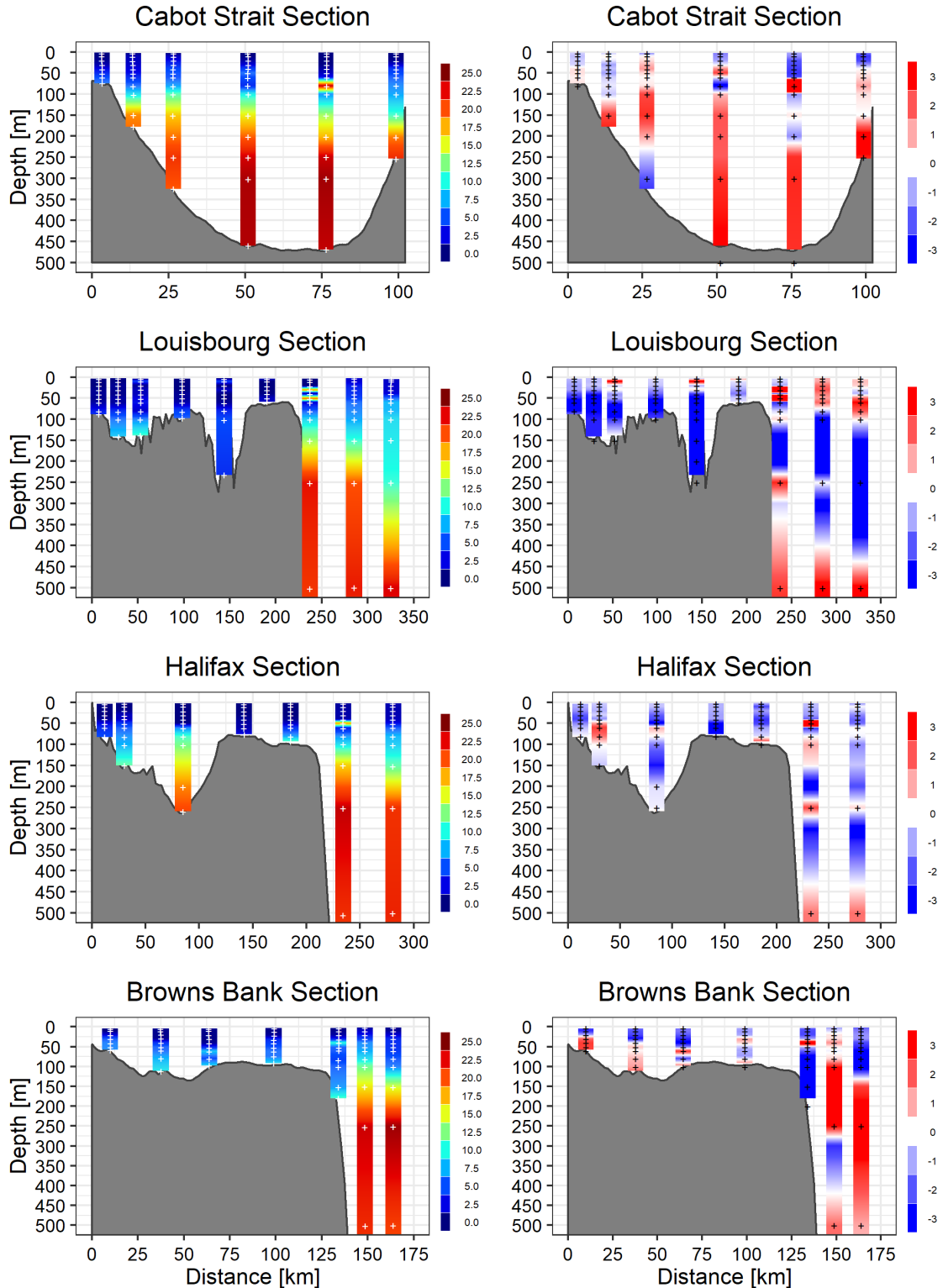


Figure 12. Vertical profiles of nitrate concentration ($\text{mmol}\cdot\text{m}^{-3}$) (left panels) and their anomalies ($\text{mmol}\cdot\text{m}^{-3}$) from 1999–2015 conditions (right panels) on the SS sections in spring 2019. White markers on the left panels indicate the actual sampling depths for 2019. Black markers on the right panels indicate the depths at which station-specific climatological values were calculated. CSL: Cabot Strait section; LL: Louisbourg section; HL: Halifax section; BBL: Browns Bank section.

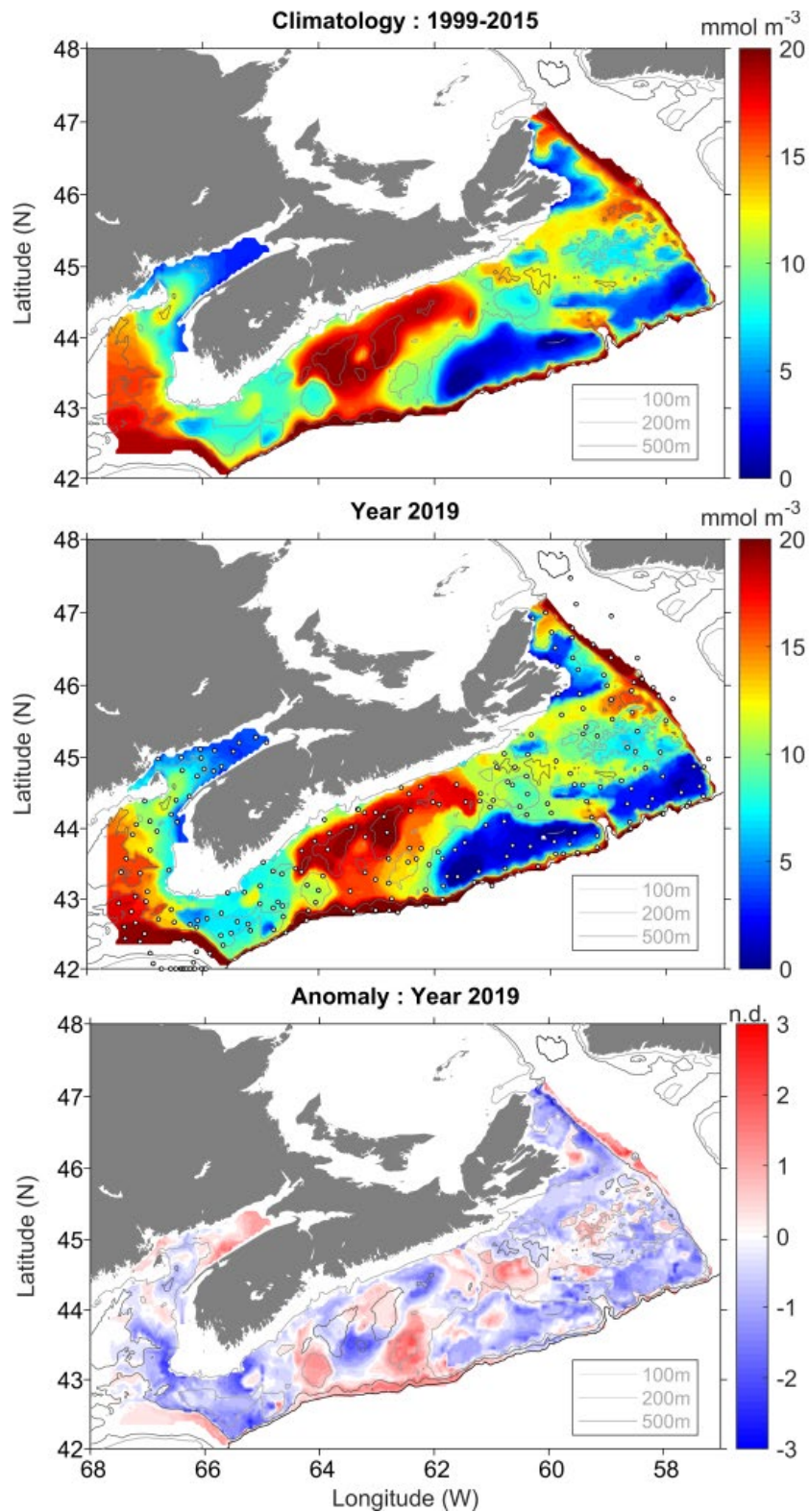


Figure 13. Bottom nitrate concentration during the annual summer ecosystem trawl survey: 1999–2015 climatology (upper panel), 2019 conditions (middle panel), and normalized anomalies from climatology (lower panel). Markers in middle panel represent the 2019 sampling locations. nd = no dimensions.

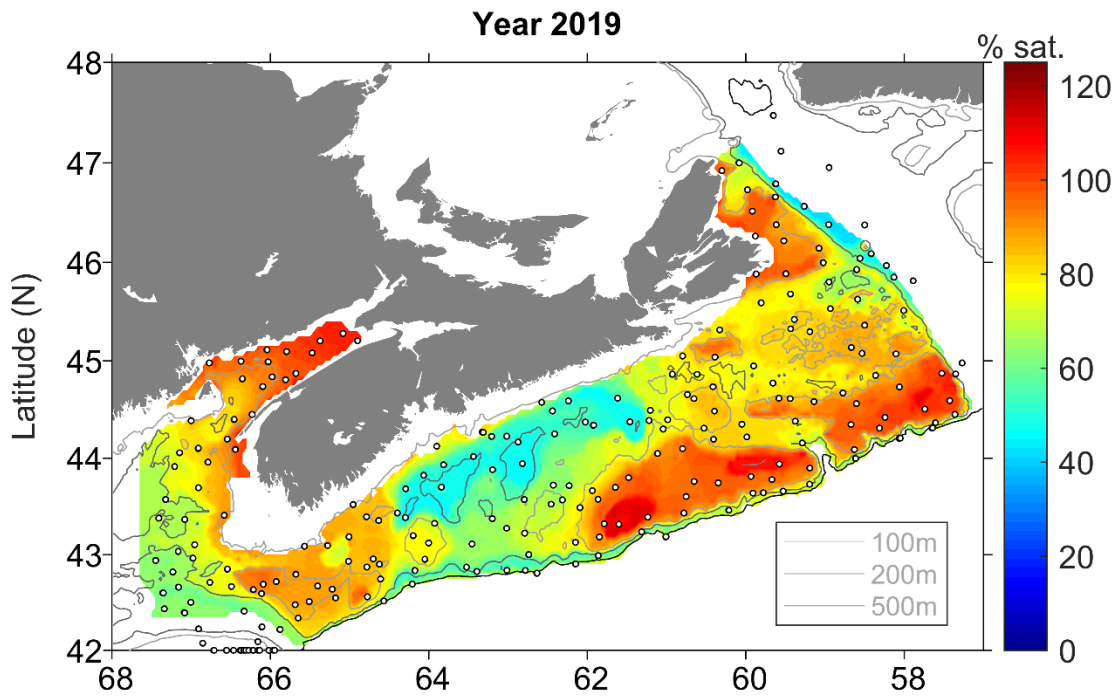


Figure 14. Bottom oxygen saturation level during the annual summer ecosystem trawl survey in 2019. Markers represent the sampling locations.

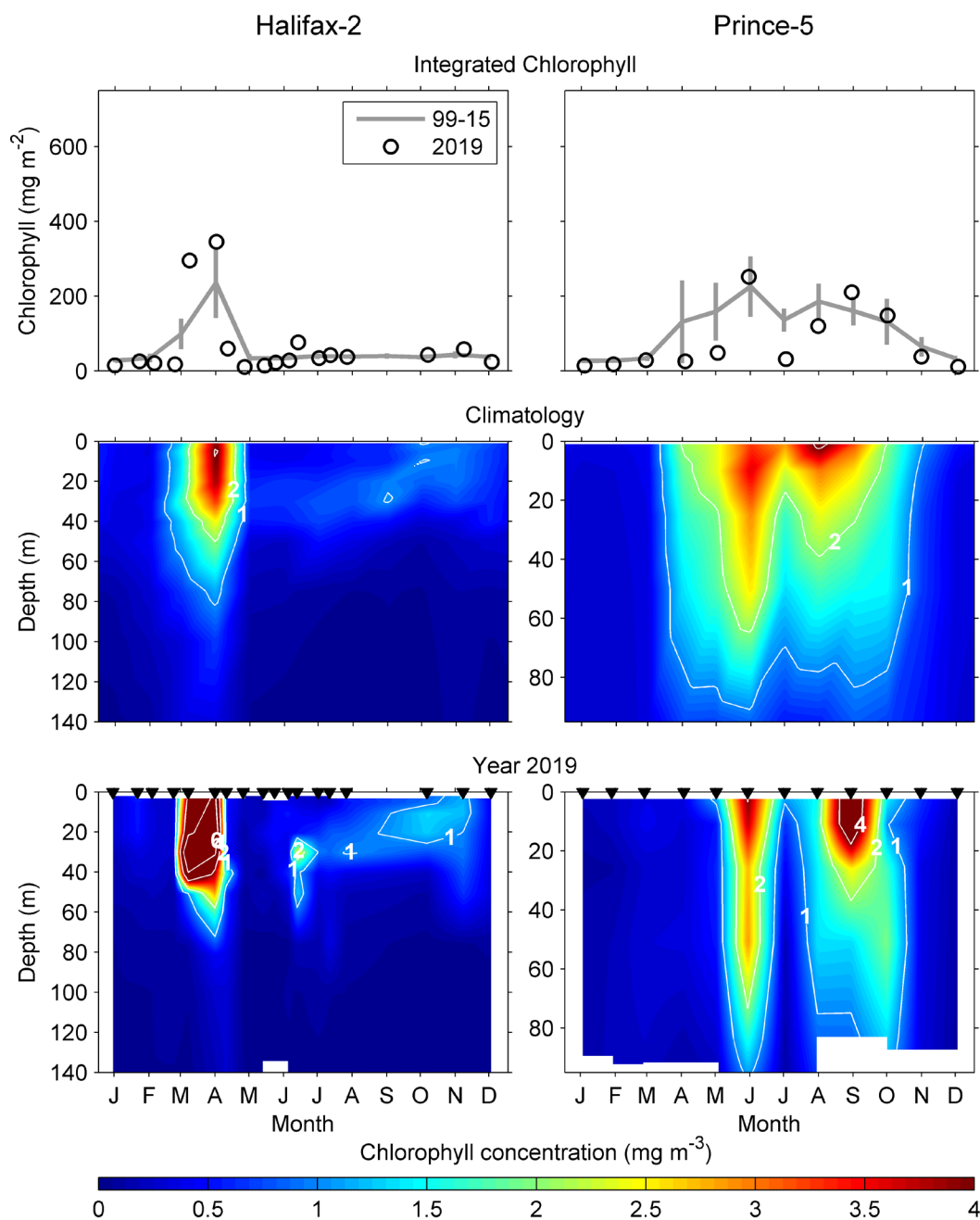


Figure 15. Annual variability in chlorophyll a concentration at the Maritimes time-series stations (left column: Halifax-2, right column: Prince-5). Top row: chlorophyll a inventories (0–100 m at Halifax-2, 0–95m at Prince-5) in 2019 (open circle) and mean values 1999–2015 (solid line). Vertical lines are 95% confidence intervals of the monthly means. Middle row: Mean (1999–2015) seasonal cycle of the vertical structure of chlorophyll a concentration ($\text{mg}\cdot\text{m}^{-3}$). Bottom row: seasonal cycle of the vertical structure of chlorophyll a concentration in 2019. Colour scale chosen to emphasize changes near the estimated food saturation levels for large copepods. Black triangles in the bottom panels indicate sampling dates. Tick marks on the horizontal axes indicate the 15th day of the month. White areas indicate no data.

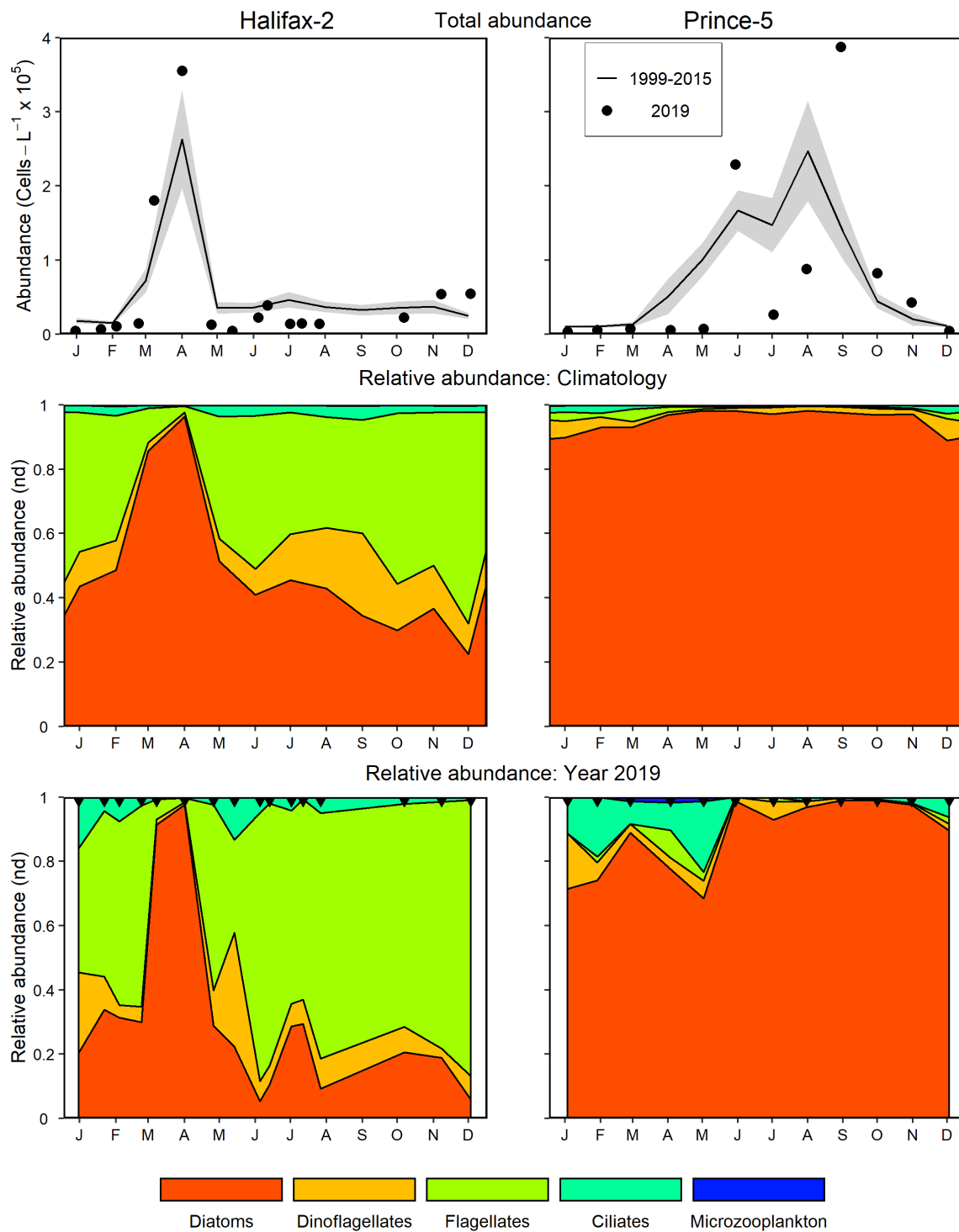


Figure 16. Comparison of 2019 microplankton (phytoplankton and protists) abundance and community composition with mean conditions from 1999–2015 at the Maritimes high-frequency sampling stations (Halifax-2 right panels; Prince-5 left panels). Upper panels: 2019 microplankton abundance (solid circle) and mean conditions from 1999–2015 (solid line). The gray shaded area represents the standard error of the monthly means. Middle panels: Climatological microplankton relative abundance from 1999–2015. Lower panels: 2019 microplankton relative abundance. nd = no dimensions. Black triangles in the bottom panels indicate sampling dates. Tick marks on the horizontal axes indicate the 15th day of the month.

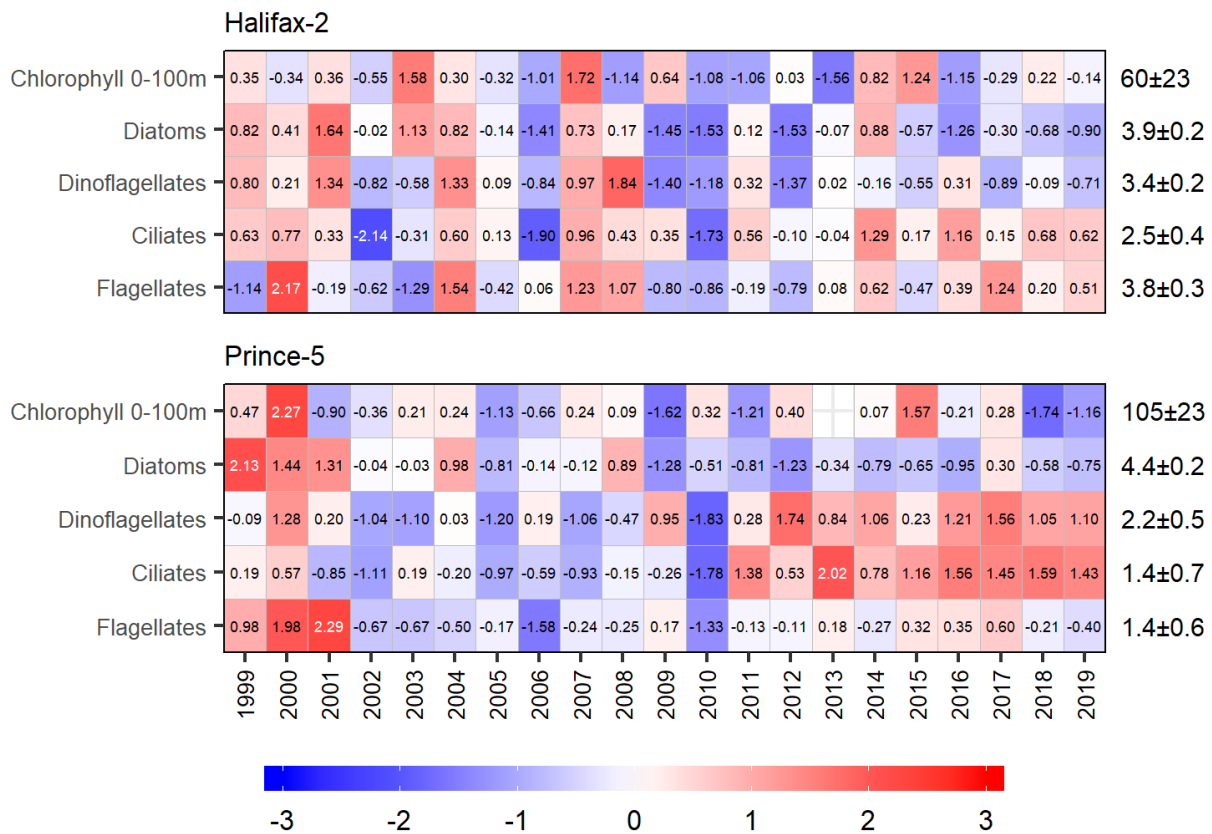


Figure 17. Annual anomaly scorecard for chlorophyll a inventory (0–100 m at Halifax-2, 0–95 m at Prince-5) and microplankton abundance at the Maritimes high-frequency sampling stations. Values in each cell are anomalies from the mean for the reference period, 1999–2015, in standard deviation (sd) units (mean and sd listed at right). Red (blue) cells indicate higher- (lower-) than-normal chlorophyll a inventories or microplankton abundances.

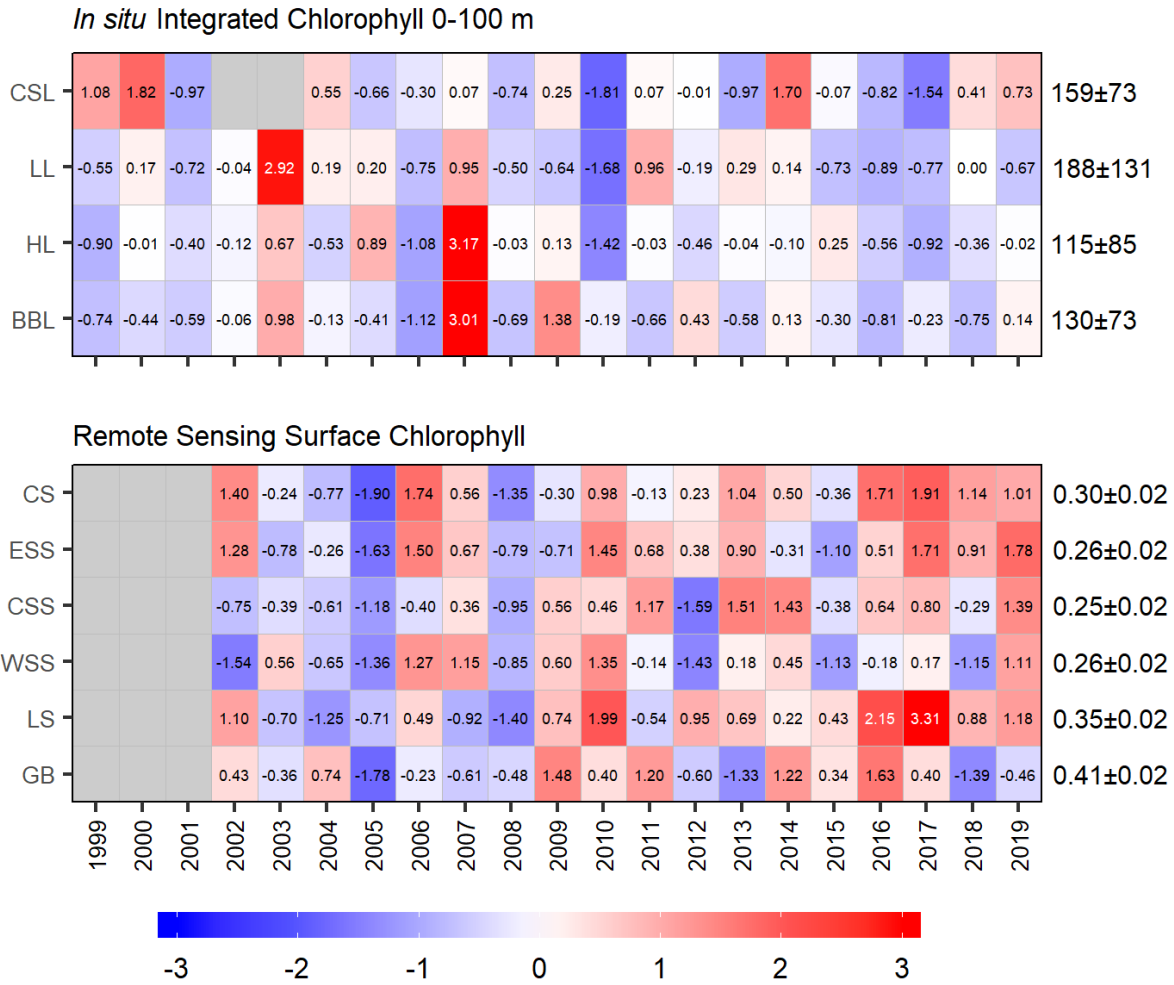


Figure 18. Annual anomaly scorecard for chlorophyll *a* inventory (0–100 m) from in situ sampling on the Cabot Strait [CSL], Louisbourg [LL], Halifax [HL] and Browns Bank [BBL] sections (top panel) and for surface chlorophyll *a* concentrations from weekly remotely sensed ocean colour data in the Cabot Strait [CS], Eastern Scotian Shelf [ESS], Central Scotian Shelf [CSS], Western Scotian Shelf [WSS], Lurcher Shoal [LS], and Georges Bank [GB] statistical sub-regions (bottom panel). Data from MODIS 2002–2019. Values in each cell are anomalies from the mean for the reference period, 1999–2015 for in situ chlorophyll *a* inventory and 2003–2015 for remotely sensed surface chlorophyll *a*, in standard deviation (sd) units (mean and sd listed at right). Red (blue) cells indicate higher- (lower-) than-normal chlorophyll *a* inventories or surface chlorophyll *a* concentrations.

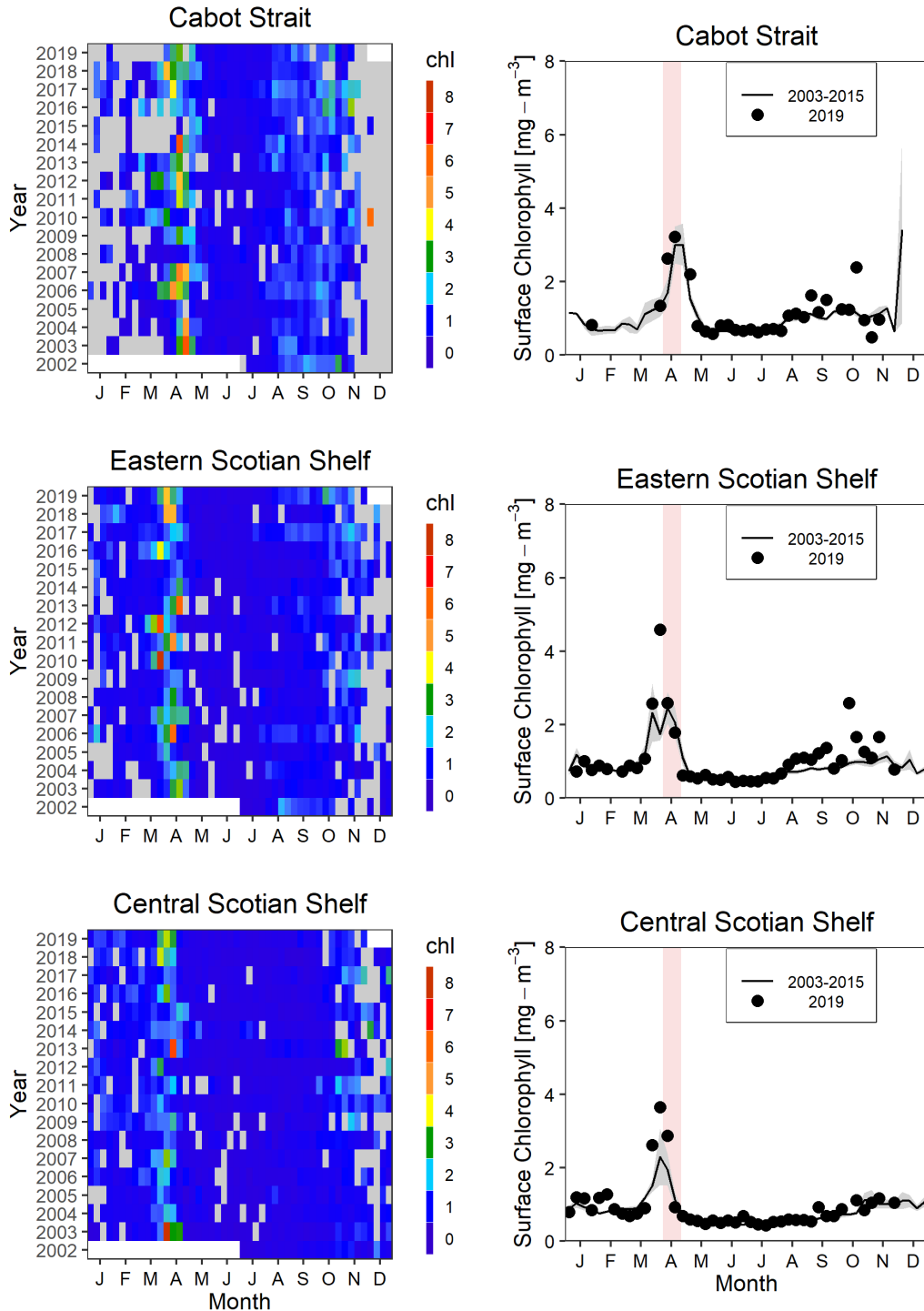


Figure 19a. Estimates of surface chlorophyll a concentrations from weekly remotely sensed ocean colour data in the Cabot Strait (top), Eastern Scotian Shelf (middle), and Central Scotian Shelf (bottom) statistical sub-regions. Data from MODIS 2002–2019. Left panels: Time series of annual variation in chlorophyll a concentrations. Right panels: Comparison of 2019 (solid circle) surface chlorophyll a estimates with mean conditions from 2003–2015 (solid line) in the same sub-regions. Gray shaded area is the 95% confidence interval of the weekly means. Pink vertical stripes indicate the timing of the seasonal missions. Tick marks on the horizontal axes indicate the 15th day of the month. White pixels on the left panels delimit the range of data availability and gray pixels indicate missing data.

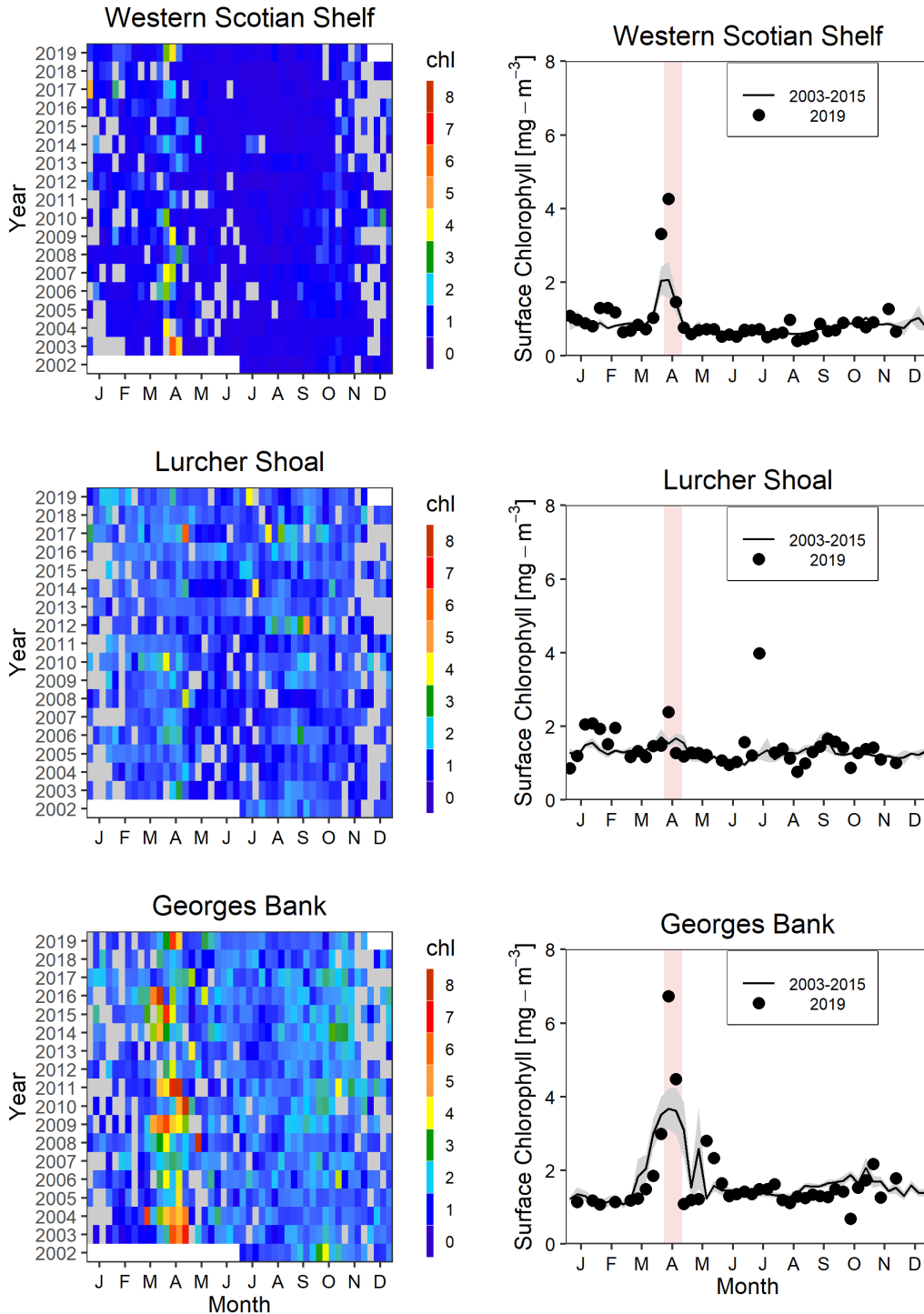


Figure 19b. Estimates of surface chlorophyll a concentrations from weekly remotely sensed ocean colour data in the Western Scotian Shelf (top), Lurcher Shoal (middle), and Georges Bank (bottom) statistical sub-regions. Data from MODIS 2002–2019. Left panels: Time series of annual variation in chlorophyll a concentrations. Right panels: Comparison of 2019 (solid circle) surface chlorophyll a estimates with mean conditions from 2003–2015 (solid line) in the same sub-regions. Gray shaded area is the 95% confidence interval of the weekly means. Pink vertical stripes indicate the timing of the seasonal missions. Tick marks on the horizontal axes indicate the 15th day of the month. White pixels on the left panels delimit the range of data availability and gray pixels indicate missing data.

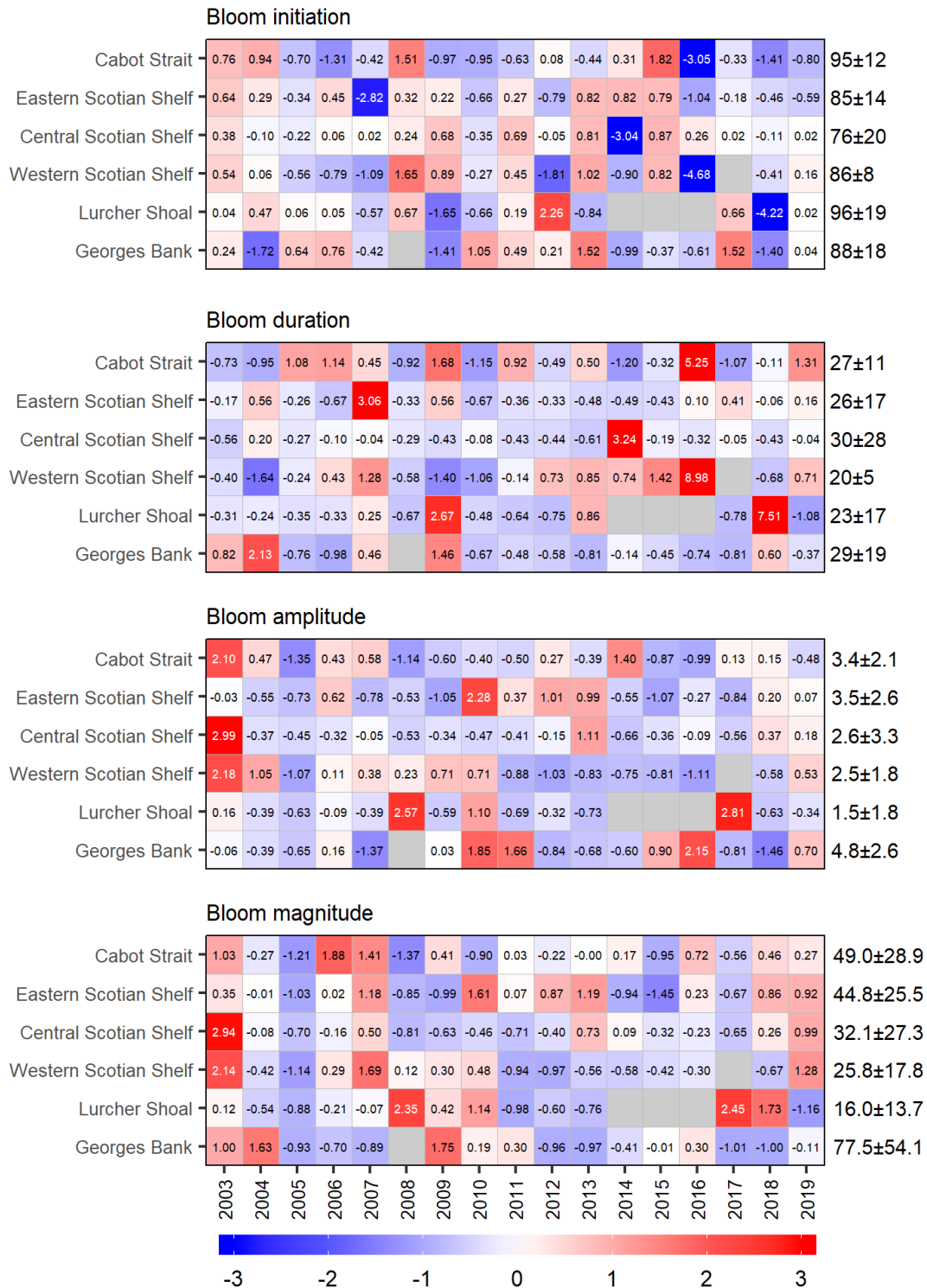


Figure 20. Annual anomaly scorecard for spring-bloom parameters. Values in each cell are anomalies from the mean for the reference period, 2003–2015, in standard deviation (sd) units (mean and sd listed at right). A grey cell indicates missing data. Red (blue) cells indicate later (earlier) initiation, longer (shorter) duration or higher- (lower-) than-normal amplitude or magnitude.

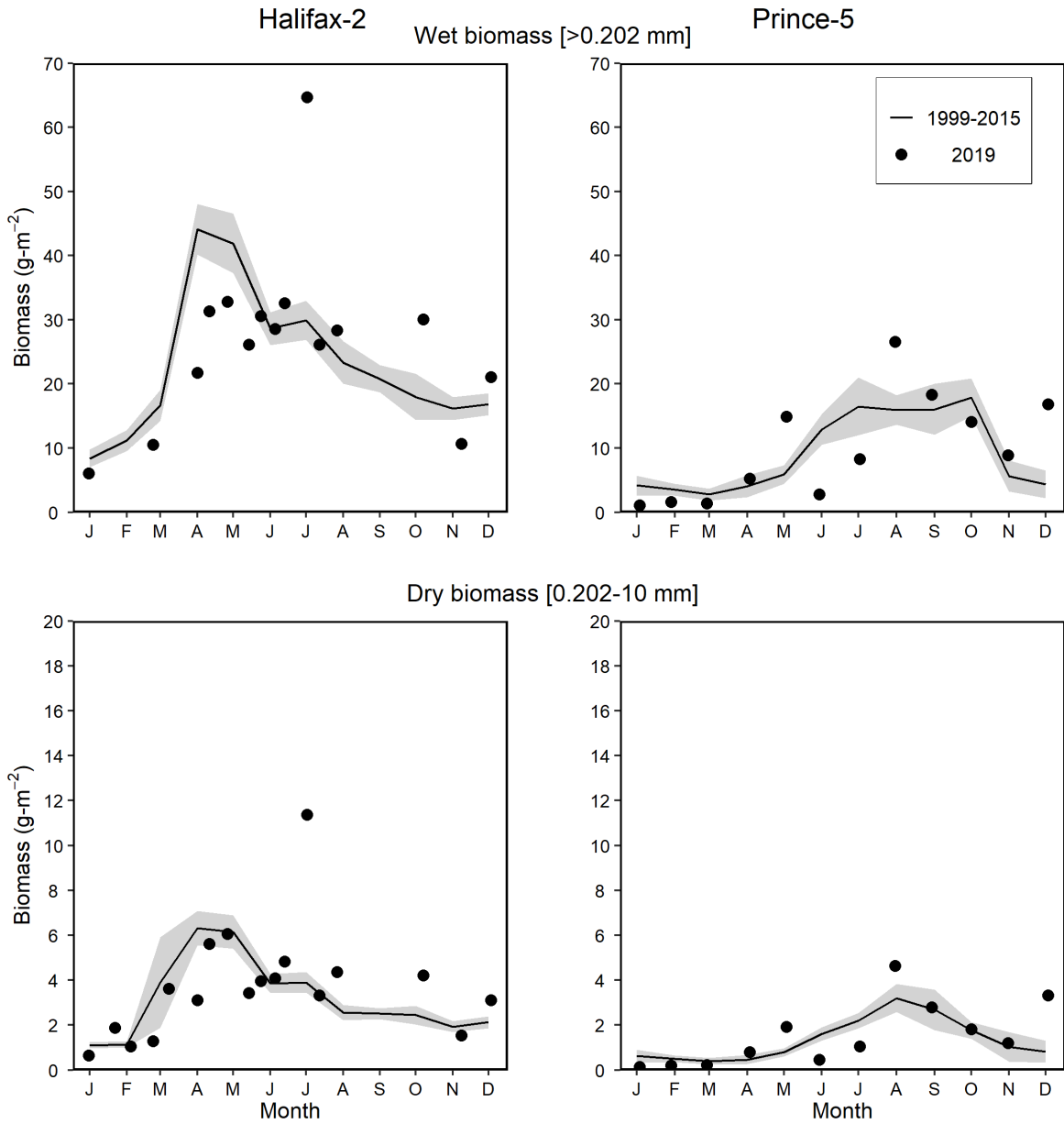


Figure 21. Zooplankton total wet biomass (upper panels) and mesozooplankton dry biomass (bottom panels) (integrated surface to bottom) in 2019 (solid circle) and mean conditions 1999–2015 (solid line) at the Maritimes high-frequency sampling stations. The gray shaded area represents the standard error of the monthly means. Left panels: Halifax-2; right panels: Prince-5. Tick marks on the horizontal axes indicate the 15th day of the month.

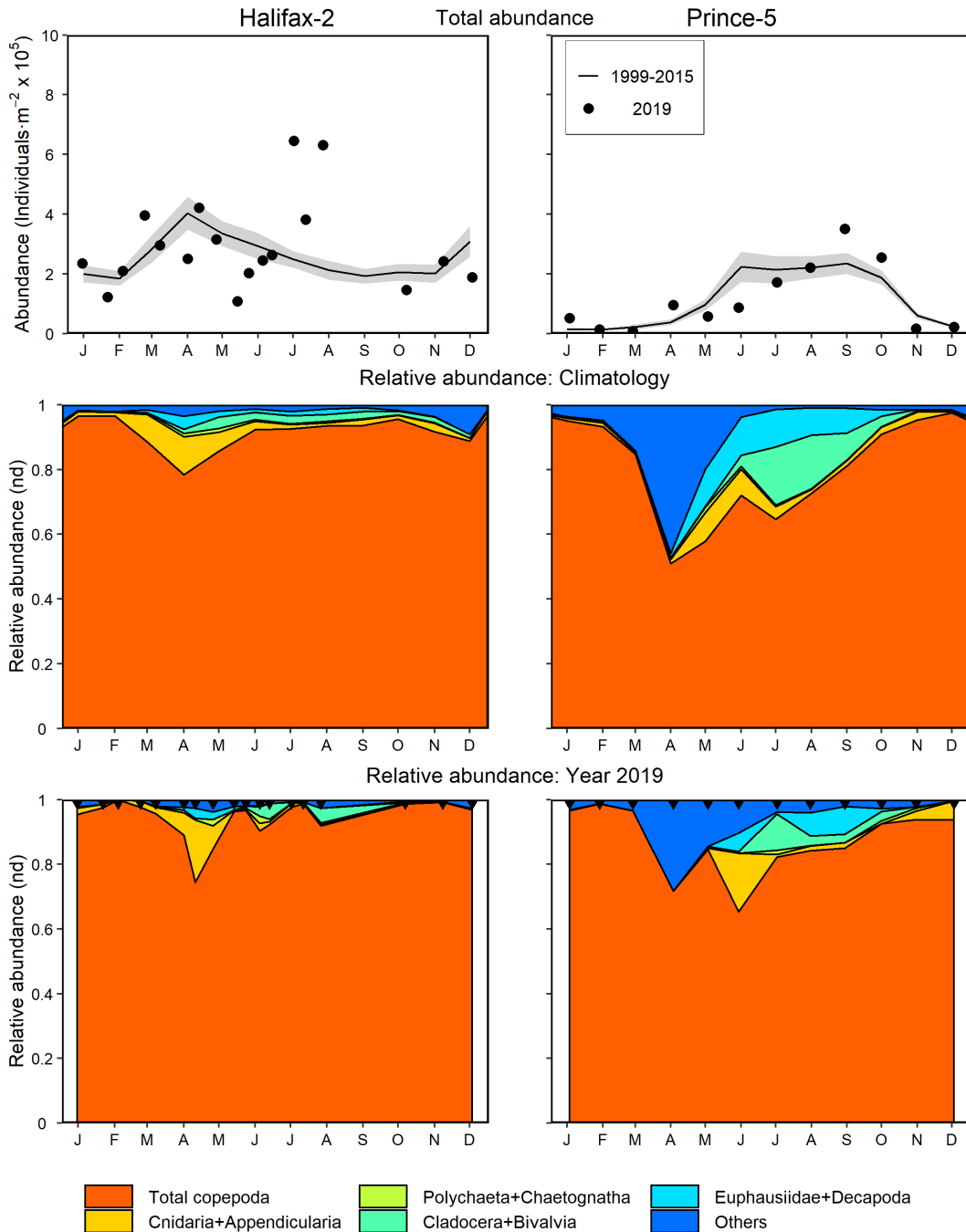


Figure 22. Zooplankton (>200 μm) abundance and community composition in 2019 and mean conditions 1999–2015 at the Maritimes high-frequency sampling stations (Halifax-2, left panels; Prince-5, right panels). Upper panels: Zooplankton abundance in 2019 (solid circle) and mean conditions 1999–2015 (solid line). The gray shaded area represents the standard error of the monthly means. Middle panels: Climatology of major groups relative abundances 1999–2015. Lower panels: major groups relative abundances in 2019. nd = no dimensions. Black triangles in the bottom panels indicate sampling dates. Tick marks on the horizontal axes indicate the 15th day of the month.

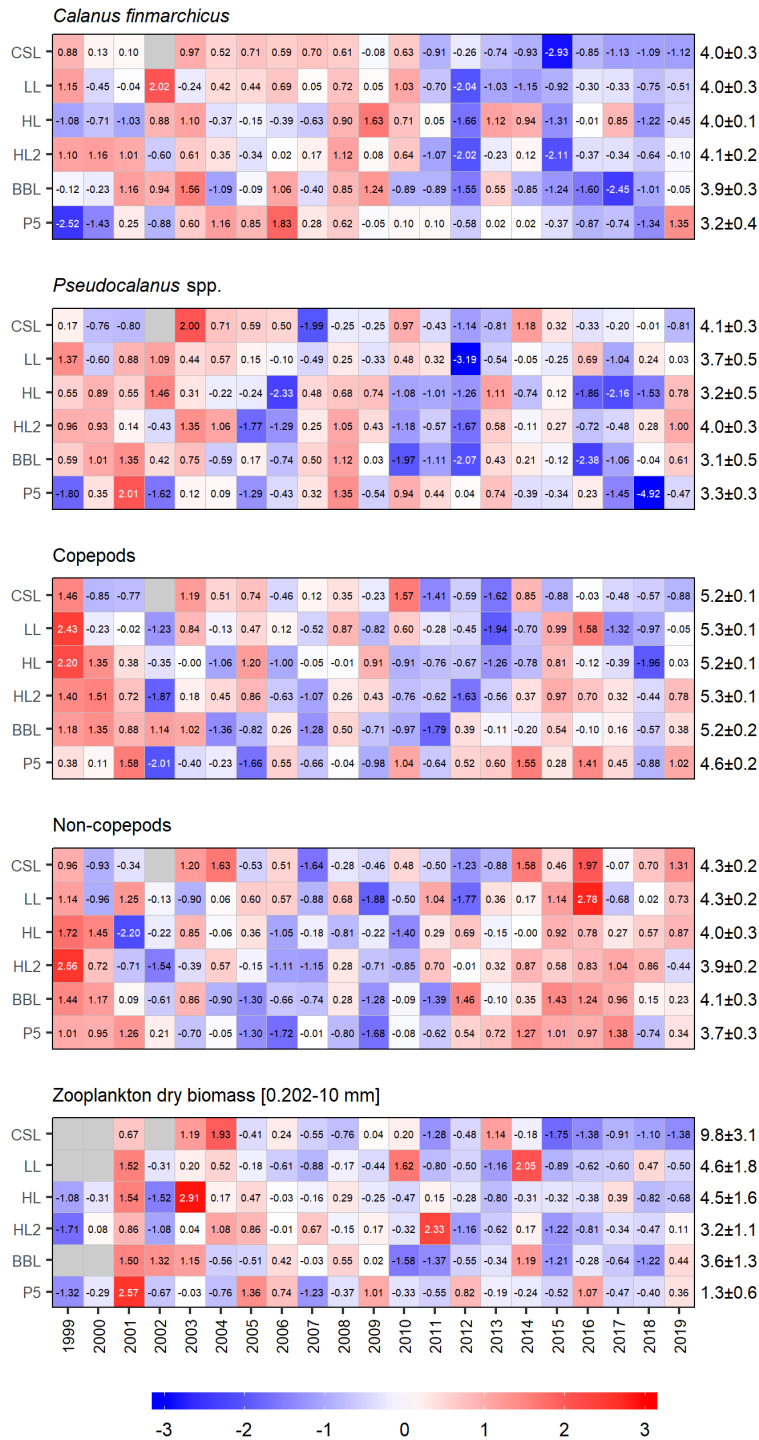


Figure 23. Annual anomaly scorecard for zooplankton abundance and biomass. Values in each cell are anomalies from the mean for the reference period, 1999–2015, in standard deviation (sd) units (mean and sd listed at right). A grey cell indicates missing data. Red (blue) cells indicate higher- (lower-) than-normal abundances or biomass. CSL: Cabot Strait section; LL: Louisbourg section; HL: Halifax section; HL2: Halifax-2; BBL: Browns Bank section; P5: Prince-5.

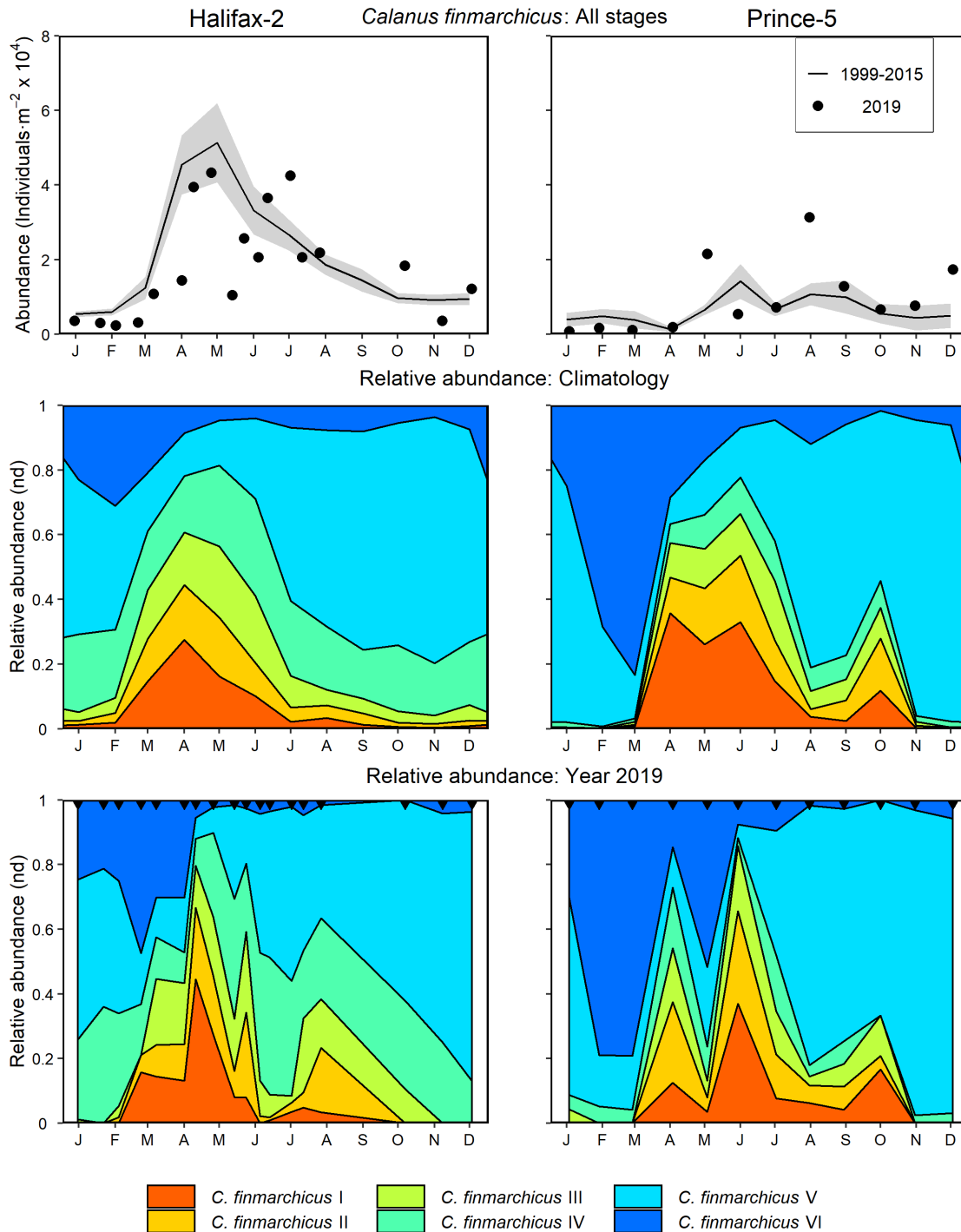


Figure 24. *Calanus finmarchicus* abundance and developmental-stage distributions in 2019 and mean conditions 1999–2015 at the Maritimes high-frequency sampling stations (Halifax-2, left panels; Prince-5, right panels). Upper panels: *C. finmarchicus* abundance in 2019 (solid circle) and mean conditions 1999–2015 (solid line). The gray shaded area represents the standard error of the monthly means. Middle panels: Climatological *C. finmarchicus* stage relative abundances, 1999–2015. Lower panels: *C. finmarchicus* stage relative abundances in 2019. nd = no dimensions. Black triangles in the bottom panels indicate sampling dates. Tick marks on the horizontal axes indicate the 15th day of the month.

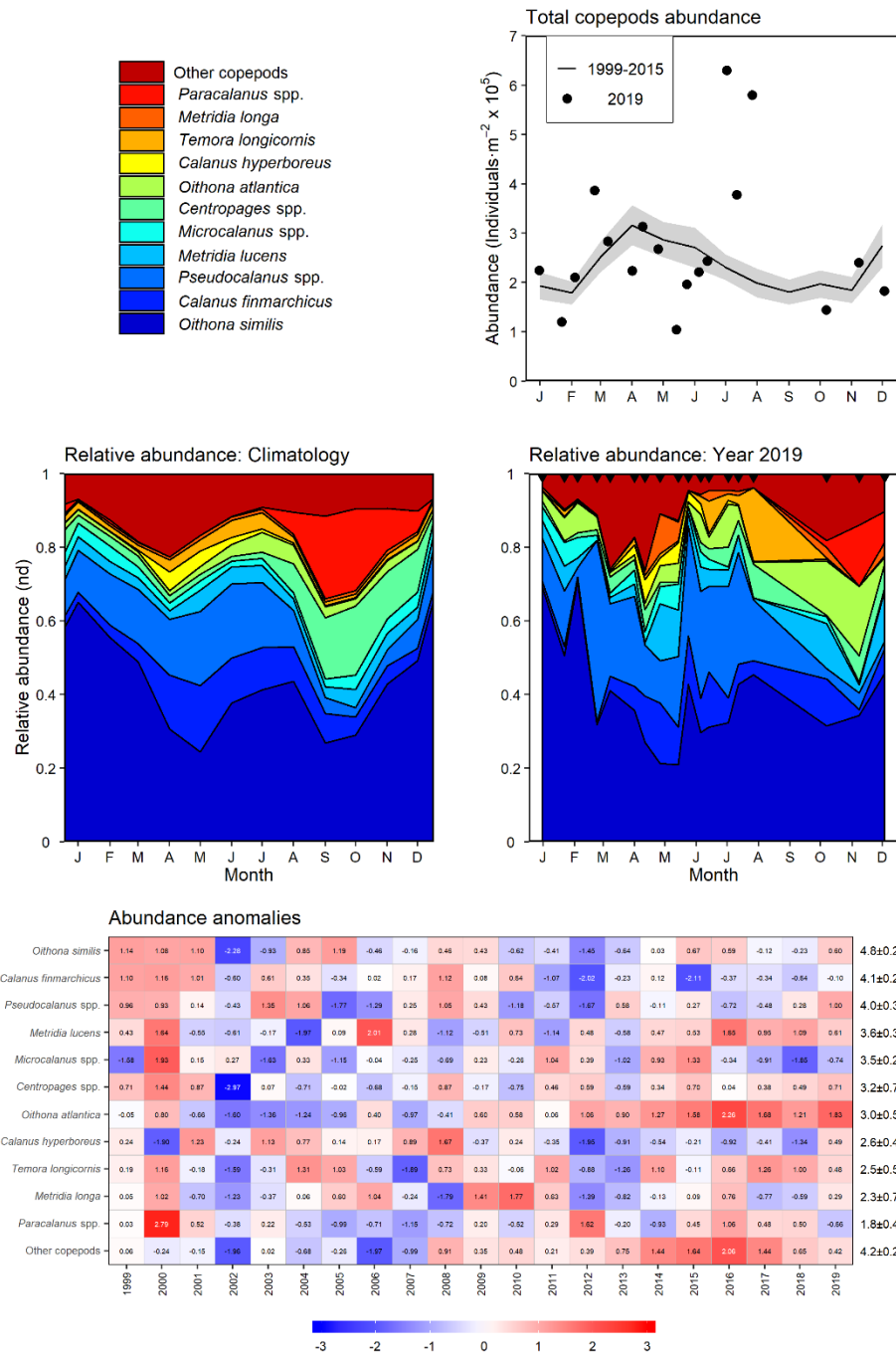


Figure 25a. Variability of dominant copepods at Halifax-2. The top 95% copepod taxa by abundance are shown individually; unidentified copepods (mostly nauplii) are grouped as “others.” Upper right panel: copepod abundance in 2019 (solid circle) and mean conditions, 1999–2015 (solid line). The gray shaded area represents the standard error of the monthly means. Middle left panel: Climatology of copepod relative abundances, 1999–2015. Middle right panel: copepod relative abundance in 2019. nd = no dimensions. Black triangles in the middle right panel indicate sampling dates. Tick marks on the horizontal axes indicate the 15th day of the month. Bottom panel: Annual anomaly scorecard for copepod abundance. Values in each cell are anomalies from the mean for the reference period, 1999–2015, in standard deviation (sd) units (mean and sd listed at right). A grey cell indicates missing data. Red (blue) cells indicate higher- (lower-) than-normal abundances.

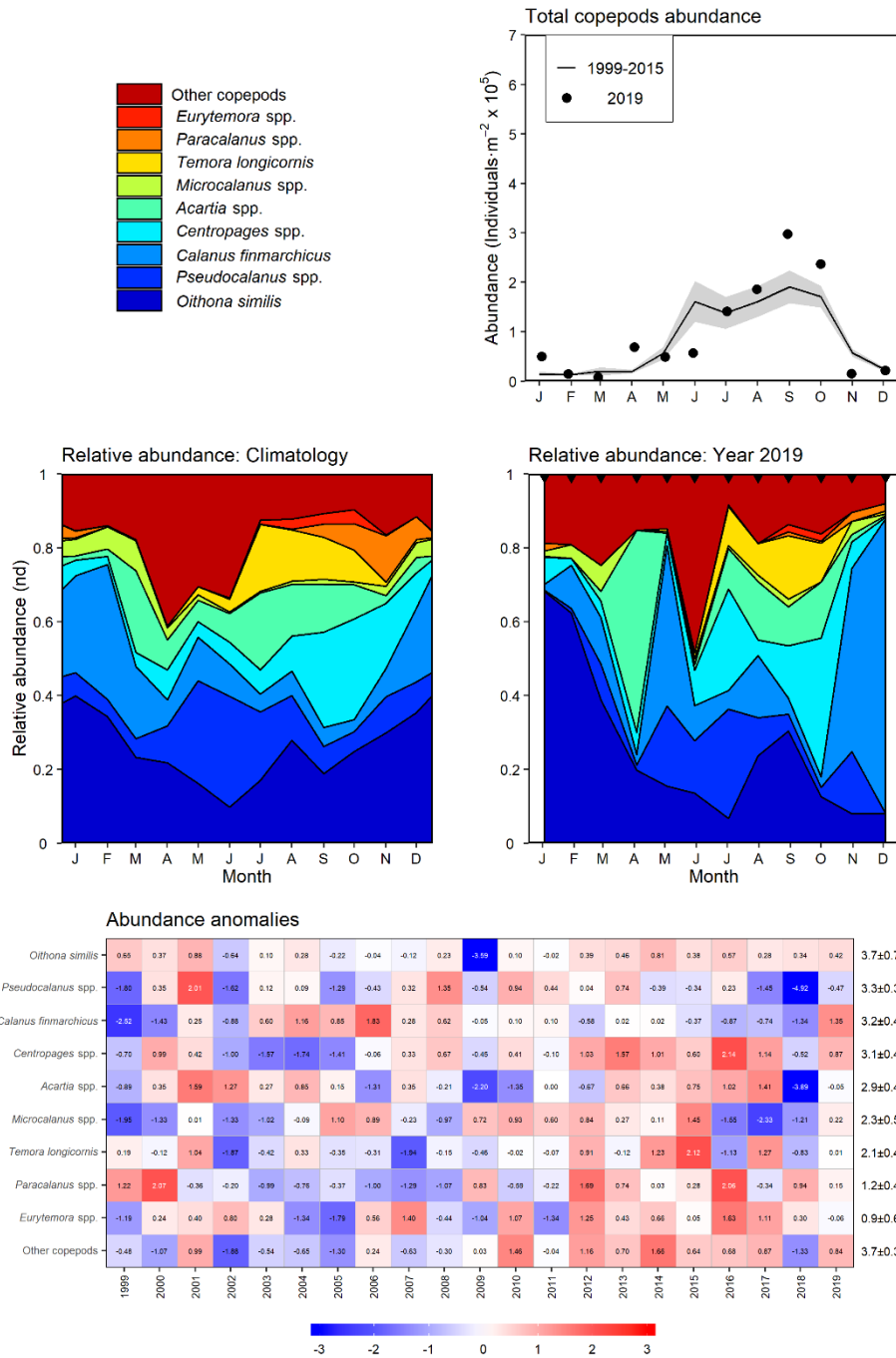


Figure 25b. Variability of dominant copepods at Prince-5. The top 95% copepod taxa by abundance are shown individually; unidentified copepods (mostly nauplii) are grouped as “others.” Upper right panel: copepod abundance in 2019 (solid circle) and mean conditions, 1999–2015 (solid line). The gray shaded area represents the standard error of the monthly means. Middle left panel: Climatology of copepod relative abundances, 1999–2015. Middle right panel: copepod relative abundance in 2019. nd = no dimensions. Black triangles in the middle right panel indicate sampling dates. Tick marks on the horizontal axes indicate the 15th day of the month. Bottom panel: Annual anomaly scorecard for copepod abundance. Values in each cell are anomalies from the mean for the reference period, 1999–2015, in standard deviation (sd) units (mean and sd listed at right). A grey cell indicates missing data. Red (blue) cells indicate higher- (lower-) than-normal abundances.

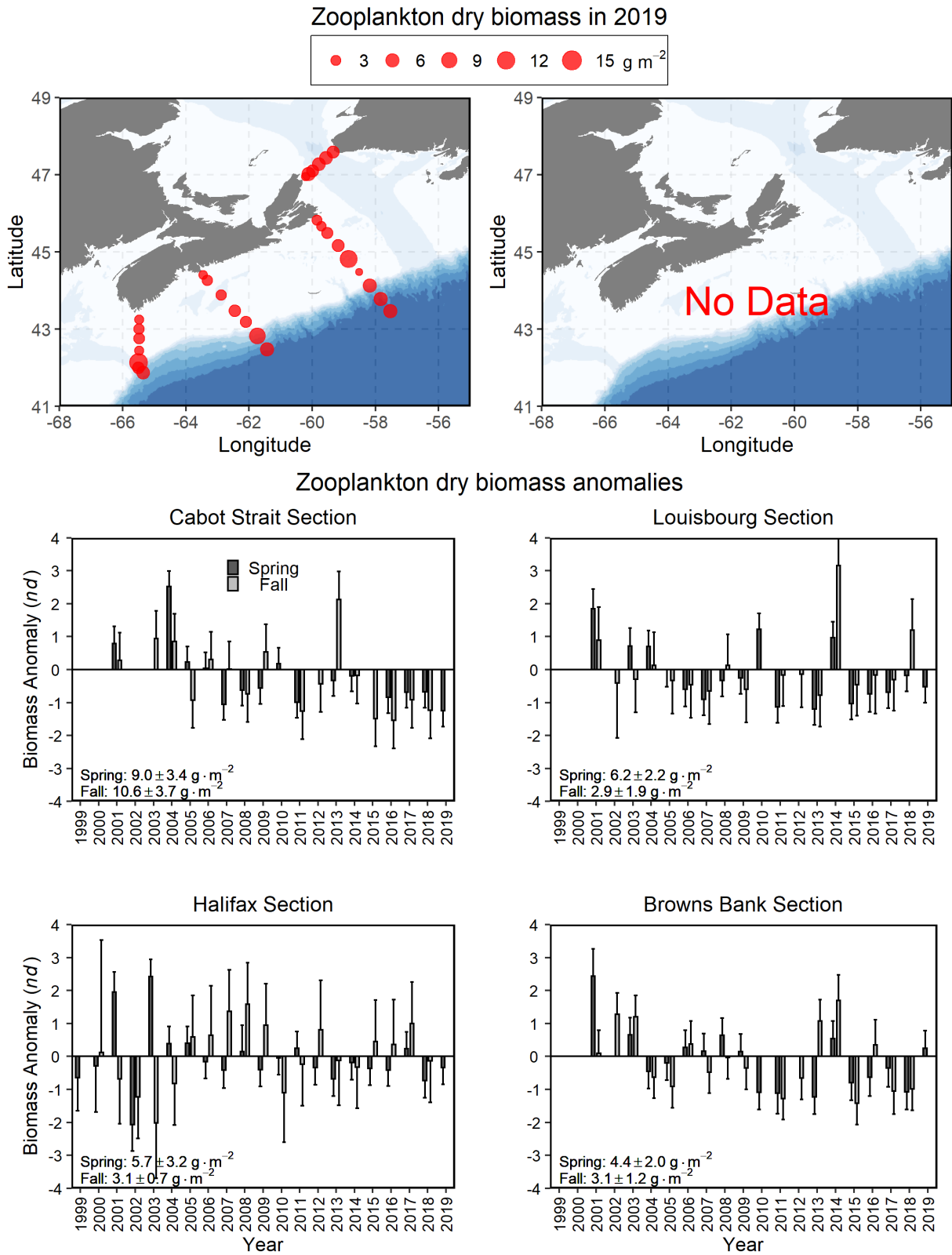


Figure 26. Spatial distribution of zooplankton dry biomass in 2019 (upper panels) and time series of zooplankton dry-biomass anomalies on Scotian Shelf sections (middle and lower panels) in spring and fall, 1999–2019. Vertical lines in lower panels represent standard errors.

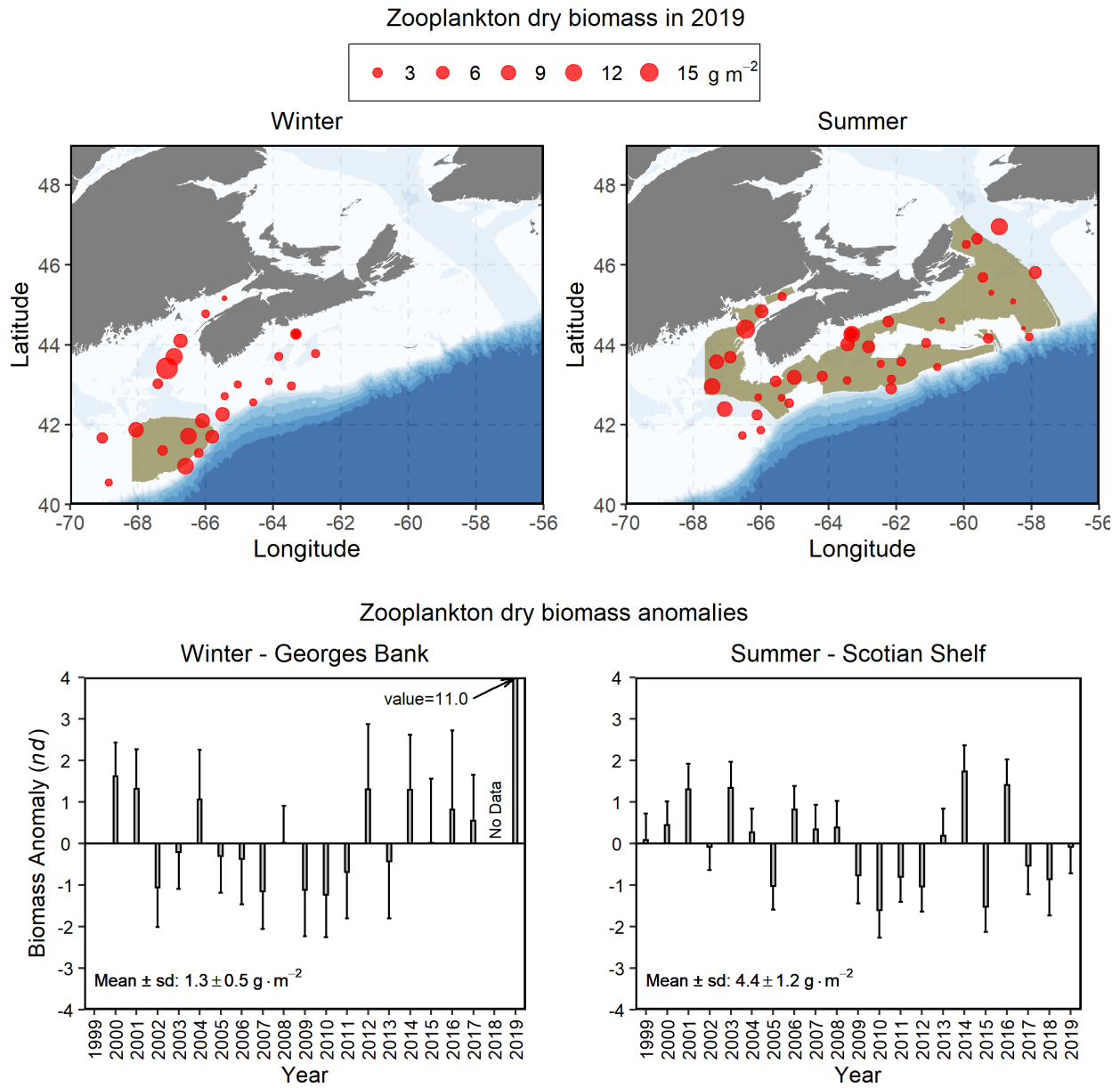


Figure 27. Spatial distribution of zooplankton dry biomass in 2019 (upper panels) and time series of zooplankton dry biomass anomalies (lower panels) from ecosystem trawl surveys on Georges Bank (winter) and the Scotian Shelf and eastern Gulf of Maine (summer), 1999–2019. Light-brown shaded areas in the upper panels represent the strata used to calculate the seasonal means. Vertical lines in lower panels represent standard errors.

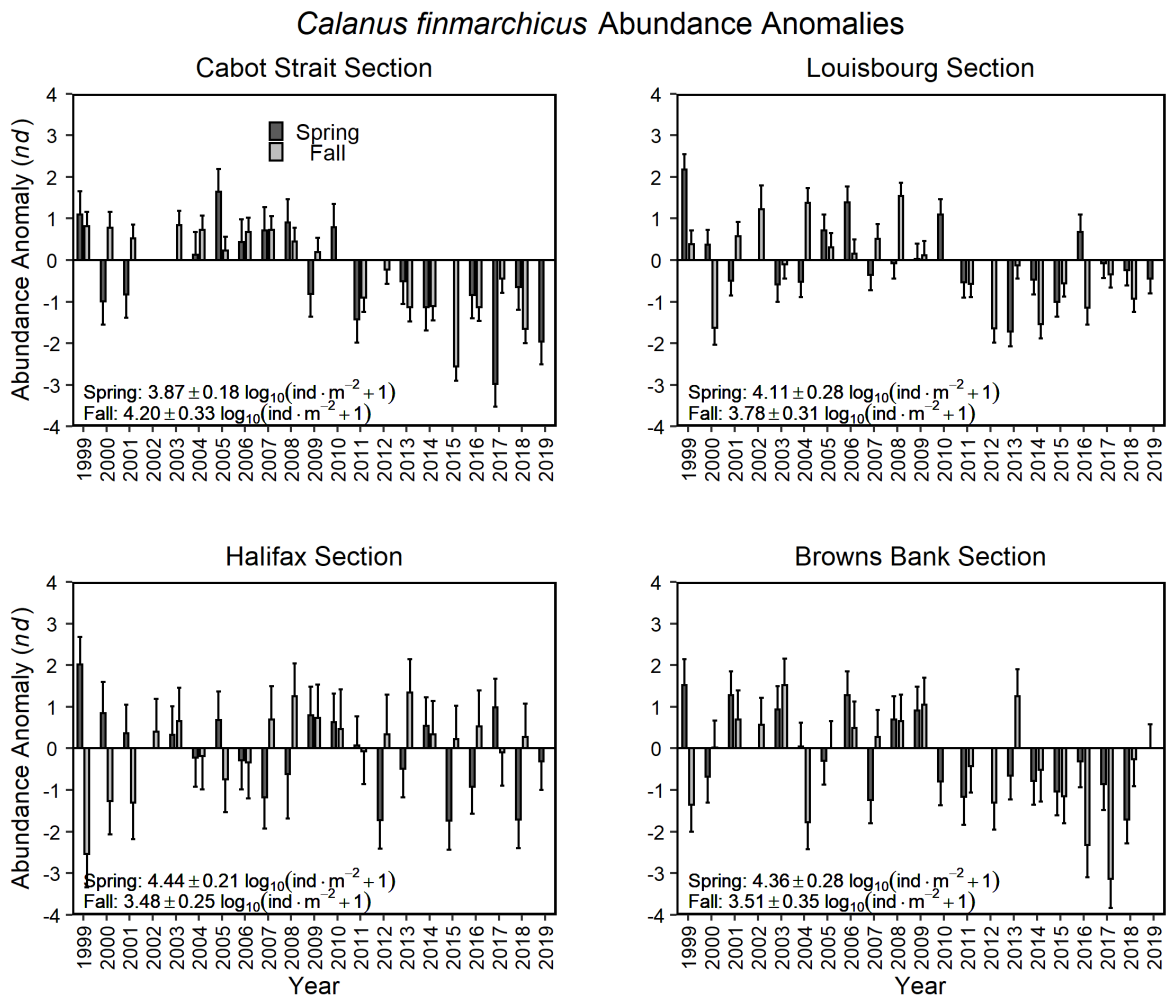
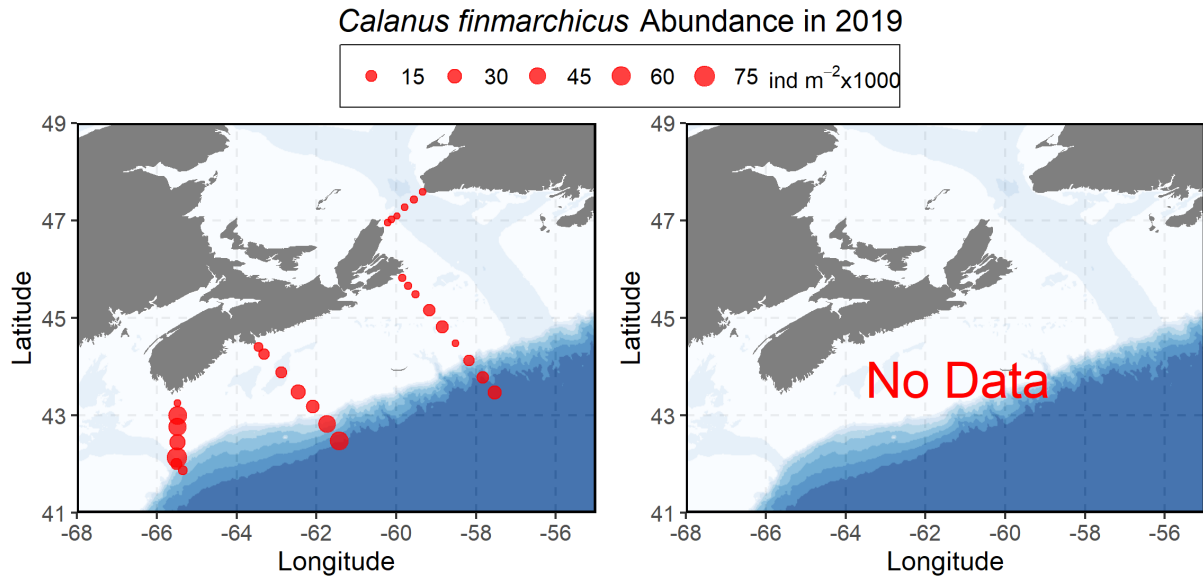


Figure 28. Spatial distribution of *Calanus finmarchicus* abundance in 2019 (upper panels) and time series of *C. finmarchicus* abundance anomalies on Scotian Shelf sections (middle and lower panels) in spring and fall, 1999–2019. Vertical lines in lower panels represent standard errors.

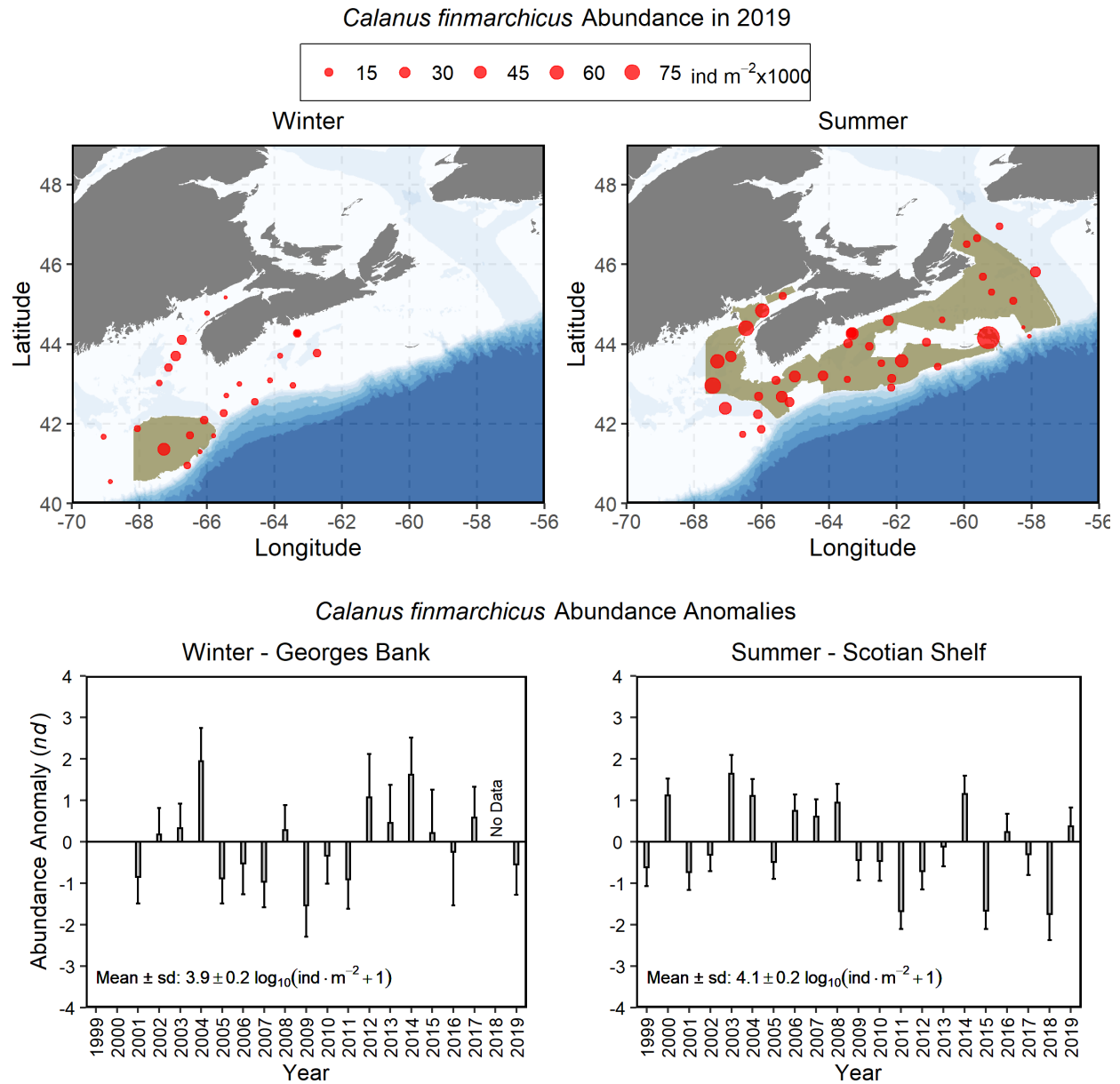


Figure 29. Spatial distribution of *Calanus finmarchicus* abundance in 2019 (upper panels) and time series of *C. finmarchicus* abundance anomalies (lower panels) from ecosystem trawl surveys on Georges Bank (winter) and the Scotian Shelf and eastern Gulf of Maine (summer), 1999–2019. Light-brown shaded areas in the upper panels represent the strata used to calculate the seasonal means. Vertical lines in lower panels represent standard errors.

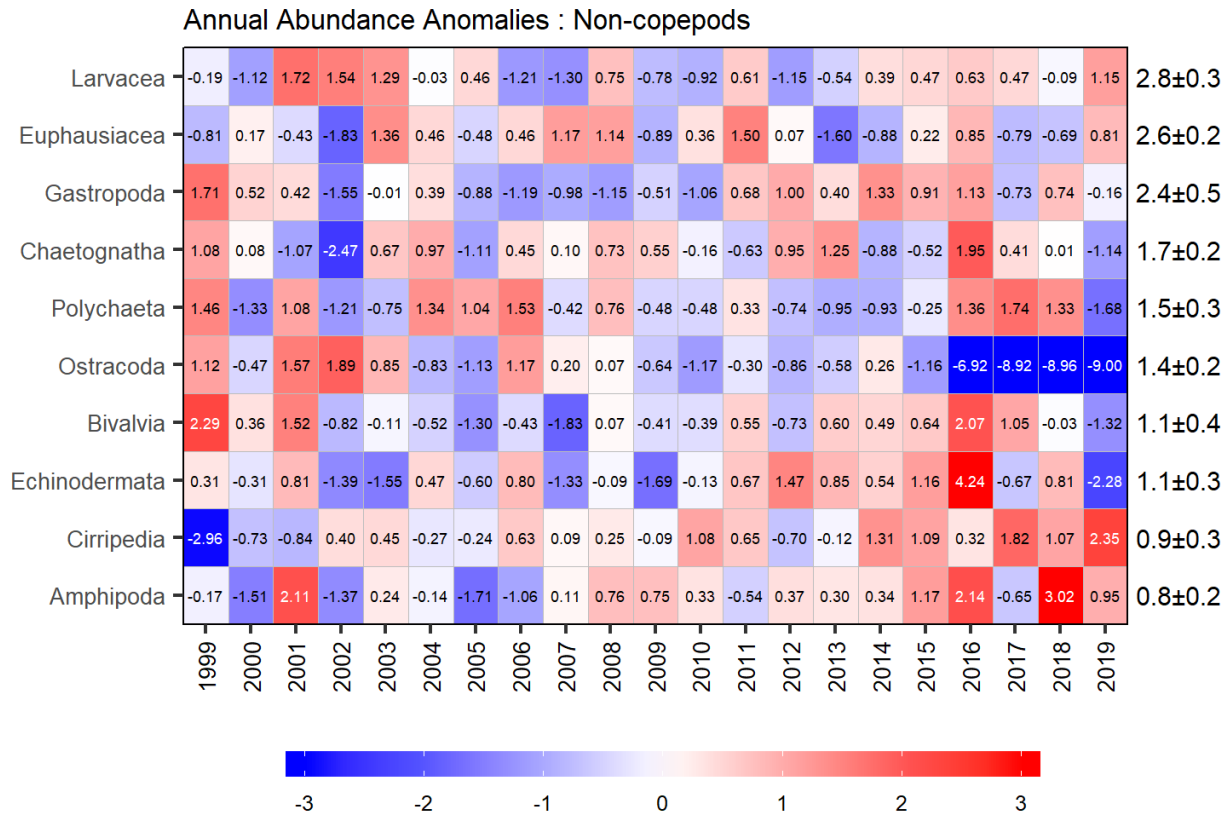


Figure 30. Annual anomaly scorecard for non-copepod groups abundances on the Scotian Shelf sections, ordered from higher- to lower-abundance. Values in each cell are anomalies from the mean for the reference period, 1999–2015, in standard deviation (sd) units (mean and sd listed at right). A grey cell indicates missing data. Red (blue) cells indicate higher- (lower-) than-normal abundances.

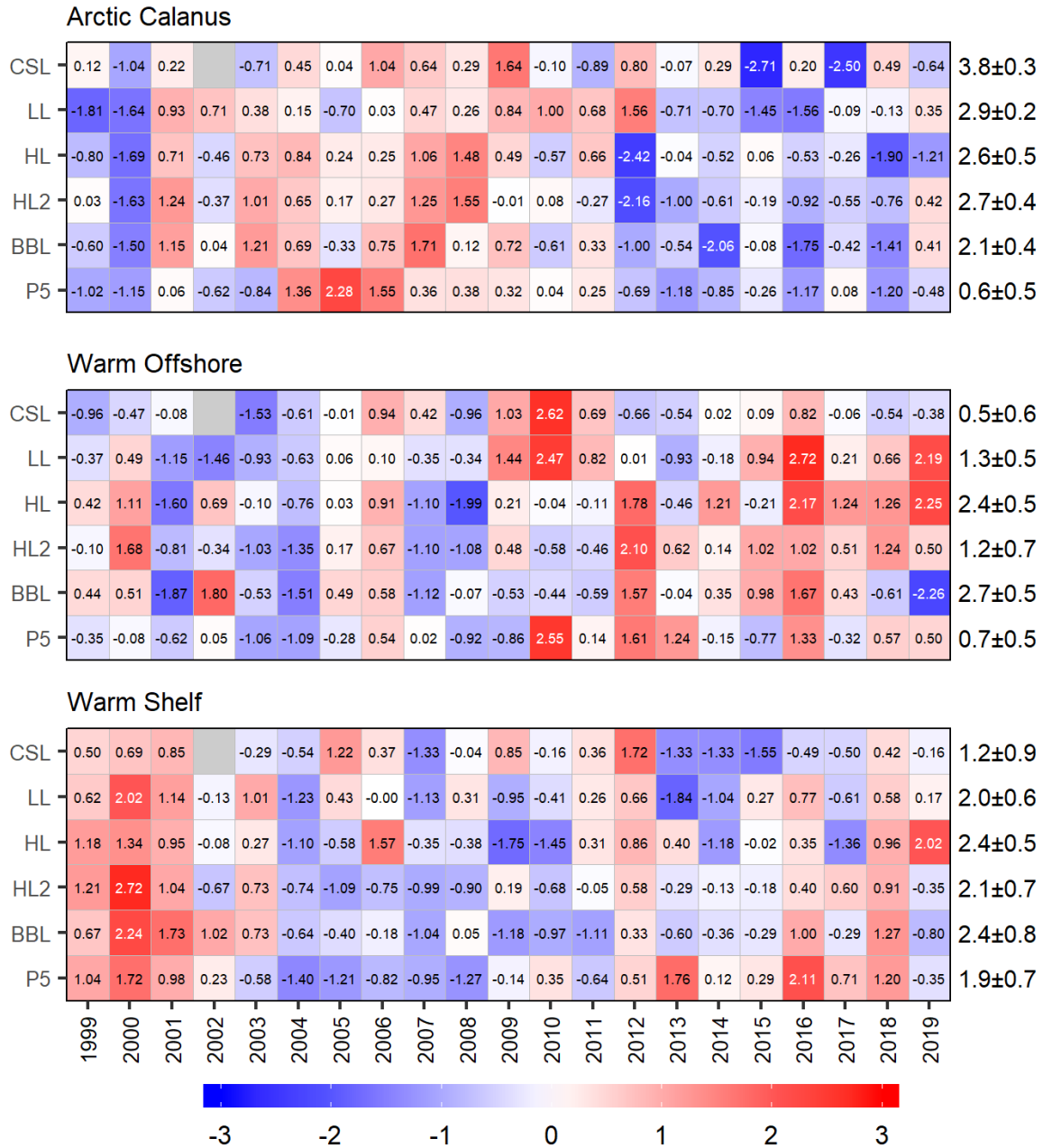


Figure 31. Annual anomaly scorecard for copepod indicator species grouped abundances. Values in each cell are anomalies from the mean for the reference period, 1999–2015, in standard deviation (sd) units (mean and sd listed at right). A grey cell indicates missing data. Red (blue) cells indicate higher- (lower-) than-normal abundances. CSL: Cabot Strait section; LL: Louisbourg section; HL: Halifax section; HL2: Halifax-2; BBL: Browns Bank section; P5: Prince-5.

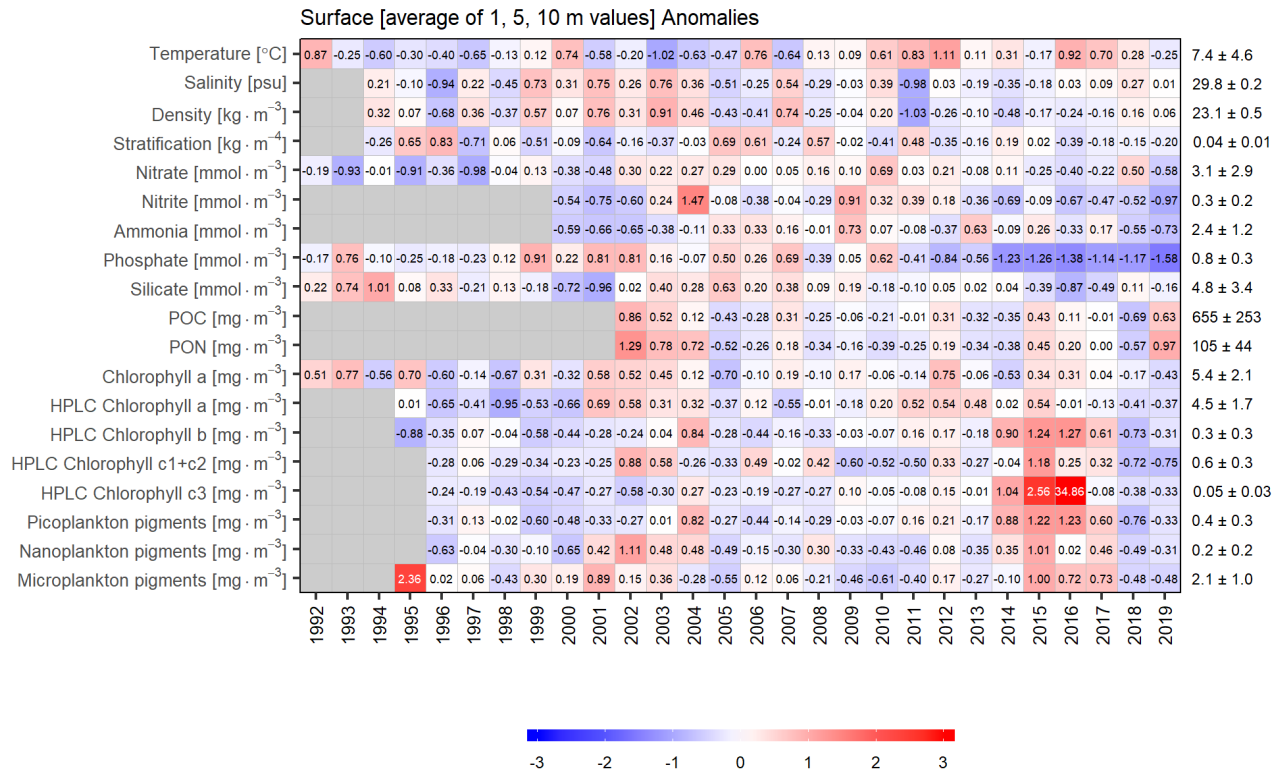


Figure 32. Annual anomaly scorecard for environmental and phytoplankton conditions in the upper water column (2, 5, and 10 m) in Bedford Basin. Values in each cell are anomalies from the mean for the reference period, 2000–2015, in standard deviation (sd) units (mean and sd listed at right). A grey cell indicates missing data. Red (blue) cells indicate higher- (lower-) than-normal levels for a given variable. POC and PON represent particulate organic carbon and nitrogen, respectively.

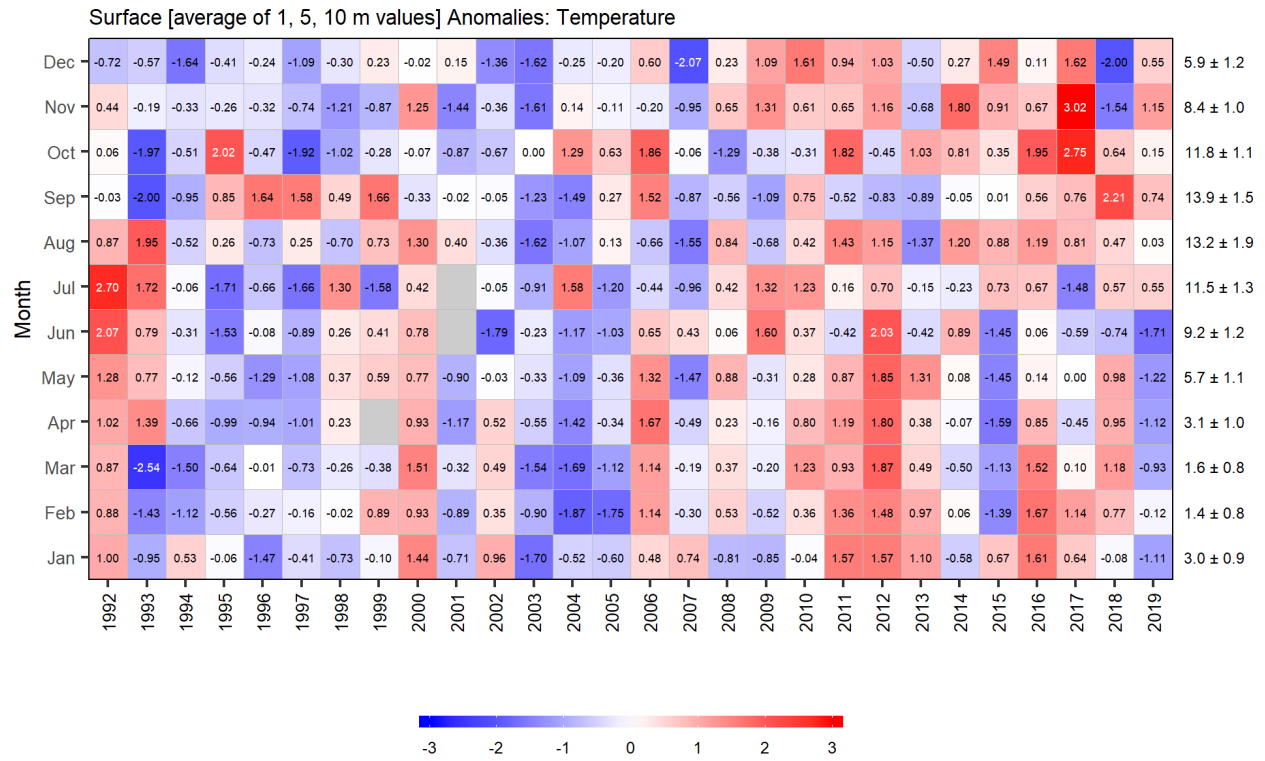


Figure 33. Average monthly temperature anomalies in the upper water column (2, 5, and 10 m) in Bedford Basin. Values in each cell are anomalies from the monthly means for the reference period, 2000–2015, in standard deviation (sd) units (mean and sd listed at right). A grey cell indicates missing data. Red (blue) cells indicate higher- (lower-) than-normal temperature.

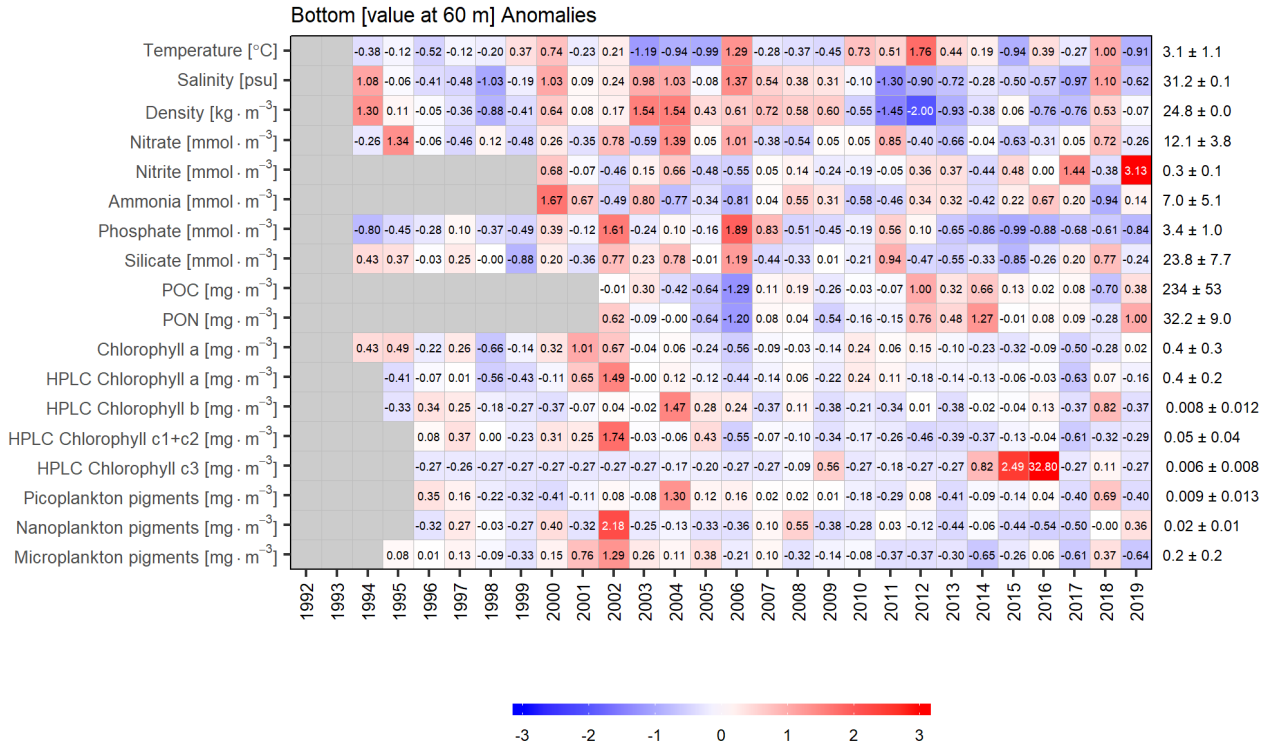


Figure 34. Annual anomaly scorecard for environmental and phytoplankton conditions at 60 m in Bedford Basin. Values in each cell are anomalies from the mean for the reference period, 2000–2015, in standard deviation (sd) units (mean and sd listed at right). A grey cell indicates missing data. Red (blue) cells indicate higher- (lower-) than-normal levels for a given variable. POC and PON represent particulate organic carbon and nitrogen, respectively.

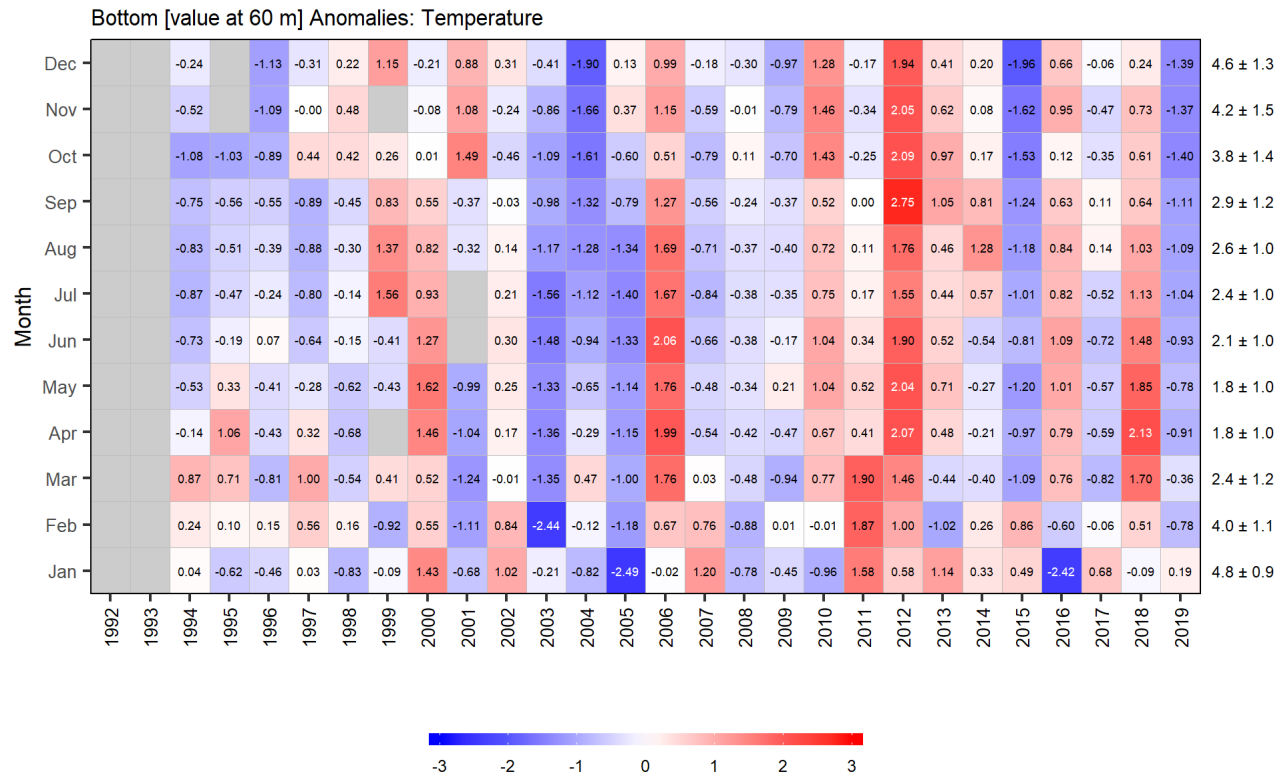


Figure 35. Bottom monthly temperature anomalies at 60 m in Bedford Basin. Values in each cell are anomalies from the monthly means for the reference period, 2000–2015, in standard deviation (sd) units (mean and sd listed at right). A grey cell indicates missing data. Red (blue) cells indicate higher- (lower-) than-normal temperatures.

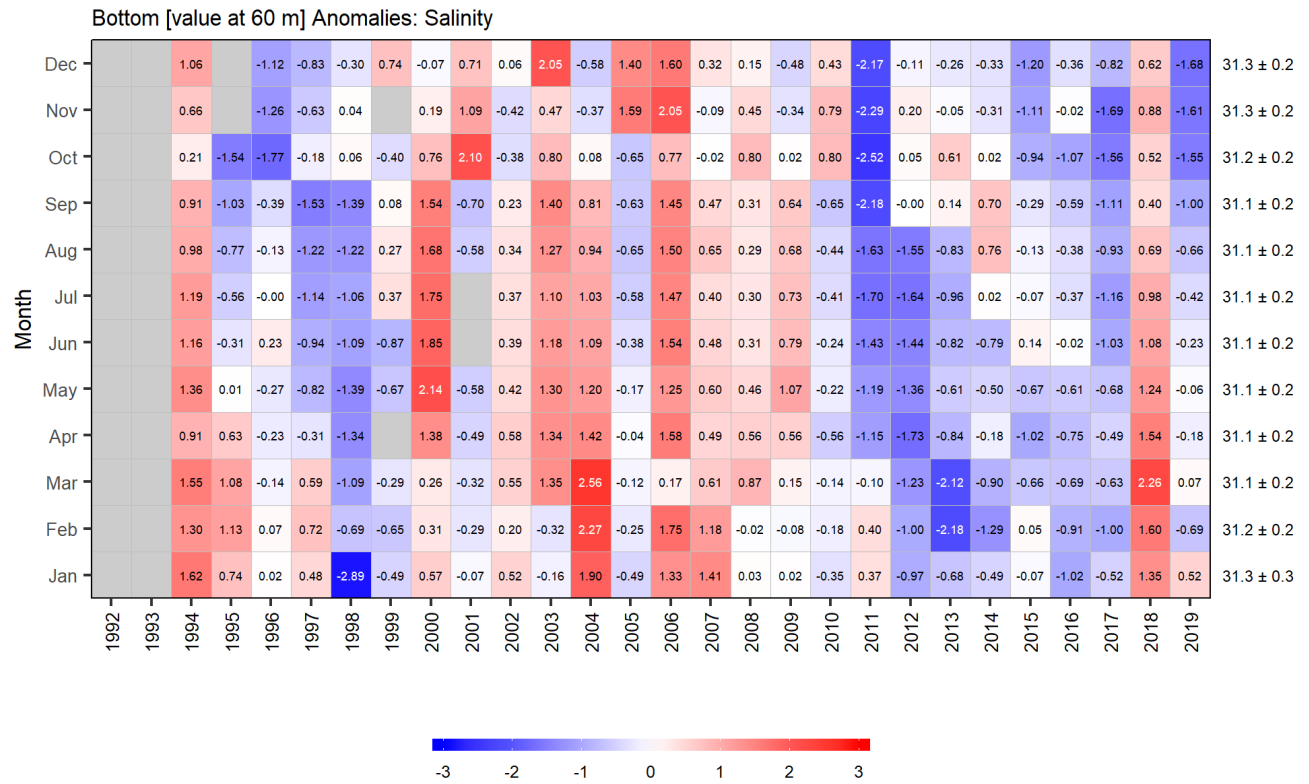


Figure 36. Bottom monthly salinity anomalies at 60 m in Bedford Basin. Values in each cell are anomalies from the monthly means for the reference period, 2000–2015, in standard deviation (sd) units (mean and sd listed at right). A grey cell indicates missing data. Red (blue) cells indicate higher- (lower-) than-normal salinities.

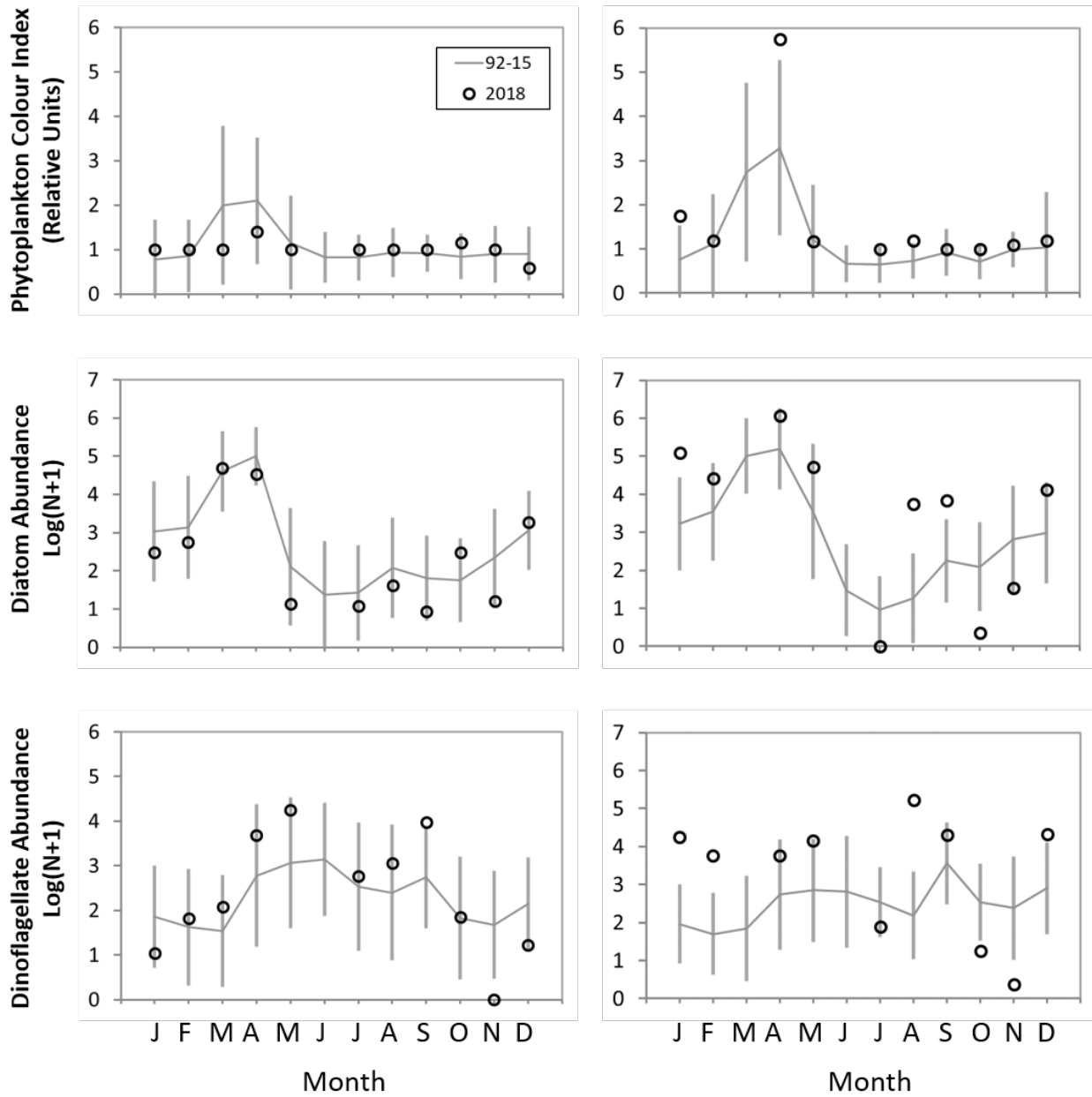


Figure 37. CPR phytoplankton abundance indices in 2018 and mean conditions, 1992–2015 (solid line) on the Western Scotian Shelf (left column) and Eastern Scotian Shelf (right column). Vertical lines show the standard deviations of the monthly averages.

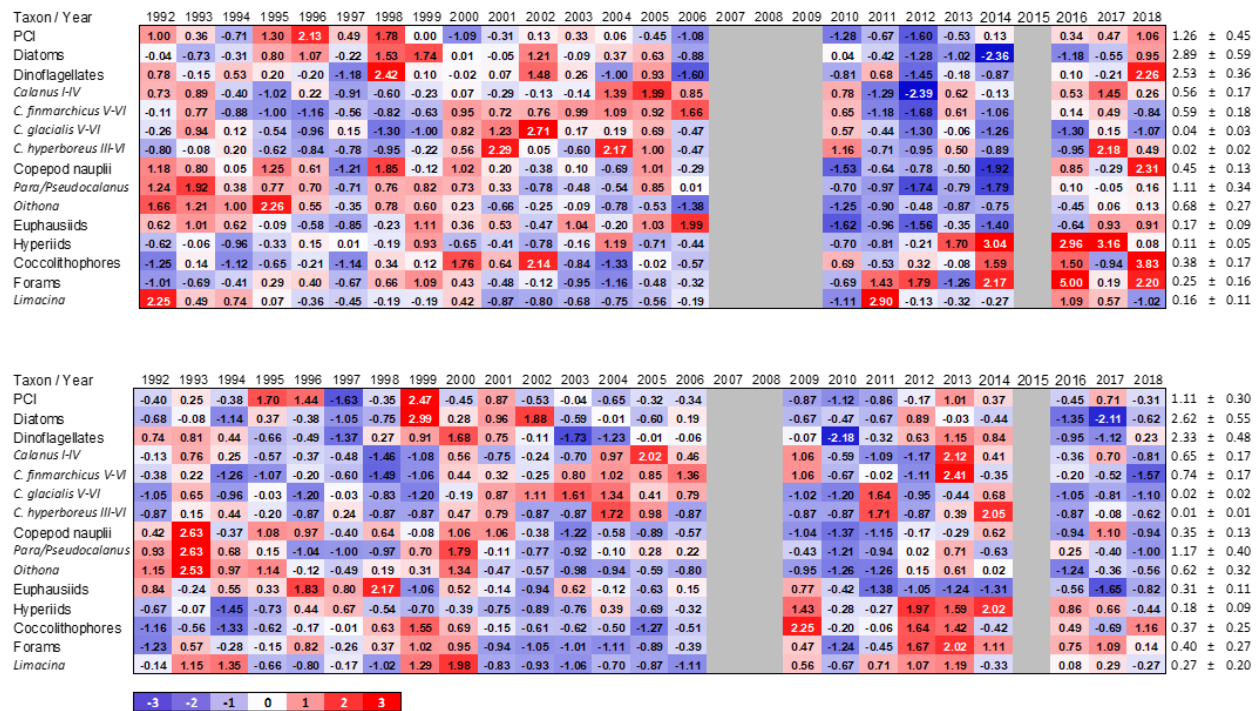


Figure 38. Annual anomaly scorecard for the abundances of phytoplankton and zooplankton taxa observed with the CPR on the Eastern Scotian Shelf (upper panel) and Western Scotian Shelf (lower panel). Blank cells correspond to years where either there was sampling in 8 or fewer months, or years where there was a gap in sampling of 3 or more consecutive months. Red (blue) cells indicate higher- (lower-) than-normal abundances. The reference period is 1992–2015. The numbers in the cells are the standardised anomalies.

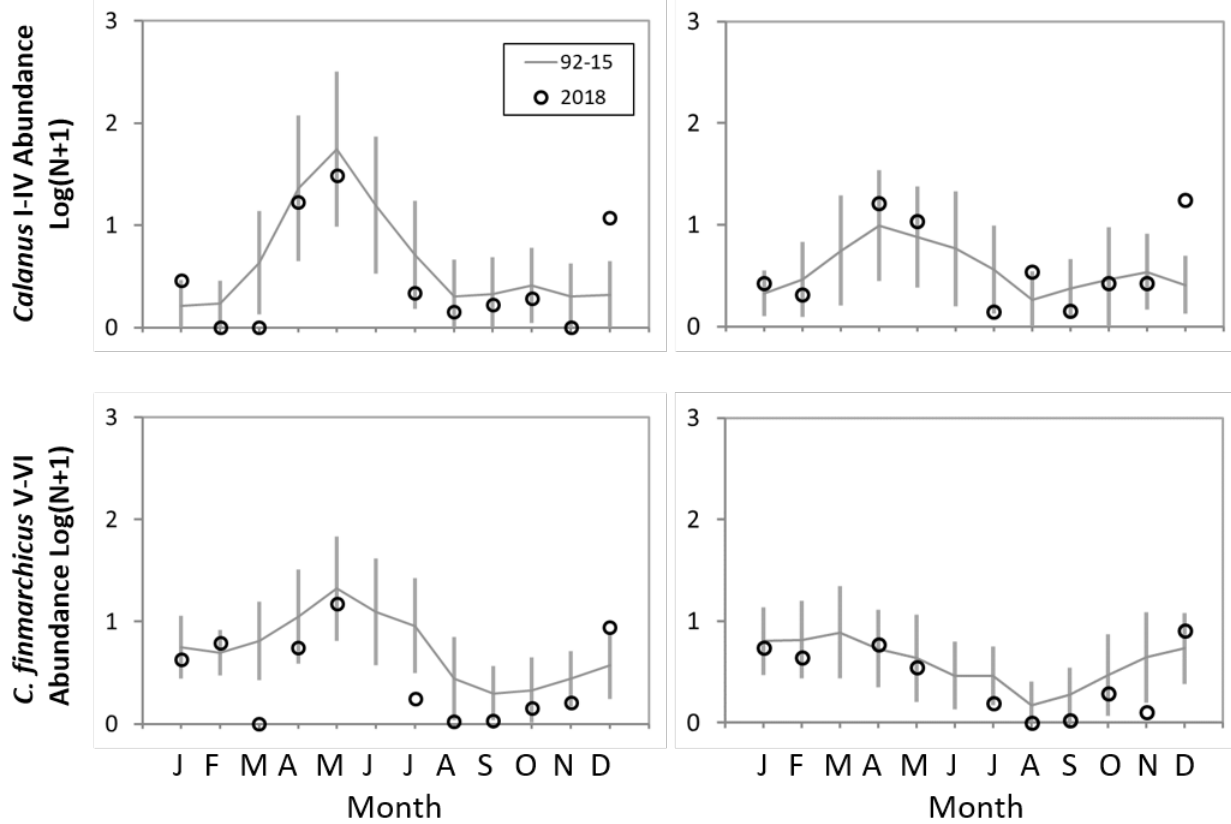


Figure 39. CPR abundance indices for *Calanus* I-IV (mostly *Calanus finmarchicus*, upper row) and *C. finmarchicus* V-VI (lower row) in 2018 and mean conditions, 1992–2015 (solid line) on the Western Scotian Shelf (left column) and Eastern Scotian Shelf (right column). Vertical lines represent standard deviations of the monthly averages.